



Universidade do Porto  
Faculdade de Engenharia  
**FEUP**

# REACTIVE POWER CONTROL IN MICROGRIDS

**BHARAT CHETRY**

*Doctoral thesis submitted to the  
Faculty of Engineering, University of Porto*

Supervisor  
**Prof. Adriano da Silva Carvalho, Ph.D.**

Co-Supervisor  
**Prof. Rui Miguel Monteiro de Brito, Ph.D.**

Departamento de Engenharia Electrotécnica e de Computadores  
Faculdade de Engenharia da Universidade do Porto  
University of Porto

July 2018  
Porto-Portugal

The research leading to these results has received funding from the **Interweave** project under **Erasmus Mundus Program** from 2014 to 2017 and SYSTEC from 2017 to 2018

©2018 Bharat Chetry. All rights reserved

Dedicated to my twin sons *Arpan* and *Arpit*

# ABSTRACT

---

The distribution of electrical energy started in 1882 by Edison and his company in direct current form. The alternating current system came into use in 1885 with the advantages of the transformer and multiple phase system. The high voltage transmission system encouraged bulk amount of energy production at remote places. The rising demand of electrical energy and the increase in bulk production of electrical energy with traditional sources like coal and oil cause environmental problems, namely emissions of carbon dioxide. These emissions are causing the greenhouse effect with the increased production of carbon.

All these factors cause the recent and present movement to alternate and renewable sources of electrical energy that address the above issues. The needs of high penetration of renewable push the conventional grid to migrate to a Microgrid, what handles the challenge of electricity demand and supply imbalance caused at integrating renewable energy sources into the main grid, without redesigning the distribution system. However, increased penetration of renewable energy resources in the conventional power system leads to new challenges as well, in order to face issues like loss of rotating inertia, low short circuit ratio, reactive power support, storage in islanded condition, which need to be handle properly. One of the major issues to face is the reactive power sharing in a Microgrid as it allows handling the voltage limit violation and limiting the losses.

This Ph.D. thesis proposes a new methodology to control the reactive power sharing adopting a distributed and local approach, which put each power source contributing within a high dynamics frame. This approach is based on measuring the needs of reactive power in the microgrid making use of the Thevenin's equivalent impedance across the terminals of the Voltage Source Converter, the output of the renewable power source, and observing the microgrid from its Thevenin's equivalent.

The VSC is controlled based on vector control in a dq reference frame and decoupling the active and reactive power in order to handle direct and orthogonally the reactive power



generation. Due to the thesis framework active power generation by the VSC is controlled as a constant power just to show the individual contribution to the reactive power sharing independent from the active power generation, supervised by MPPT conditions. The reactive power demand is estimated based on the impedance observed by the controller at the Point of Common Coupling (PCC). The consequent researched algorithm has been implemented in a conventional Microgrid using PSIM simulation platform as the right tool for this implementation. Although almost all the simulations are in PSIM but some of the simulations are performed in MATLAB Simulink to show the problem of reactive power sharing in microgrid.

# RESUMO

---

A distribuição de energia elétrica em corrente contínua foi iniciada em 1882 por Edison e sua empresa. O sistema de corrente alternada foi introduzido em 1885 com as vantagens do transformador e do sistema de fase múltipla. O sistema de transmissão em alta tensão incentivou a produção de energia em grande escala e em locais remotos. A crescente demanda de energia elétrica e o aumento generalizado da produção de energia elétrica através de fontes tradicionais como o carvão, o petróleo e a energia nuclear contribuíram para o aparecimento crescente de problemas ambientais, em particular com a produção excessiva de dióxido de carbono.

Estes fatores causaram o movimento para fontes alternativas e renováveis de energia elétrica de modo a resolver os problemas supramencionados. A Micro-rede é uma resposta adequada para lidar com o desafio da demanda de eletricidade e com a oferta crescente de integração de fontes de energia renováveis na rede elétrica sem redesenhar o sistema de distribuição. No entanto, o aumento da instalação de fontes de energia renováveis no sistema de energia convencional também conduz a novos desafios, causados pelas novas características da rede, tais como: a perda de inércia rotativa, a baixa taxa de curto-circuito, a dificuldade em suporte de energia reativa, unidades de armazenamento em modo ilha, que precisam de ser tratados adequadamente. Um dos principais problemas a enfrentar é a partilha da energia reativa numa Micro-rede, que permite lidar com a violação do limite de tensão e o aumento das perdas que podem ocorrer nas Micro-redes.

Esta tese de doutoramento propõe uma nova metodologia para controlar a partilha da energia reativa, adotando uma abordagem distribuída e local que permite o contributo dinâmico de cada fonte de energia de forma a resolver os problemas novos associados. Esta abordagem baseia-se na medição das necessidades de energia reativa na Micro-rede, fazendo uso da impedância equivalente de Thévenin aos terminais do Conversor de Potência Fonte de Tensão, que interliga a fonte de energia renovável com a rede elétrica, e observando a Micro-rede no seu equivalente de Thévenin.

O conversor, fonte de tensão, é controlado com base no controlo vetorial, no referencial “dq”, com desacoplamento das componentes d e q de modo a controlar direta e ortogonalmente a produção de potência ativa e reativa. No contexto da tese, a potência ativa gerada à saída do conversor de tensão é controlada como potência constante, apenas para mostrar a produção individual de energia reativa independente da produção de energia ativa, esta supervisionada pelas condições de máximo ponto operacional de produção. A demanda de energia reativa é estimada com base na impedância observada pelo controlador no ponto de acoplamento comum. O algoritmo investigado foi desenvolvido e aplicado numa Micro-rede convencional utilizando a plataforma de simulação PSIM como ferramenta apropriada a esta implementação. O contexto inicial de análise foi trabalhado com suporte na plataforma MATLAB Simulink fundamentalmente por razões de comparação com o estado da arte.

## Publications

---

- [i] Bharat Chetry, Adriano da Silva Carvalho, Rui Brito, “*Voltage Source Converter in Microgrid*” International Journal of System Assurance Engineering and Management (2018). <https://doi.org/10.1007/s13198-018-0741-x>.
- [ii] Bharat Chetry, Adriano da Silva Carvalho, Rui Brito “*A Novel Distributed Approach based Reactive Power Support in Microgrids*” In: 2017 IEEE Conference on Technologies for Sustainability, DOI: 10.1109/SusTech.2017.8333536.
- [iii] Khagendra Thapa, Pradip Khatri and Bharat Chetry “*Voltage Control of a DFIG-Based Wind Power Plant Using Adaptive Reactive Current Capability and Measured Admittance Schemes.*” (ICDERT, 2018), Kathmandu, Nepal.
- [iv] B. Chetry and N. R. Karki, “*Adequacy Assessment of Integrated Nepal Power System,*” U.Porto J. Eng., vol. 1, no. 2, pp. 13–22, 2015.
- [v] Bharat Chetry \*, Mohammad Meraj Alam 2, Adriano Carvalho 1, and Rui Brito 3, “*A new Method to Share Reactive Power in Microgrids*” Submitted in Journal ‘Energies’.

# Acknowledgements

---

I consider myself very lucky to be among so many good people around me without whom it would not be possible carry out this Ph.D. work. There are many people whose continuous support was with me during the entire period of my thesis work.

I take the opportunity to express my deep gratitude to my supervisor Prof. *Adriano Da Silva Carvalho* for his extreme dedication and valuable contributions, which were sufficient for allowing me to stay, focused. It was very difficult for me to complete the Ph.D. in three years after taking one year on regular courses. My supervisor always supported me whenever I was in trouble. I would also like to express my gratitude to my co-supervisor Prof. *Rui Miguel Monteiro de Brito* for his continuous support. He treated me like a helpful friend. I found him as a very kindhearted person. Beside my two supervisors I am extremely grateful to Prof. *Carlos Coelho Leal Moreira* who introduced me to the problem of reactive power sharing in microgrid for the first time. He even provided me some simulations from his thesis which were very helpful to me for analyze the problem.

I would like to express special thanks for helping me out in this work to my friends *Jorge Pinto, Mohammad Meraj Alam, Agostinho Rocha* and *Yola Marinheiro*. Many thanks to *Ataollah Mokhberdoran* and *Elias Yousefi* for being a good friend while working together as a researcher and motivating in many occasions. I feel lucky to get friends like *Ricardo, Alexandre*, and *Vitor* as a labmate. You were very cooperative for understanding a person from the Future (as you often called me as our calendar is advanced than the A.D.)

I want to show my deepest respect to my supervisor from MSC Prof. *Navaraj Karki* for guiding and motivating me for going for the Ph.D. My special thanks are with Dr. *Bishnu Bhattari* for giving valuable suggestions from the USA.

I am very thankful to my parents and the whole family for their continuous blessings and love. I will never forget the sacrifice of my wife while doing the Ph.D. and of course last but not

the least this Ph.D. work has kept my sons away from the love of their father. I hope after completing the work I will be able to compensate by loving them even more. Thanks for keeping patient and missing me sons.

## Table of Contents

1	INTRODUCTION .....	1
1.1	General Background and Motivation .....	1
1.2	Problem Definition .....	1
1.3	Objective and Research Question .....	4
1.4	Contributions of the Thesis .....	4
1.5	Outline and Approach .....	5
2	MICROGRID AND ITS DEVELOPMENT .....	8
2.1	Conventional Electrical Power Grids .....	8
2.2	Microgrid and its development .....	10
2.2.1	Consortium for Electric Reliability Technology Solutions (CERTS) .....	11
2.2.2	European Concept of Microgrid .....	13
2.2.3	Shimizu's Microgrid .....	15
2.3	Control of Microgrid .....	16
2.3.1	Frequency Control .....	17
2.3.2	Voltage Control and Power Sharing .....	20
2.3.3	Modified Voltage Control and Power Sharing .....	24
2.4	Control of Microgrid with innovative approaches .....	28
2.5	Conclusion .....	34
3	VOLTAGE SOURCE CONVERTER AND ITS CONTROL .....	35
3.1	Voltage Source Converter Modeling .....	35
3.1.1	AC side model of the VSC .....	39
3.1.2	Active and Reactive Power of the AC side .....	45
3.1.3	DC side model of the VSC .....	46
3.1.4	The Complete model of the VSC .....	48
3.2	The Laplace Model of VSC .....	49
3.2.1	Laplace Equations of the AC side of the VSC .....	49
3.2.2	Laplace Domain Equations of the DC side of the VSC .....	49
3.3	The VSC Control Principle .....	52
3.3.1	The VSC Current Controller .....	52

3.3.2	Pulse-width Modulation Techniques for Voltage Source Converters .....	55
3.3.3	Modulation Indexes.....	56
3.4	Synchronization Techniques.....	57
3.4.1	Synchronous Reference Frame PLL .....	58
3.4.2	PSIM SRF-PLL Dynamic Evaluation .....	60
3.5	VSC Working in Different Modes .....	62
3.6	Conclusion .....	69
4.	REACTIVE POWER CONTROL USING VOLTAGE SOURCE CONVERTER .....	71
4.1	Introduction.....	71
4.2	The problem with reactive power sharing .....	71
4.3	Reactive Power Flow with different line parameters. ....	77
4.4	Power Flow conducted using the designed controller in PSIM. ....	80
4.4.1	Description of the Simulation System .....	81
4.4.2	Components of PSIM used in this Thesis.....	82
4.4.3	PSIM Block to measure phase angle between voltage and current.....	86
4.4.4	PSIM Block to measure the inductive or capacitive part of the impedance.....	87
4.4.5	Power Flow using the designed controller in PSIM.....	87
4.5	Conclusion .....	94
5	REACTIVE POWER CONTRIBUTION BY RENEWABLE SOURCES.....	95
5.1	Introduction.....	95
5.2	Analytical derivation of the equivalent impedance observed by the VSC .....	96
5.3	Voltage and Frequency Control .....	100
5.4	Reactive Power Sharing in Microgrids.....	104
5.4.1	Role of the Controller .....	104
5.4.2	Digital Algorithm for Reactive Power Contribution.....	106
5.4.3	Reactive Power sharing with Renewable energy using VSC .....	109
5.5	Conclusion .....	121
6	CONCLUSION AND FUTURE WORK .....	122
6.1	Conclusion .....	122
6.2	Future Work.....	124
	B I B L I O G R A P H Y.....	125



## List of Figures

Figure 2.1 Stages of Power System.....	9
Figure 2.2 CERTS Microgrid Architecture [5]. ....	13
Figure 2.3 MG architecture based on European project MICROGRIDS [1]. ....	14
Figure 2.4 Shimizu Extended microgrid [24].....	16
Figure 2.5 Active power frequency droop [1].....	18
Figure 2.6 Droop controlled BESS with cooperative control [35]. ....	19
Figure 2.7 Reactive Power-Voltage droop [1].....	22
Figure 2.8 Three strategies to control reactive power flow. ....	23
Figure 2.9 P/Q sharing loops. ....	26
Figure 2.10 Reactive power sharing strategy based on secondary voltage control [15]. ....	27
Figure 3.1 Grid feeding power source with the grid side converter controlling grid voltage [76].....	36
Figure 3.2 Grid forming power source with the grid side converter controlling grid voltage [76]. ....	37
Figure 3.3 Grid Supporting VSC [79] (Current Source based and Voltage source Based). ....	37
Figure 3.4 Three-phase VSC with AC and DC sources/loads. ....	39
Figure 3.5 Three-phase VSC AC side model. ....	40
Figure 3.6 abc, $\alpha\beta$ and dq reference frame. ....	41
Figure 3.7 VSC single-phase and dq vector diagram.....	43
Figure 3.8 VSC's AC side - a) rectification at UPF; b) inversion at UPF. ....	44
Figure 3.9 Three Phase AC model of VSC in dq.....	45
Figure 3.10 Three Phase VSC DC side. ....	47
Figure 3.11 Three Phase VSC model. ....	48
Figure 3.12 DC side of the VSC with battery modeled as a capacitor and a Resistor in series. ....	50
Figure 3.13 VSC DC side representation of a battery modeled as a large capacitor.....	50
Figure 3.14 Laplace Model of VSC including a large capacitor as a battery.....	51
Figure 3.15 Decoupled current controller of three phase VSC.....	53
Figure 3.16 Current controller and VSC Laplace model with a battery modeled as a capacitor in the DC side. ....	54
Figure 3.17 VSC connected with the grid. ....	55
Figure 3.18 Basic structure of PLL. ....	58
Figure 3.19 Synchronous Reference Frame PLL Model .....	59
Figure 3.20 Synchronous Reference Frame PLL comprehensive Model.....	60
Figure 3.21 PSIM SRF-PLL synchronization test circuits using a) $V_q$ or b) $V_d$ as a synchronization signal.....	61
Figure 3.22 PSIM SRF-PLL synchronization test circuits waveforms. ....	61
Figure 3.23 VSC connected with the Grid at 400 Line to Line (rms). ....	63
Figure 3.24 VSC working as rectifier and as inverter at UPF( Unity Power Factor); $I_d$ = constant = 100A; $I_d$ = single phase peak current; $I_d$ =+100A and $I_q$ =0 . ....	64
Figure 3.25 VSC working as rectifier and as inverter at UPF $I_d$ =+100A and $I_q$ =0. ....	65
Figure 3.26 Enlarged View of $I_d$ settling to $I_{d\_ref}$ and the effect shown in $I_q$ .....	66
Figure 4.1 Three phase VSC model [5].....	73
Figure 4.2 Active power supplied by the DG1while load in point 1.....	73
Figure 4.3 Active power supplied by DG2 while the loading is in point 1.....	73

Figure 4.4 Reactive power supplied by DG1 while loading in point 1.....	74
Figure 4.5 Reactive power supplied by DG2 while loading in point 1.....	74
Figure 4.6 Active power supplied by DG1 while loading in point 2. ....	74
Figure 4.7 Reactive power supplied by DG1 while the loading is in point 2. ....	75
Figure 4.8 Active power supplied by DG2 while the loading is in position 2. ....	75
Figure 4.9 Reactive power supplied by DG2 while the loading is in position 2.....	75
Figure 4.10 (a) Power flow through a line (b) Phasor Diagram.....	78
Figure 4.11 Relationship between PSIM blocks.....	81
Figure 4.12 Image and Attribute of Proportional Controller [98].....	82
Figure 4.13 Image and Attribute of Integrator [98].....	82
Figure 4.14 Image and attribute of PI controller [98].....	83
Figure 4.15 Image and attribute of FFT. ....	84
Figure 4.16 Image and circuit model of the THD block [98]. ....	84
Figure 4.17 Voltage and Current Sensor.....	85
Figure 4.18 abc to dq0 and dq0 to abc transformation block. ....	86
Figure 4.19 Phase angle measurement between voltage and current.....	86
Figure 4.20 Measurement of equivalent impedance (Inductive or Capacitive).....	87
Figure 4.21 VSC connected to a grid through a line having an inductance of 100 m H and resistance of 1 m-ohm.....	88
Figure 4.22 Single line diagram of VSC connected to a grid. ....	89
Figure 4.23 Power transfer between Grid and Voltage Source Converter. ....	92
Figure 4.24 Variation of active power flow (kw) with the variation of the phase angle between VSC and GRID. ....	92
Figure 4.25 Variation of reactive power with the variation of voltage magnitude.....	93
Figure 5.1 VSC connected to the grid.....	96
Figure 5.2 Equivalent impedance observed by the VSC.....	97
Figure 5.3 VSC connected to the grid. ....	101
Figure 5.4 Voltage and frequency drops with the increase in load current.....	102
Figure 5.5 Improvement of frequency with the injection of active power from the VSC.....	103
Figure 5.6 Voltage improvement by the increment of the reactive power from the VSC. ....	103
Figure 5.7 Controller used to generate the signals for the VSC to control reactive power. ....	105
Figure 5.8 Enlarged view of one of the section of the controller.....	106
Figure 5.9 Flowchart of the algorithm used in C-Block.....	107
Figure 5.10 C-Block used for implementation of digital algorithm.....	109
Figure 5.11 VSC connected to the grid.....	111
Figure 5.12 Circuit diagram of the VSC connected.....	112
Figure 5.13 Reactive power support by the VSC.....	113
Figure 5.14 Active power supplied by the VSC. ....	116
Figure 5.15 Change in $e_d$ and $e_q$ components of the voltage with the change in load.....	117
Figure 5.16 Generation of the $I_{q\_Reference}$ for the positive error.....	118
Figure 5.17 Generation of the $I_{q\_Reference}$ for the negative error. ....	119
Figure 5.18 Change in equivalent reactance and voltage across the load.....	120

## LIST OF TABLES

Table 4.1 Active and Reactive power between VSC and Grid.....	90
Table 4.2 Actual values of Active and Reactive power flow between VSC and Grid.....	91

# Acronyms

---

AC	Alternating Current
AI	Artificial Intelligence
ANF	Adaptive Notch Filtering
BTU	British Thermal Unit
BESS	Battery Energy Storage System
CERTS	Consortium for Electric Reliability Technology Solutions
DC	Direct Current
DFT	Discrete Fourier Transform
DG	Distributed Generation
DSC	Delayed Signal Cancellation
ETP	European Technology Platform
EU	European Union
ESS	Energy Storage Systems
ESR	Equivalent Series Resistor
FFT	Fast Fourier Transform
FLL	Frequency Locked Loop
GhG	Green House Gas
ISEN	Current Sensor
kVAR	Kilo Volt Ampere Reactive
km	Kilometer
LV	Low Voltage
MGs	Microgrids

MGCC	Microgrid Central Control
MI	Modulation Index
MV	Medium Voltage
MPPT	Maximum Power Point Tracking
mH	Milli Henry
NLS	Non Linear Least Square
OECD	Organisation for Economic Cooperation and Development
PCC	Point of Common Coupling
PLL	Phase Locked Loop
PMSG	Permanent Magnet Synchronous Generator
RMS	Root Mean Square Value
SPWM	Sinusoidal Pulse Width Modulation
SRF	Synchronous Reference Frame
SVM	Space Vector Pulse Width Modulation
THD	Total Harmonic Distortion
VSC	Voltage Source Converter
VSEN	Voltage Sensor
VSG	Virtual Synchronous Generator
VSI	Voltage Source Inverter
ZCD	Zero Crossing Detection

# 1 INTRODUCTION

## 1.1 General Background and Motivation

Microgrids (MGs) can be considered as the modern reformulation of the power system as Edison and other electrical pioneers designed it. Centralized and fossil fuel-based conventional generation stations, suffering from long distance transmission, low efficiency/reliability, heavy pollution, and energy resource shortage, will be gradually substituted by distributed and renewable energy based generation plants[1]. Increased penetration of renewable resources in the conventional power system leads to new challenges, which are to be handled with a new approach. Microgrid (MG) is one of the suitable answers to handle the challenges related to the renewable resources. MG approach not only integrates the advantages of the distributed generation but also provide new technical ways for large application of grid-connected generation of renewable energy.

MG is also emerging as a source of clean energy and resilient power source after the frequent natural calamities around the world that led to the disturbance in the traditional power system. The resiliency of MG was proved in an earthquake in Japan in 2011 when the Sendai MG continued its supply after the earthquake [2]. Similarly, after the sandy storm of the USA in 2012, the research MG at the Princeton University continued its supply. According to the criteria of European Technology Platform (ETP), future electricity networks should be accessible, flexible, reliable and economic [3]. Along with the criteria from ETP, it is also prime importance to use as many renewable resources as possible to face the environmental challenges caused by fossil fuel generation. All these circumstances lead to consider MG as the new energy supply system.

## 1.2 Problem Definition

The energy crisis and environmental issues have become increasingly prominent, it has become the general consensus of human society to develop low carbon economy and construct ecological civilization to achieve sustainable development [4]. The development of clean and renewable energy has become an important strategy of economic and socially sustainable development for all the countries in the world. It is necessary to include a large number of renewable resources to handle the energy crises and environmental issues.

## INTRODUCTION

According to United States Government official energy statistics, a scenario where the current energy policies remain unchanged in the coming years will lead to the increase by 50% of the world marketed energy consumption in the period 2005–2030. Total world energy use will rise from  $462 \times 10^{15}$  British Thermal Units (BTU) in 2005 to  $563 \times 10^{15}$  BTU in 2015 and to  $695 \times 10^{15}$  BTU in 2030. For the same reference scenario, the world net electricity generation nearly doubles from about  $17.3 \times 10^{12}$  kWh in 2005 to  $24.4 \times 10^{12}$  in 2015 and  $33.3 \times 10^{12}$  kWh in 2030. It is also expected that the total electricity generation in countries not belonging to the Organisation for Economic Cooperation and Development (OECD) will increase by an average of 4% per year from 2005 to 2030, as compared with a projected average increase of 1.3% per year for OECD countries [5].

One of the major challenges is to supply all these energy requirements in future with environmentally friendly sources. So different countries have set targets to fulfill the demand with distributed generation through renewable resources. There are many challenges to incorporate the distributed energy resources in the existing traditional power system. In order to coordinate the contradiction between the grid and distributed generation, and maximize the advantages of distributed generation in the economy, energy, and environment, the scholars put forward the concept of the microgrid. With proper control and management, MGs based power grid can offer a number of advantages, typical ones of them are [6]-[7]:

- ✚ Higher efficiency because of local generation and combined electricity/heat generation/storage.
- ✚ A well designed MG is capable of enhancing power system reliability at the customer level since two independent sources (the MV( Medium Voltage)) distribution grid and DG( Distributed Generation) units) can be used to supply the electrical loads. Also, the transmission system dynamic stability can be improved under a scenario of the provision of ancillary services by DG. Additional benefits such as voltage support or enhanced power quality can also be provided by MG [5].
- ✚ Ensure diversity of energy supply.
- ✚ Enhanced sustainability by reducing the amount of fuel based generation, and increasing the penetration of renewable energy.

## INTRODUCTION

✚ Power supply to a remote site.

Along with advantages, there come challenges, though MGs are the perfect answer to the present and upcoming distributed renewable resources worldwide still there are many challenges to be look after. The increasing interest in integrating intermittent renewable energy sources into MGs presents major challenges from the viewpoints of reliable operation and control.

Some of the technical challenges on MG are the stability issues, seamless transition between interconnected to islanded mode and operation in islanded mode. There are some stability issues due to the fact that unlike traditional power system where there are a lot of generation based on rotating machine, in MG the generations are mostly performed by renewable resources. These renewable resources are electronically integrated with the grid which is mostly inertialess that can cause a problem to the stability of the system. To overcome this problem of stability, the control algorithms must provide a solution for grid dynamics and react to the demand response of the MG.

In fact, there is a risk of phase and frequency drift for the MG is high when there is a transition to the islanded mode from the interconnected mode. Special care must be taken when there is a transition from islanded to interconnected mode, as connecting to the bigger system may damage the MG if connected directly without a blackout. The other current issues regarding islanding operation in the MG are to increase the duration of islanded mode operation. Research works are being carried out worldwide to increase the duration of islanded operation by using improved algorithms and integrating new demand response techniques.

Another technical challenge points to how to manage and control the reactive power sharing relevant functionality to guarantee a good regulation of the grid voltage. The proposed work of this research is to solve this issue using the distributed approach with the help of controlling techniques of the VSC (Voltage Source Converter). In comparison to the frequency which is a global variable, voltage is a local variable which is to be controlled using local control approach. In this thesis, a methodology to control the reactive power compensation and voltage control is carried out.





## INTRODUCTION

### 1.3 Objective and Research Question


This Ph.D. thesis work is on reactive power control and regulation of voltage in the microgrid. Many works have been done in frequency control but voltage and reactive power control still have to be harnessed. The voltage drop is compensated to a large extent by the capacitive compensation of both loads and transmission lines in the high voltage traditional network [8]. Moreover, the synchronous generators exhibit a self-stabilizing feature due to their high rotational inertia [9].

In case of a MG, the scenario is different with Distributed Generation (DG) because the DG are located near to each other and lines connecting them are more resistive than inductive what prohibits easy voltage control. So, a proper load sharing mechanism is required in a MG to prevent overloading of the sources and to control the voltages of their terminals. Since most of the generation units integrated into the MG are not of the synchronous generator type thus, MG needs to somehow mimic the droop characteristic existing in those synchronous generators to control the voltage. This research work is carried out addressing the following issues: -

1. Analytical formulation to

-  Establish a mathematical Laplace model of the controller of the VSC (Voltage Source Converter) in order to guarantee a good enough dynamical response.
-  Design a controller of the VSC to guarantee mathematically a fast operation of VSC in which active and reactive power are controlled independently.

2. Work within PSIM Software a formulation of MG operation

-  To control the reactive power at the point of interconnection of renewable resources using VSC which will finally help the MG to maintain reactive power balance.

### 1.4 Contributions of the Thesis

This thesis handles one of the major problems of a MG which is sharing of reactive power. Many works on this direction has been done using different approaches which are discussed in state of art in detail in chapter two. After going through the state of art it is found that most of

## INTRODUCTION

the work is based on central supervision of the MG using a communication network to perform it. The reactive power sharing problem has been dealt with virtual impedance approach in a lot of research work. There are many works going on worldwide with many voltage control loops used in the controller which makes the system slow which becomes hard to deal with the fast dynamics of the system.

A distributive control of reactive power is implemented in this thesis using the local variables like voltage and current across the VSC terminal. The work is started with the design of a vector controller of the VSC in dq reference frame in order to demonstrate its feasibility. The detail model of the VSC is developed both in time domain and frequency domain. The advantages of using Laplace model is described with operational conditions simulation. The controller designed is verified using different modes of operation of the VSC such as Rectifier consuming power from the grid and as an inverter supplying power to the grid. It is shown that using the dq vector control the active and reactive power can be controlled independently. If a decoupling method is properly done there is only just a mutual coupling for a very short while during the switching period which settles very fast.

Using the controller designed the VSC is used to share the active and reactive power of the synchronous generator controlling the frequency and voltage in open loop. After verifying the controller in open loop control test it is used to share the reactive power of the MG using an algorithm to share the reactive power in case of demand from the load. It is shown with many simulations that the reactive power is contributed within a fast dynamic frame after the load change. There is no communication needed by the VSC as it measures the local variables present across the terminal of the VSC. In this way it calculates the equivalent Thevenin's impedance and contributes according to the change in the load.

### 1.5 Outline and Approach

In order to achieve the objectives of the research laid down in objective & research questions, a systematic approach to identify and investigate the challenges of the MGs in the presence of VSC is adopted. The mathematical modeling of the controller of the VSC is done

## INTRODUCTION

which guarantees the reactive power support and voltage regulation within the limit. The simulations are done in PSIM showing how VSC can support the MG with reactive power support. The outline of the thesis is presented in the following section.

### *Chapter 2*

Chapter two starts with the state of art of the MG development. MGs are presented from the development from Consortium for Electric Reliability Technology Solutions (CERTS), European MG to latest development. The voltage control and frequency control of the MG are also described in detail. Some of the recent work in active and reactive power sharing is described along with their control approaches. The modified voltage control methods adopted recently are presented with detailed circuit diagrams.

### *Chapter 3*

Chapter three describes the modelling of the VSC which is used to control the reactive power in this work. The AC side modelling and the DC side modelling of the VSC are described in detail. The Laplace model is also presented with necessary diagram. The modulation technique and the synchronization techniques used are explained in brief. The vector control used to control the VSC in dq axis is described with circuit diagram. VSC working in both Inverter and Rectifier mode in which it either supplies or consumes power from the grid is described with simulations. The effect of decoupling is described in detail showing the transients while controlling one and the effect on the other which settles quickly. This chapter shows how VSC can be used to control the reactive power in MG.

### *Chapter 4*

This chapter describes the problem related with reactive power sharing in MG with a simulation example in MATLAB. The detail description of the simulation system used (PSIM) is described. The modified power flow equation in MG is explained and the power flow using the VSC is presented. It is shown that VSC can be used to control the power flow in any direction and in any amount using the controller as designed in the chapter three. The VSC along with the controller is very much efficient to supply the load with required active or reactive power demand.

## INTRODUCTION

### *Chapter 5*

Chapter five presents the main outcome of this thesis. It is shown how reactive power can be contributed by the vector control of the VSC using renewable resources to the MG. The controller designed in chapter three is used along with the VSC to control the reactive power flow to the MG. It is shown that by changing the reference of quadrature component of the current the reactive power can be contributed. Similarly, by controlling the direct component of the current the active power can be controlled. The open loop control of voltage and frequency using the controller designed and MG with synchronous generator is shown as an example. A functional block is used which uses a digital algorithm to share the reactive power of the grid and is implemented in the PSIM as an external functional block to control the reactive power supplied to the MG by the VSC. It is shown successfully the contribution of the VSC to supply reactive power when there is load change.

### *Chapter 6*

Finally, chapter six presents the conclusion of the work along with some works suggestion for future. The work which can be further carried forward is presented as a future work.

## 2 MICROGRID AND ITS DEVELOPMENT

This chapter presents the development of MG. The description is presented from the conventional power system to the recently used MG technology. The components of conventional power system as well as the requirements of MGs are described. The development of MGs is presented according to state-of-the-art. The technology used in the MGs and their limitations are presented. The recent technologies applied to solve the challenges of the MG are also presented and discussed. The evolution of the MGs is discussed in detail, from the CERTS, European System approaches to present technology.

### 2.1 Conventional Electrical Power Grids

The first distribution system was established in 1882 by Edison and his company in DC. Finally, the AC system was established in 1885 [10]. The growth of ac systems was further encouraged in 1888 when Nikola Tesla presented a paper in a meeting of the American Institute of Electrical Engineers describing the two-phase induction and synchronous motors, which made evident the advantages of poly-phase versus single-phase systems. The three main stages of the conventional power system are Generation, Transmission, and Distribution as shown in Figure 2.1. The main purpose of the generation of the traditional power system is to generate bulk amount of electrical energy at a place where it is available and suitable to produce at a reasonable price. The purpose of transmission system is to transmit the generated electrical power to the point of consumption. Similarly, the distribution system distributes the transmitted electrical energy to the consumer's point at the suitable form to use.

The generation of electrical energy consists of transforming other forms of energy into electrical energy either ac or dc. The commonly used generators are synchronous generators for the production of electrical energy that are driven by prime movers using steam turbines, hydro turbines and gas turbines. The common fuel of choice for power plants has been coal since early 20th century, while nuclear power plants in the 1960s and natural gas in 1990s were later utilised [11]. The renewable resources are also incorporated in the medium voltage or low voltage level.

The transmission is done by stepping up the voltage level so that it is possible to transfer the electrical energy to a long distance at low losses as the higher voltages leads to lower currents

for the same power rating. The step up of the voltage level is done using transformers. As the amount of power and the distance increases, the level of voltage also increases to maintain the power losses within the limit. The power is then stepped down to suitable voltage level using a step down transformer at the point of use.

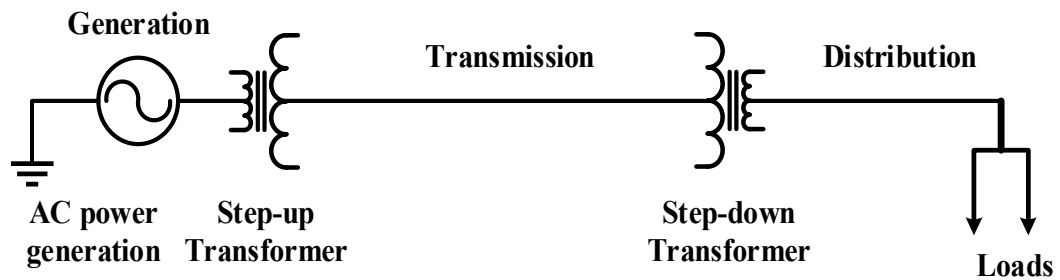


Figure 2.1 Stages of Power System.

The main issue in the conventional power system is to maintain the voltage and frequency within the operating range. It is done by controlling the parameters of the synchronous generator (SG). If the amount of electrical load is suddenly increased keeping the mechanical input to the synchronous generator constant, the synchronous generator releases some energy to compensate by decreasing the speed. The speed is sensed by the governor and the mechanical input to the shaft is increased to maintain the frequency constant. Similarly, to maintain the voltage level constant the excitation system of the synchronous generator plays an important role. If the voltage level goes down to that of the required value, then the excitation current is increased and opposite action is taken if the voltage level increases.

When there is more than one synchronous generator (SG) connected in the system then to ensure a stable operation of the grid a proportional frequency control mechanism is incorporated into the speed governor of each SG. For this mechanism [12], the power command to the prime mover of the synchronous generator is calculated based on a linear droop function of the frequency error, with a negative slope. The negative slope will guarantee a decrease in active power with the increase in frequency and vice versa. This stabilises the operation of the whole grid, and, if all SGs use the same droop function, results in equal sharing of the active power between the different synchronous generators.

### 2.2 Microgrid and its development

The expansion of the electrical power grid has also led the conventional power system to become increasingly vulnerable to cope with the reliability requirements and the diverse demand of power users [13]. The problem of pollution also has led the world to think of alternate ways of electrical energy generation. The advantages of distributed generation (DG) like pollution reduction, high-energy utilization rate, flexible installation location, and low-power transmission losses have made the world to go for distributed renewable energy resources [14].

The development of clean and renewable energy has become an important strategy of economic and socially sustainable development for all the countries in the world [4]. Worldwide policies have been brought forward by different countries to promote renewable energy resources by including feed-in tariffs, renewable portfolio standards, tradable green certificates, investment tax credits and capital subsidies etc. In Europe, the UK is aiming for 15% of its electricity to be generated from renewable energy sources by 2015/16, which represents an increase of around 10% compared to the existing share; Germany, with a more aggressive policy, targets a 25–30% share by 2020, and 50% by 2030 [15]. The European Union (EU) Energy and Climate Package, proposed on March 2010, set out ambitious targets for 2020: a 20% reduction of GhG emissions, 20% reduction in the primary energy used and a 20% increase of RES in the final energy consumption [2].

Similarly, in the US, the state of California has set a target of 33% for the retail load to be served from renewable sources by 2020 [16]–[17]. In Canada, the province of Ontario has an aggressive policy for the promotion of energy conservation and investments in renewable energy sources, as part of an overall climate change action plan; according to the Ontario Green Energy Act (2009) [4], renewable energy sources are granted long-term contracts with predefined feed-in tariffs in order to reduce the risk for investors, and progressively phase out the existing coal-fired generators.

The traditional power system with a central management system is not capable of coping with the challenges posed by the incoming large-scale integration of different distributed generation which is increasing day by day [18]. To overcome this problem there is a need for management system near to the consumer's point. With the advanced metering system added

## MICROGRID AND ITS DEVELOPMENT

to the distribution system, the load can be made more responsive. This entire requirement is making the supply providers go for another interactive, resilient, reliable power system which is MG. MG combines distributed power, load, energy storage devices and control devices, forming a single and controllable power supply system [19]. Europe, North America, and Japan are leading the revolution being faced in the conventional electric power systems operation paradigm, by actively promoting research, development, demonstration, and deployment of MG[20]. Some of the early MGs from these countries are described within CERTS (Consortium for Electric Reliability Technology Solutions) in section 2.2.1 and European Microgrid section 2.2.2. and Shimizu's Microgrid in section 2.2.3.

### 2.2.1 Consortium for Electric Reliability Technology Solutions (CERTS)

The MG concept was originally introduced in the United States by the Department of Energy, who have actively supported considerable work in the area. More specifically, the Consortium for Electric Reliability Technology Solutions (CERTS) was founded in 1999 to research, develop and disseminate new methods, tools, and technologies in order to protect and enhance the reliability of the United States electric power system and the efficiency of competitive electricity markets [21].

The MG defined by CERTS is a micro power system including a cluster of loads, storage and multiple DGs as shown in Figure 2.2 [22]. The main objective of the CERTS was to develop solutions for the technical challenging problems resulting from the Distributed Energy Resources (DER) integration and finally to prove that these sources have the ability to improve the reliability of supply. CERTS developed MG as a single unit which provides power and heat to its customers and meets local reliability. The main three components of MG structure under CERTS include three components [2]:

1. MS Controller or Power Flow Controller: - Micro source controller controls the power flow and the voltage level according to the predefined value. Micro source controller is able to respond quickly to the load changes based on local voltage and current measurement.
2. Energy Manager: - Energy Manager manages the energy use by minimizing energy losses and it is also responsible for satisfying the interconnection requirements.



## MICROGRID AND ITS DEVELOPMENT

3. Protection scheme constituted by protection coordinator and MG separation device which isolates the MG from upstream. The MG control architecture follows a plug and play approach which means that critical control functionalities such as frequency and voltage regulation are provided locally by each MS (Micro Source).

The three components of the CERTS discussed above make it possible for the system to work autonomously. The CERTS appears to the grid as indistinguishable from other currently legitimate customer sites. Maintaining this profile relies on the flexibility of advanced power electronics that control the interface between micro sources and their surrounding AC system [23]. The basic CERTS MG architecture is shown in Figure 2.2, where it represents as a typical LV distribution system with several radial feeders (in these case A, B, and C). The LV side of the distribution transformer is the Point of Common Coupling (PCC) between the MG and the distribution system and it is used to define the boundary between the both systems.

## MICROGRID AND ITS DEVELOPMENT

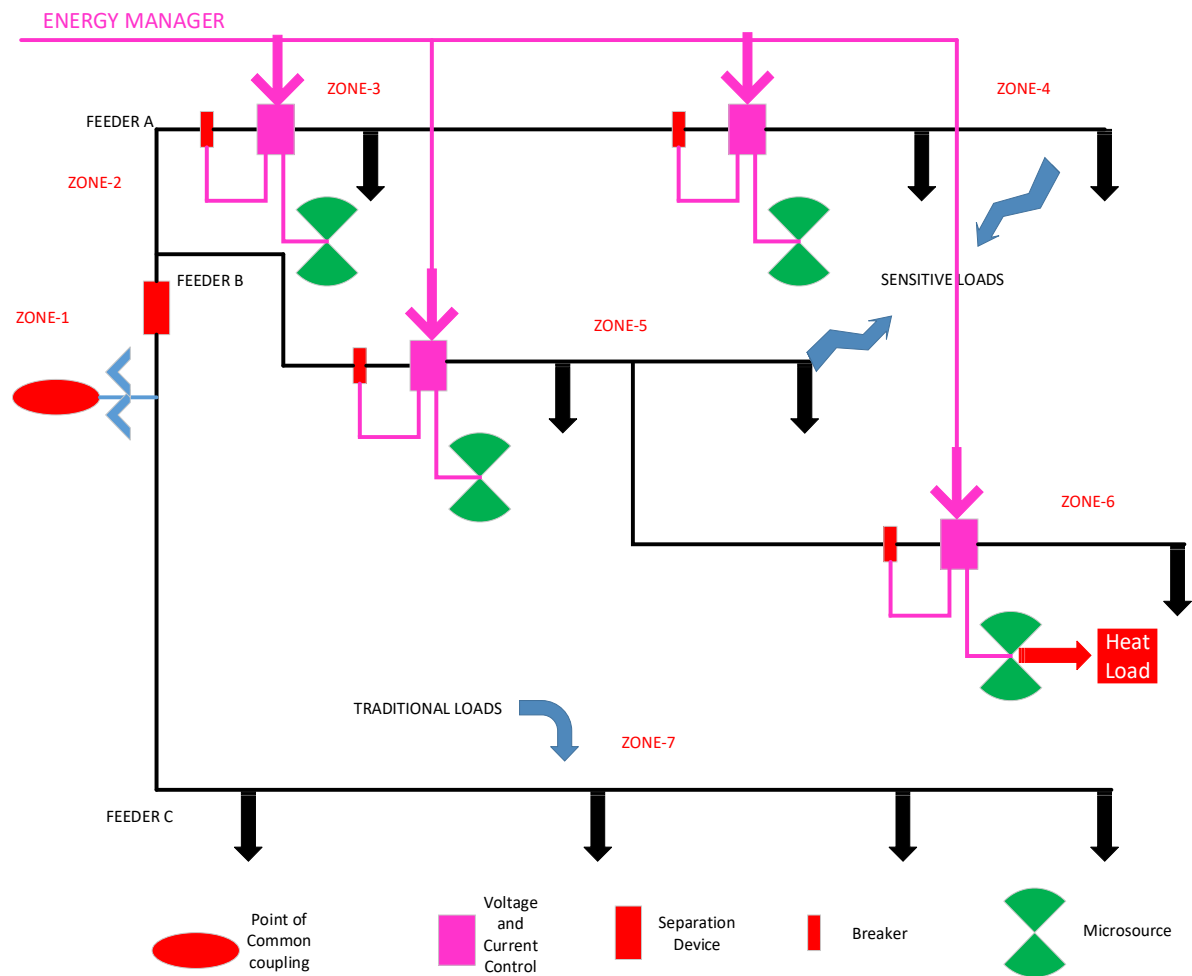


Figure 2.2 CERTS Microgrid Architecture [5].

### 2.2.2 European Concept of Microgrid

Microgrid in Europe is being developed in order to enable the safe integration of large amounts of MS (Micro Source) based on the renewable energy resources. The main focus of the MG and MMG (Multiple Microgrids) is the development of active management strategies for the distribution networks. The common thing in both the CERTS and European concepts is that the MG is dominated by inverters. The reason behind this was the rapid development of power electronic equipment. Compared to electrical machines, the inverters impose additional power quality challenges, requiring the adoption of filters to reduce the emission of high-frequency distortion produced. The major parts of MG as described by Microgrids project (Europe) is as shown in Figure 2.3.

## MICROGRID AND ITS DEVELOPMENT

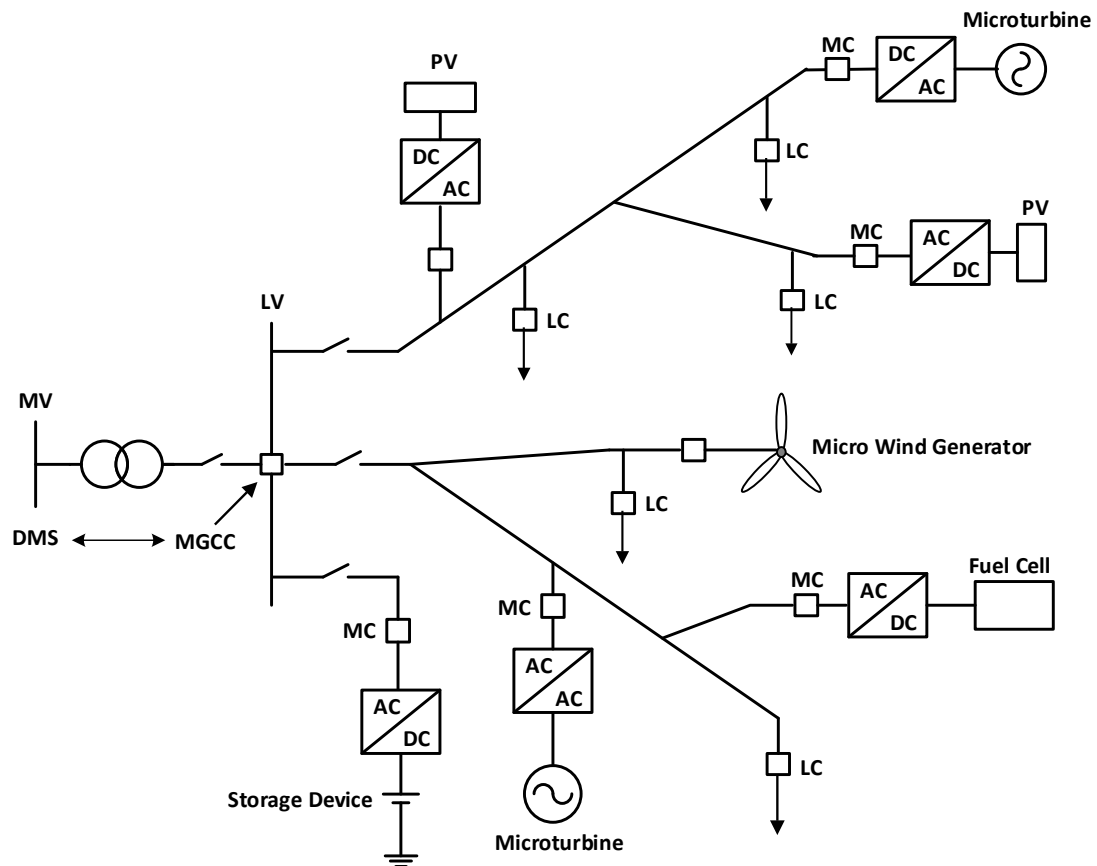


Figure 2.3 MG architecture based on European project MICROGRIDS [1].

As shown in Figure 2.3 the major parts of MG's are MGCC (Microgrid Central Controller), Load Controller (LC), Micro source Controller (MC) and storage. The MGCC is responsible for the monitoring and technical management of the LV (Low Voltage) distribution network and will assess the situation on the lower level and send information to the higher level (upper level) of the microgrid. The MGCC (Microgrid Central Controller) ensures the interface with the higher control layers of the distribution management system (DMS). The MC is responsible for controlling and maintaining the active and reactive power of the system. One of the key elements of MG is storage which makes the system capable of operating in autonomous operation. Storage technologies are characterized by their power capacity, energy storage capacity, response time and cost. The recently added Electric Vehicle (EV) to the distribution system is also rapidly developing as a solution to the storage system. When operating in the islanded mode the MG in European concept will utilize its storage system to supply the load connected to the system. If the storage is insufficient and the MG is in islanded operation, then there will be load shedding

## MICROGRID AND ITS DEVELOPMENT

in certain parts. The other storage units generally used in MG are Battery, Superconducting Magnetic Energy storage, Flywheel, and Super capacitor.

As can be seen from Figure 2.3, there is the dominance of inverters in MG compared to the traditional power system. The majority of the MG components, namely the MS (Micro Source), Storage units and EV (Electric Vehicle) require a power electronic interface. The power electronics interface can be divided into two groups as the input side converter and grid side converter. The input side converter manages the power extracted from the primary source (like solar) being controlled to operate close to the Maximum Power Point Track (MPPT). The grid side inverter controls the active and reactive power flow with the grid, dc link voltage and synchronization between MS and the grid. Similarly, one of the major parts of the MG is the management and control architecture. A strong MG management and control system is required to enable real-time monitoring and control of the resources connected downstream and interacts with external entities namely the Distributed Management System, Markets, and Agents.

Similar to Europe and America the works on MG are also under development in Japan through MGs like Shimizu's MG, Hachinohe project, Kyoto Eco-Energy Project, Aichi Project, and Sendai project[24]. Among MGS mentioned Shimizu's MG is one of the early stage work done which is described in 2.2.3.

### 2.2.3 Shimizu's Microgrid

The Shimizu Corporation has built both a pilot and a larger scale MG at its research labs in Tokyo, Japan. The layout of Shimizu's MG is shown in Figure 2.4. Initially, a small scale MG was constructed to support a company load in laboratories of Shimizu. Besides supplying load to the company it was made a pilot project to study about the different control of the MG. This MG was later upgraded in 2006 by adding two gas engines of 90 kW and 350 kW. There was also storage of 400 kWh NiMh battery and 100 kW ultra-capacitor added to the system. The upgraded version of the MG is shown in Figure 2.4. Many studies were done in this project that which showed that there should be uniformity in the electronic devices otherwise there would be many challenges for the smooth operation of the MG.

## MICROGRID AND ITS DEVELOPMENT

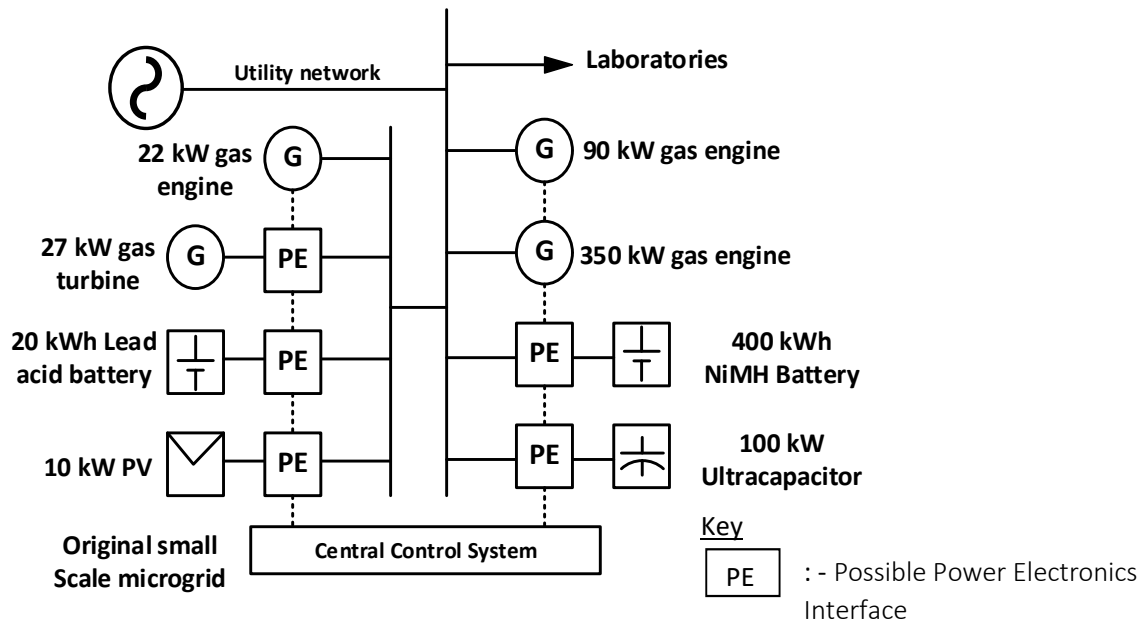


Figure 2.4 Shimizu Extended microgrid [24].

Besides, the MGs discussed above there is a lot of work going on in different parts of the world. Although the development work is rapidly growing in a MG, there are still many challenges to efficiently design, control, and operate MGs when connected to the grid, and also when in islanded mode, where extensive research activities are underway to tackle these issues. Some of the works on technical challenges of MG like control and other issues are discussed in next section.

### 2.3 Control of Microgrid

The control of power, frequency, and voltage in a MG is different from the traditional power distribution system [25]. The power ratings of the sources, loads and the voltage levels are lower in a MG [26]. More importantly, the generation sources in a MG, the distributed generators, are mainly based on the renewable energy resources which have completely different characteristics to conventional power plants. The storage in the MGs puts another dimension to the approach [27]. There has been a great amount of research on the different aspect of the control and protection of MGs. The two common architectures for MGs are centralized and distributed. Standardized procedures and easy implementations are among

advantages of the centralized approach [3]. In the centralized type of control scheme, the central controller makes a decision about the dispatch of all DGs and ESSs (Energy storage systems) according to the objective functions. On the other hand, MGs, where each DG has its own controller-distributed control near the consumer, has great application. The number of transmitted messages between different individual components and the MG controller increases as the size of the MG increases, which requires a large investment and structure for communication. If decentralized control is applied with the proper approach it will reduce the scale of the problem. The problem can be solved making small section sub problems and can be solved locally. The approach of this work is also to apply this distributed approach in which it is expected to use the converter of each grid side to act as a small helping unit to the MG.

The other major challenging part of the MG is the energy balancing of the MG. Unlike the traditional utility system, which is based on the vast majority of generation occurring through rotating machines, MGs have a magnitude of less inertia, especially MGs with high percentages of renewable generation. Thus, control algorithms and demand response may need to operate much more quickly in order to preserve the energy balance and system stability, with an eye on the architecture and interaction [28].

Besides the above challenges, the most common other problem is less inertia in renewable generation. In most of the distributed generation there are no synchronous machines to balance demand and supply, through its frequency control scheme, so in this case, the inverters should also be responsible for frequency control during an islanded operation. In addition, a voltage regulation strategy is required; otherwise, the MG might experience voltage and/or reactive power oscillations of power [29]. The primary control applied in distributed generation stabilizes frequency and voltage using droop controllers, whereas secondary control compensates for the steady-state deviations in voltage and frequency caused by the primary control, and tertiary control that takes into account the economic considerations and determines power flow between the MG and utility grid to achieve the optimal operation [3]. The section 2.3.1 and 2.3.2 describes the frequency and voltage control applied in the MGs respectively.

### 2.3.1 Frequency Control

## MICROGRID AND ITS DEVELOPMENT

Frequency is one of the key indexes for the stable operation and good control of MG. It is relatively easy to control frequency rather than voltage as the frequency is a global variable whereas voltage is a local variable [30]. Since frequency is one of the key indexes to stable operation of the power grid, and operation characteristics of the distribution generators are totally different from the operating principle of the synchronous generator, therefore, the frequency is one of the important topics for research in MG [30]-[31]. Controlling the frequency, the active power can be shared among the available DG sources can be done in proper ratio if proper decoupling is done.

Many works are being carried out worldwide on frequency control using different approaches. Traditionally the frequency deviations can be limited by introducing the frequency droop characteristic that uses the MG frequency as a communication means, among the fast acting DG units, to dynamically balance the real power generation of the islanded MG[32]. During the grid-connected mode, where the frequency of the system is fixed, real power generation of the DG units is controlled by the real power references assigned to the units [33]. The frequency droop equation is shown in equation (1) and the drooping figure is given in Figure 2.5 [34], [1].

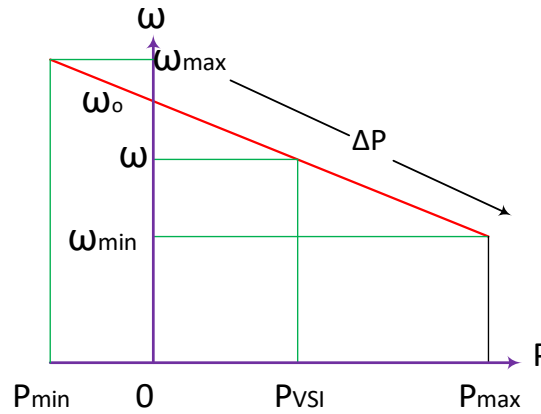


Figure 2.5 Active power frequency droop [1].

As shown in Figure 2.5 active power is proportional to frequency and it is an approach to mimic the behavior of the synchronous machine. Conventional droop control was preferred over the alternative strategies because it was found very effective active power sharing between more than one VSI connected to the system, and by only measuring frequency it was possible to share the loads between VSI's [1]. The equation generally used for the frequency droop control can be written as below.

$$\omega = \omega_0 - k_p P \quad (1)$$

The equation 1 shows the relation between the frequency and active power. A modified approach in which frequency can be controlled using the multi-agent co-operative control system dynamic energy level balancing between distributed storage devices as shown in Figure 2.6. This cooperative control method provides secondary frequency control, restoring the MG to the reference frequency. In this work, it is shown that the co-operative control system improves frequency regulation compared to traditional droop control strategies, when the storage device begins at different energy levels and the MG experiences generation or demand variability. A distributed cooperative control structure utilizing neighbor to neighbor communication is used to achieve a balanced energy level among the BESS (Battery Energy Storage System) to make full use of their power capacities. The block diagram used for cooperative frequency regulation is shown in Figure 2.6 [35]. As shown in Figure 2.6 it has 1. Battery 2. Voltage source inverter 3. LC output filters 4. Grid connection impedance and the inverter control system. The control system consists of the power controller, voltage controller, the current controller and a co-operative controller.

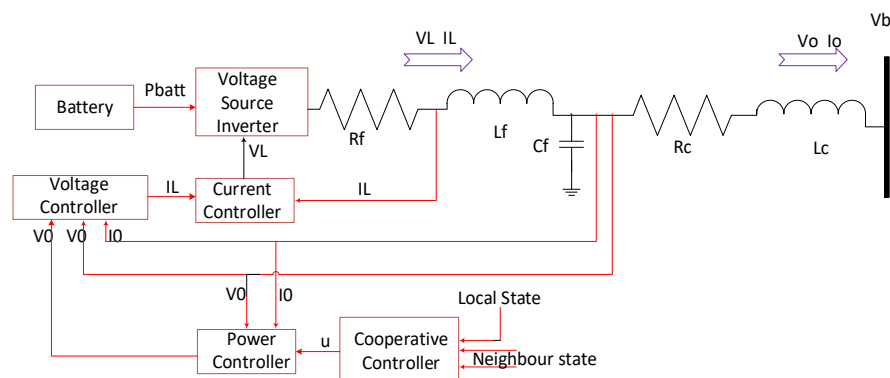


Figure 2.6 Droop controlled BESS with cooperative control [35].

The co-operative controller is designed based on co-operative state variable feedback control, assuming each BESS has access to its full state and the states of its neighbor. Finally, the dynamic energy level balancing between storage devices is applied to improve the frequency regulation over traditional and energy weighted droop approach. The co-operative control applied in this work gives system stability and allows the speed of energy convergence to make



balanced energy level. Moreover, a control input saturation constraint has been developed which ensures that the storage devices of the MG are not overloaded.

Frequency in MG can also be controlled using secondary control approach [29]. In this approach, the storage system will act according to the final value of the frequency and accordingly either supply or consume energy from the grid. Distributed control of frequency control is also done using distributed averaging proportional integrator (DAPI)[34]. These proposed controllers use the sparse communication between the neighbor and decentralized control action to maintain the frequency within the limit [36]. There is a lot of other research work on frequency control which is discussed in general section. The section 2.3.2 below discusses voltage control and power sharing.

### 2.3.2 Voltage Control and Power Sharing

In high voltage, traditional network voltage control and power sharing is not a problem due to capacitive compensation of both loads and transmission line [34]. Voltages are regulated by the excitation system of the synchronous generators in the traditional system. Synchronous generators exhibit a self-stabilizing feature due to their high rotational inertia [9]. In the case of a microgrid, the scenario is different from small DG sources, less distance between sources and resistive lines connecting them. So a proper load sharing mechanism is required in a microgrid to prevent overloading of the sources and to control the voltages of the renewable source terminal. Most of the generation units integrated into the MG are not of the synchronous generator type and thus MG needs to somehow mimic the droop characteristic existing in those generators to control the voltage as was discussed in frequency control above. In this section how the voltage control and power-sharing are done in a microgrid are discussed briefly.

Voltage and Reactive Power Control in MV Networks integrating a MG is done considering the minimization of loss as the main objective function in [37]. The work done in this reference is considering the MG is interconnected with MV network and it is assumed that the required active power is exchanged with the network according to requirement. The main objective function of this work is to reduce the losses maintaining the sharing of reactive power within limits among all the sources. The objective function and the constraints are given below.

## MICROGRID AND ITS DEVELOPMENT

$$\text{Min } OF = P_{loss}$$

Subjected to

$$\begin{aligned} V_i^{\min} &\leq V_i \leq V_i^{\max} \\ S_{ik}^{\min} &\leq S_{ik} \leq S_{ik}^{\max} \\ t_i^{\min} &\leq t_i \leq t_i^{\max} \\ Q_i^{\min} &\leq Q_i \leq Q_i^{\max} \end{aligned}$$

Where:

OF is Objective Function X

Ploss – Active Power Losses

$V_i$  – Voltage at Bus  $i$ ,  $V_i^{\min}$ ,  $V_i^{\max}$  – Minimum and Maximum voltage at bus  $i$

$S_{ik}$  – Power Flow in Branch  $ik$ ,  $S_{ik}^{\min}$ ,  $S_{ik}^{\max}$  – Minimum and maximum power flow in branch  $ik$

$t_i$  – Transformer tap of or capacitor step position,  $t_i^{\min}$ ,  $t_i^{\max}$  – Minimum and maximum tap

The algorithm is solved using an EPSO technique and the reactive power is shared among five DG sources. Along with other constraints voltage is also maintained within range and loss reduction of 3.38% achieved during the peak hour and reduction of 39.13 % during Valley hour. An EPSO approach was adopted in order to deal with the voltage/VAR control problem at the MV level and the algorithm has proved to be efficient in order to achieve the main objective function.

DG control and reactive power management strategies can be applied using the local measurements without using communication system. The reactive power problem is solved by applying conventional droop ( shown in Figure 2.7) characteristics in [33]. In conventional droop control, it is assumed that the line is inductive as a traditional power system. So the active power is controlled by P-F droop equation and the reactive power is controlled by Q-V droop equation. The active and reactive power management is described in this reference using d-q axis control. The d axis controls the active power management and the q axis controls the reactive power of the MG. As shown in figure 6, following are the three strategies defined in which the reactive power of DG unit is controlled [8].

1. Prevent deviations in terminal voltages using a preset V-Q characteristic.
2. Achieve voltage regulation at a specific load-bus.

## MICROGRID AND ITS DEVELOPMENT

3. Compensate reactive power demand of a load based on the power factor set-point of the load.

Strategy 1 can be applied using voltage droop characteristics. Figure 2.8 shows a reactive power control strategy based on a voltage droop characteristic. The input to the block is the r.m.s voltage at the point of common coupling of the distribution generator. As shown in the figure below the PI controller specifies the q axis current set point to adjust the reactive power of the distribution generator. Finally, the electronic interfaced distributed generator reacts to the q-axis current and adjusts the reactive power according to the voltage.

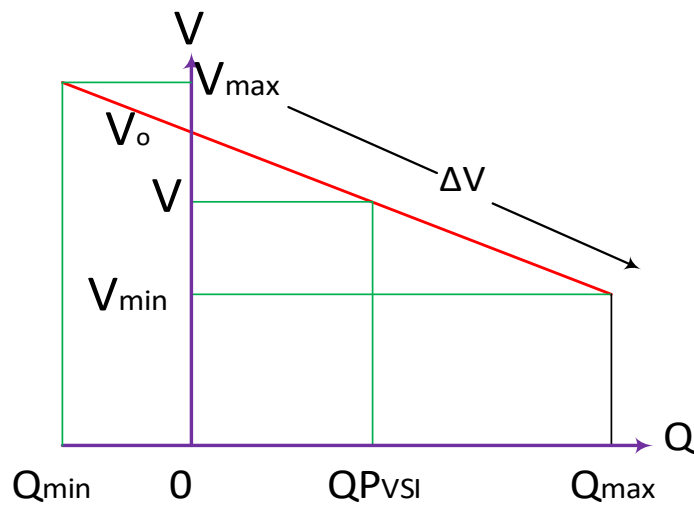


Figure 2.7 Reactive Power-Voltage droop [1].

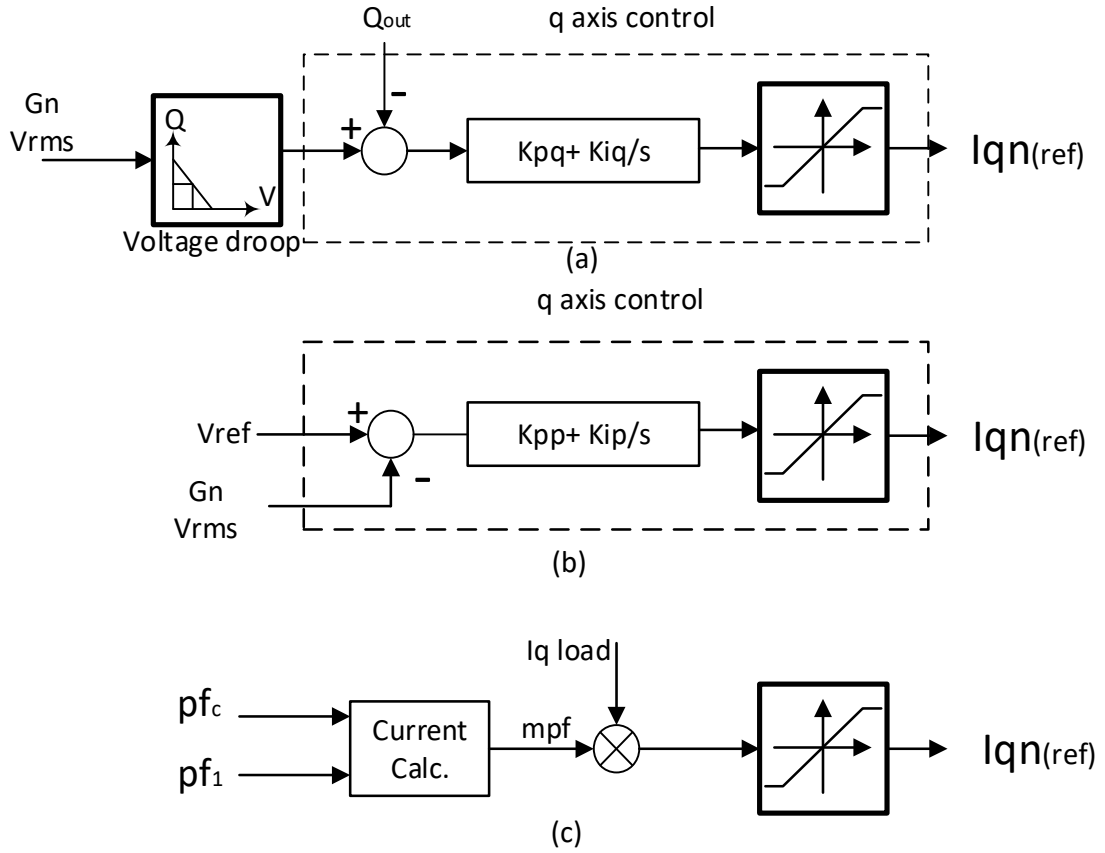


Figure 2.8 Three strategies to control reactive power flow.

In Strategy 2, the reactive power of the DG unit is controlled to regulate the PCC (Point of Common Coupling) voltage at a pre-specified level. Thus, this control strategy can be considered as a special case of voltage droop characteristic, where the tangent of the V-Q characteristic is set to zero and implicitly specifies reactive power reference of the unit. In this approach, a reference current is generated from deviations in reference RMS voltage, through a PI controller. Similarly, in strategy 3, the power factor is improved to meet reactive power requirements of a load through a fast reactive power variation characteristic. This control strategy is adopted for the MG system to locally compensate reactive power of a load by a DG unit connected to the load bus. Thus, the load power factor is assigned at a pre-set value regardless of the load variations. So this is one of the strategies used in voltage control.

### 2.3.3 Modified Voltage Control and Power Sharing

The methods discussed in section 2.3.2 are voltage controlled used in the initial stage of the MG. This approach is reliable as it has plug and play approach. It can avoid high cost, complexity, and requirement of a supervisory control. On the other hand, it has certain disadvantages which can be written point wise as below [2]-[7].

1. In case of steeper droop, the voltage and frequency changes are larger which causes more deviations and may cause instabilities in the MG.
2. The power-sharing is affected by the line impedance between the parallel inverters.
3. The performance of conventional droop is poor with renewable energy resources due to the changing nature of active output power of these sources.

Some of the recent research work in recent time to overcome these drawbacks is described in this section. The conventional droop control used above assumes that the line is inductive as a traditional line. The active and reactive power injected by every unit is given by

$$P = \left( \frac{EV}{Z} \cos\phi - \frac{V^2}{Z} \right) \cos\theta + \frac{EV}{Z} \sin\phi \sin\theta \dots\dots\dots (2)$$

$$Q = \left( \frac{EV}{Z} \cos\phi - \frac{V^2}{Z} \right) \sin\theta - \frac{EV}{Z} \sin\phi \cos\theta \dots\dots\dots (3)$$

Where E is the amplitude of the inverter output voltage, V is the common bus voltage,  $\phi$  is the power angle, and Z and  $\theta$  are the magnitude and the phase of the output impedance, respectively. In the case of a MG, the lines are assumed to be resistive in comparison to the inductive lines of the traditional transmission lines. So if the lines are assumed resistive the active power becomes directly proportional to V and the reactive power with phase angle  $\phi$ .

So the traditional V-Q and P-F droop does not work well in the MG. There are some modifications in the traditional loop in many works done. A novel wireless load-sharing controller for islanding parallel inverters in an AC distributed system is proposed in [38]. In contrast to the conventional droop mentioned above the proposed controller uses resistive output impedance. The modified power equations for the MG assuming  $Z \approx R$  can be written as below[38].

$$P = \frac{EV}{R} \cos\phi - \frac{V^2}{R} \dots\dots\dots (4)$$

$$Q = -\frac{EV}{R} \sin\phi \dots\dots\dots (5)$$

Practically angle  $\phi$  is very small so  $\cos\phi \approx 1$  and  $\sin\phi \approx 0$  can be assumed and the above equations can be modified as below [38].

$$P \approx \frac{V}{R} (E - V) \dots\dots\dots (6)$$

$$Q \approx -\frac{EV}{R} \cdot \phi \dots\dots\dots (7)$$

The above equations show that the active power can be controlled by the inverter voltage  $E$  and the reactive power can be controlled by angle  $\phi$ . Considering the above equations a controller is designed which consists of three loops. (Figure 2.9). 1) The inner output voltage regulation control loop, 2) The resistive output impedance loop and the 3) P/Q sharing outer loop. The circuit used for this controller including the above three control loops is shown in Figure 2.9 [38]. The control loops in the following work are designed taking into account the special nature of low voltage MG. A power-sharing approach without much intercommunication dynamical action is proposed in this work.

The controller designed is implemented by using a digital signal processor board, which only uses local measurements of the unit. This method of using the local measurements helps to make the approach more reliable, which is independent from the communication system action. Finally, this approach increases the modularity, reliability, and flexibility of the distributed system. Some experiments were conducted using two 6-kVA inverters which were connected in parallel whose expected results proofs the successful implementation of the idea.

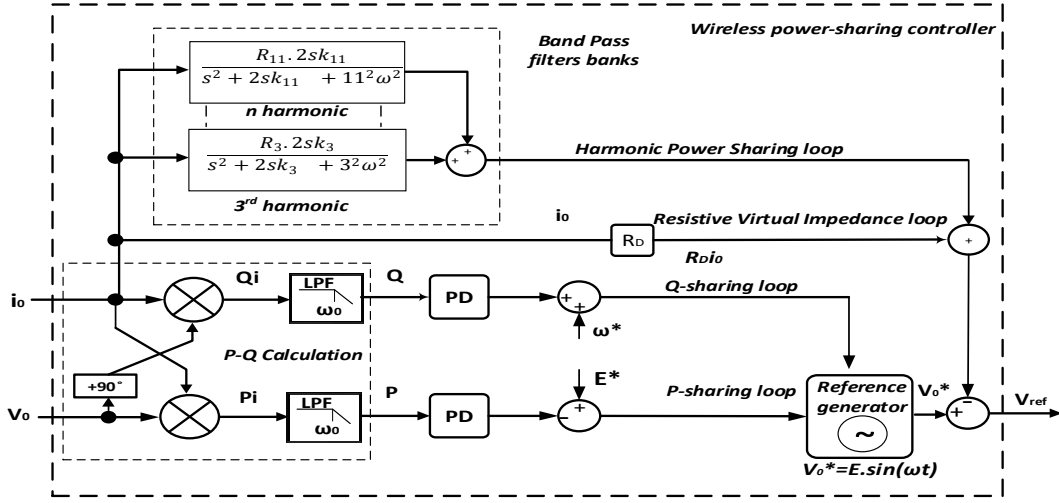


Figure 2.9 P/Q sharing loops.

As shown in Figure 2.9 there are three loops for P/Q sharing, Resistive virtual impedance loop and output voltage control loop which automatically controls harmonics. A novel reactive power sharing algorithm can be developed considering the instantaneous active power and apparent power [39]. A proportional reactive power sharing algorithm is developed in this reference by considering the instantaneous active power and the nominal reactive power by using the formula given below.

$$Q_{max} = \sqrt{S_n^2 - P^2} \dots\dots\dots (8)$$

Where  $Q_{max}$  the maximum possible reactive power of the converter,  $S_n$  is the nominal power and  $P$  is the instantaneous active power of the converter. If there are many converters connected in the system and the power is balanced, then the vector sum of the total apparent powers of the converter is equal to the total apparent power of the load irrespective of the power control strategy used. The algorithm is used to share the reactive power among three DG through power electronic converters. Though this algorithm gives a good control on sharing of reactive power it may be difficult to work for a system if there is more number of DG's.

The Figure 2.10 shows the circuit diagram of a methodology in which the voltage and reactive power sharing is controlled and improved using secondary voltage control [40].

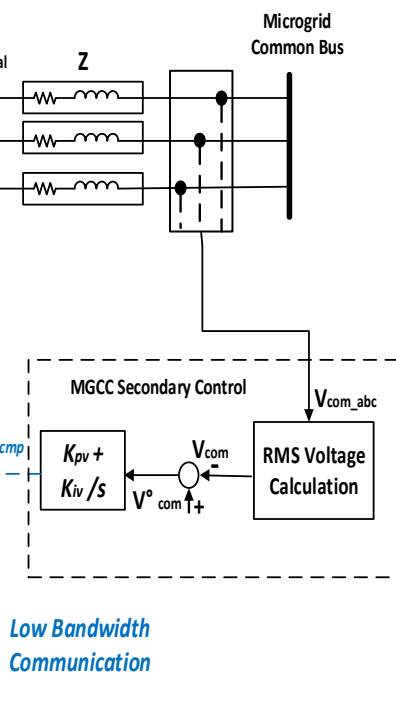


Figure 2.10 Reactive power sharing strategy based on secondary voltage control [15].

As shown in the Figure 2.10 voltage compensation signal  $E_{cmp}$  is generated from a PI controller which is given by the equation below. A slow proportional–integral (PI) controller will eliminate the voltage amplitude error and produce the amplitude restoration compensation signal  $E_{cmp}$ .

$$E_{cmp} = K_{pv}(V_{com}^* - V_{com}) + K_{iv} \int (V_{com}^* - V_{com}) dt \text{-----} (9)$$

Where  $K_{pv}$  and  $K_{iv}$  are the PI controller parameters of the secondary control voltage,  $E_{cmp}$  is the voltage compensation signal provided by the secondary voltage controller.

This is a modified approach to control the reactive power sharing using a secondary controller. In this method, only one-way communication is sufficient in which it is necessary to update each DG sources with the new value of the  $E_{cmp}$ . The microgrid common bus voltage  $V_{com}$  is maintained constant by using the signal  $E_{cmp}$ . In this way, the reactive power is maintained according to the demand without the necessity to know the parameters of the line. In contrast to the earlier version of the central communication approach here, the communication between the DG's and the communication between the MGCC and the DG's are no longer required. In this way, the communication system no longer remains busy.



The methods discussed above are some of the recent works done worldwide regarding voltage control and reactive power sharing in the MG. The works done in this field are mostly based on a central control method having MGCC as the heart of the control system. The method proposed in this thesis is a distributed control approach in which the voltage and the reactive power will be controlled using the local measurement of the voltage across the VSC terminal.

### 2.4 Control of Microgrid with innovative approaches

During evolution of the concept, the need of changing the paradigm was more perceptible due to the connection of large amounts of DG sources to Medium Voltage (MV) distribution networks. However, recent technological developments are contributing to the maturation of some DG technologies, such that they are becoming suitable to be connected to Low Voltage (LV) distribution grids. Regarding a scenario characterized by a massive integration of DG in the network, several technical issues need to be tackled. Apart from the control schemes discussed in section 2.3, there are a lot of studies done in the development of MGs around the world.

Although the components of the MGs are quite different from the traditional power system, the requirements from both the systems are quite similar i.e. Voltage regulation and Frequency. Similar to conventional distribution system here also the expectation from the consumer is to get supply at rated voltage and frequency and of course continuously. To obtain these objectives different innovative approaches are adopted in different research works. To supply continuous and reliable supply the DGs of the MGs should share the active and reactive power among themselves both in interconnected or islanded situation. If equal power sharing can be granted it reduces the chances of power mismatch [41]-[42].

The two important features of MGs described in [43] are peer to peer and plug and play features. The peer to peer features means every DGs of the MG has the capability to share the load if any one of the DG fails to supply. It will help the MG to maintain the continuous supply even in the case of any DG failure. Similarly, the plug and play features make the MG capable of adjusting any DG newly added to the system. Plug and play feature enables to add any new DG

## MICROGRID AND ITS DEVELOPMENT

in the system and forget. That is to say, any DG unit can be added to the MG and start operation without concerning the other DG.

In many kinds of literature, it is tried to establish a general control scheme which is called Hierarchical control structure[44]. In this approach, all the control of the MGs from the basic control of DGs to communications control with the MGCC has been classified into three categories. i) Level 0 control ii) Primary level control iii) Secondary level control and iv) Tertiary Control. In Level 0 control the output of the DGs is controlled by taking the reference from the higher level. If the MG is interconnected with the grids the DGs get the current reference and it gets the voltage reference if it is in islanded mode. The primary level control provides either the current reference or the voltage reference to the DGs by calculating it taking the required power flow as a reference. The secondary level of control uses certain algorithms to maintain the regulated voltage, frequency, and current if level 0 and primary level fails to maintain these values within the limit. Tertiary control is to maintain any special requirement if any of the MG like special power flow pattern, any special support to the grid is necessary.

One of the other fields in which a lot of research work has been done is the droop control in MGs. The frequency- active power and voltage- reactive power droop has been used in many works in which it is tried to mimic the characteristic of a synchronous generator in the conventional power system. When there is a considerable amount of load decreases in MG or higher generation from DGs then it is required to go for hard load curtailment which brings ON-OFF oscillations[45]. In the reference [45] the voltage droop which was originally developed for power sharing is used to soft curtailment to avoid the oscillations. The droop control is combined with PQ control to generate new references and control the MG in reference [46]. Weak droop control equations with a small power- dependent variation are used for generating the reference signal for PQ control after islanding has occurred. It is shown that the droop control along with PQ control can be used both for islanded and interconnected MGs. Three phase P/Q droop is used in [47] where the inverters are of unequal power ratings and the loads are nonlinear and unbalanced in nature.

The drooping of the virtual flux is done instead of the inverter output voltage in [48]. At first, the mathematical relation between flux and power (active and reactive) is developed and

## MICROGRID AND ITS DEVELOPMENT

then the droop slope between flux and power is used instead of the output voltage. [49] shows that adding derivative and integral gains to the conventional proportional droop function can increase the stability and dynamics of the power sharing. In [49] it is tried to use the droop slope without communication between DGs though the loops become slow to interact. The reactive power sharing is improved in [50]. The problem of power sharing due to line impedance is addressed in [50] by improving the conventional droop equation. A control strategy based on virtual resistance and phase locked loop is used in [51]. The drawbacks of conventional droop like the slow response have been tried to improve.

A triple droop control scheme for power management is presented in [52]. The first level is based on conventional P/f and Q/V droop. The second droop scheme regulates the output power of the micro source in response to the DC bus voltage, and the third level adjusts the output parameters for the first level to select between constant  $P_{dc}$ , constant  $V_{dc}$ , or  $P_{dc}$  sharing. [53] puts forward an idea to improve the conventional droop equation by estimating the reactive power sharing errors of DG units through injecting small real power disturbances. The problem of inaccurate power sharing has been improved using the central communication system MGCC in [54]. It presents a MG control strategy based on a combination of droop control and centralized control. Droop control for the highly resistive line for rural area( resistive line) is presented in [55]. The first method considers no communication among the distributed generators (DGs) and regulates the converter output voltage and angle ensuring proper sharing of the load in a system having strong coupling between real and reactive power due to high line resistance. The second method, based on a smattering of communication, modifies the reference output voltage angle of the DGs depending on the active and reactive power flow in the lines connected to point of common coupling (PCC). The communication system improves the performance of load sharing. Most of the references mentioned till now seem to be different at a first glance but basically, they all are using the controlled voltage loop to share active and reactive power.

This section describes the research work done in the hierarchical control scheme. In order to structurally organize the different control loops, the hierarchical control scheme is used in many research studies. A hierarchical control structure is presented [56] in which, firstly, smart MGs deal with local issues in a primary and secondary control. Secondly, these MGs are

## MICROGRID AND ITS DEVELOPMENT

aggregated in a virtual power plant that enables the tertiary control. The dc control system is used for enhancing the economics and the resilient operation of a dc MG in [57]. The proposed hierarchical control strategy that applies to a dc MG improves the DC MG using V/I droop and MPPT [57]. A supplementary control loop is added in [58] to improve the stability of the system when using high angle droop in case of the weak system. The hierarchical control of three stages is proposed in [44]. The three hierarchical stages are 1) The primary control is based on the droop method, including an output-impedance virtual loop; 2) the secondary control allows the restoration of the deviations produced by the primary control, and 3) the tertiary control manages the power flow between the MG and the external electrical distribution system.

The works undergoing in research world other than droop control and hierarchical level in MG are virtual impedance. The assumptions in droop control discussed in above section assume the impedance of the lines inductive as the droop in a conventional generation through the synchronous generator. In reality, the case is different in MG where the lines are highly resistive so it is not correct to neglect the resistance and assuming the lines to be inductive. The research works conducted to handle this problem are discussed in this section. The main problem with the complex impedance is the coupling between active and reactive power which makes the droop theory less applicable. To handle this problem in most of the research, work the virtual impedance is taken into consideration. [59] presents an approach with P/f and Q/V droop, while regulating the DG unit interfacing virtual impedance at fundamental and harmonic frequencies. The virtual resistance is modified (in [60]) in the droop controllers in accordance with the state in charge of each energy storage unit. The virtual resistance in [60] is adjusted to reduce the voltage deviation at the common dc bus. The investigation of the characteristics of the active and reactive power sharing in a parallel inverters system under different system impedance conditions is carried out in [61]. Instead of pure inductive or resistive loop intentional complex loop is considered in [61].

The resistive nature of low voltage lines in MG is neutralized by connecting virtual inductance at the interfacing inverter output in [62]. It is shown that the virtual inductance can effectively prevent the coupling between the real and reactive powers by introducing predominantly inductive impedance even in a low- voltage network with resistive line

impedances. A transform matrix where only the knowledge of ratio of resistance and inductance of the lines are used to modify the power sharing in [3]. Each inverter supplies a current that is the result of the voltage difference between a reference ac voltage source and the grid voltage across virtual complex impedance.

Many works are done in the storage of the MGs. The necessity of storage system and the operation of MG in islanded mode is described in [29]. It evaluates the performance of different control strategies such as  $P/f - Q/V$  droop and master slave controllers with storage systems and load shedding strategies in an islanding process of a medium voltage MG. In [63] a control strategy for a converter that interlinks AC and DC NGs is presented which is made possible with energy storage systems. A lot of research work has been done in which the renewable with MPPT are incorporated in MG. During load change (increase) the frequency is maintained constant by using a boost converter to get a partial power from solar panel's maximum power point [64]. During an increase in load, the boost converter tracks closer to the PV panel's maximum power point, to output more power in order to keep the frequency in the desired value. [65] proposes a control scheme in which the converters connected in wind and PV sources generates active current according to the output of the MPPT.

Smooth transition from interconnected mode to islanded mode is also a challenge for MGs. Many research works have been done in this area also. MGs are generally operated in current control mode while interconnected with the grid and in voltage control mode while operated in islanded condition [66]. The unified controller is used in [67] which can be used both for interconnected and islanded mode. So there is no need to change the mode of control as it was necessary for [66]. Although it was necessary to incorporate synchronization algorithms which make the implementation complicated. In both the cases, the MG must always resynchronise to the utility grid before reconnecting back to the grid once the grid disturbance is cleared [68]. The study of the dynamic response on planned and unplanned switching is studied in [69]. It also presents a control strategy with doubly fed induction generator, a synchronous generator, and a voltage source inverter. An algorithm is used which detects the islanding operation and changes the control approach.

## MICROGRID AND ITS DEVELOPMENT

The control approach for the output of a VSI based DG unit is not uniform across the literature. In [70] the control strategy, used with each distributed generation system in the MG is developed so as to combine the advantages of the current control and the voltage control strategies. In other words, the combination of voltage control and current control are used as a control strategy for this work. In the island mode of operation of the MG, it has to supply the full local load demand without the grid support and it has to maintain the voltage itself. P+ multiple resonant controllers instead of PI controller is used in reference [71] to solve the issues of distorted voltage in case of an unbalanced load. An analytical method to determine the best possible gains that can be achieved for any class of practical linear ac current controller is presented in [72]. The optimum gains for PI and PR current regulators in grid-connected VSIs is also calculated in [72]. The voltage control strategies for current regulated PWM inverters are studied and a decoupling feedback control strategy is presented in [73], which eliminates the steady state error.

Synchronous generators are a very important component of the traditional power system in terms of stability. It can provide some amount of power to instantaneous load demand surges at the expense of losing their angular momentum. The absence of synchronous generator in DG is tried to fulfil in many research by mimicking the behaviour of the synchronous generator. In this way, governor and swing equations are virtually implemented on the VSI to give it an inertial behaviour. In [74] the comparison is made by developing small signal analysis between the virtual synchronous generator (VSG) and droop equations method applied in MG. These two methods are used to mimic the behaviour of a synchronous generator in grid connected or islanded inverters. The use of inverters mimicking the behaviour of a synchronous generator is further studied as synchro converters in [75]. It is shown that the active and reactive power delivered by synchro converters connected in parallel and operated as generators can be automatically shared using the well-known frequency- and voltage-drooping mechanisms.

### 2.5 Conclusion

This chapter presents the approaches, development and different work going on in the field of MG as the development of MG, Control of MG and innovative control approach of the MG. Most of the work around the world is on droop control of the MG. Many modifications and improvements are done in the droop control method developed in the initial stage to mimic the behaviour of SG. Many modified droop control methods are presented for the special cases. The other field which has drawn the interest of researchers is the problem of solving the resistive nature of the MG lines which are different from the traditional power system. Many works have been observed to reduce the harmonics content which is introduced due to the power electronics component of the MGs.

Although a lot of works are being carried out still there are many challenges to be solved in MGs. The complex impedance of MG line in comparison to the inductive line of traditional power system still is a problem in estimating the power sharing. The voltage loops used are not fast enough in responding as it is required. There are many complicated control structures being applied in many works. The absence of inertia in DGs has not yet been solved though a partial solution is done by mimicking the behaviour of the synchronous generator. The reactive power sharing is also still a problem as the complex impedance of the MG lines does not allow using the traditional approach of power flow. All these unsolved issues will be discussed in coming chapters and the reactive power problem will be handled in this thesis work.




### 3 VOLTAGE SOURCE CONVERTER AND ITS CONTROL

A MG is a very fast developing power system, mainly due to high local power generation, with renewable power sources. The interaction of these power sources with the MG is based on electronic power conversion. So the operation of the power converters typically voltage source converters is critical when one evaluates the power quality as a key element within a MG. VSC permits to implement advanced control solutions to enhance the operation of the electrical system in a MG [76]. This chapter discusses the Voltage Source Converters (VSC) modelling, modulation techniques, synchronization with the grid, and power flow with the developed control technique.

#### 3.1 Voltage Source Converter Modeling

VSC is used in MGs to integrate the distributed renewable energy sources and using VSC helps not only to integrate the renewable resources but provide system functions such as real and reactive power contribution according to the requirements of the grid. VSCs, also known as a PWM Rectifiers/Inverters, are widely used bi-directional power electronics converters [77]. In these converters active and reactive power may be independently defined, i.e. the Power Factor may be controlled, and thus they may behave as a balanced resistive load to the grid -Unity Power Factor (UPF). They have a very good dynamic response showing a good robustness to disturbances from load parameters. They guarantee almost sinusoidal line currents as well as a high-quality voltage in the DC-side [1].

VSCs are popular in interfacing renewable resources like wind and solar to MG. They are also useful in high-power, high-performance applications, not only in a renewable generation but also in the automotive industry, where pure electric and hybrid vehicles require high performance drives to respond to frequent accelerations, decelerations, and braking. Recently they have been used also in high-voltage direct current (HVDC) electric power transmission system. They are connected in three modes while interfacing with the MG [78].

-  Grid-feeding VSC
-  Grid Forming VSC
-  Grid Supporting VSC



## VOLTAGE SOURCE CONVERTER AND ITS CONTROL

Grid-feeding VSC is controlled through an active and reactive (PQ) control strategy. The VSC is a current-controlled voltage source, designed to deliver a controlled amount of power (active and reactive) to the grid. In some literature, they are also referred as Grid tied converters. The Grid feeding converters do not have the ability to impose voltage and frequency. In the grid feeding configuration of Figure 3.1, the power source injects power to the electrical grid, regardless of the electrical demand and regardless of the operation mode of the MG. Generally, the grid feeding converters are connected in such a scheme that they extract maximum power from the source like wind, PV etc.

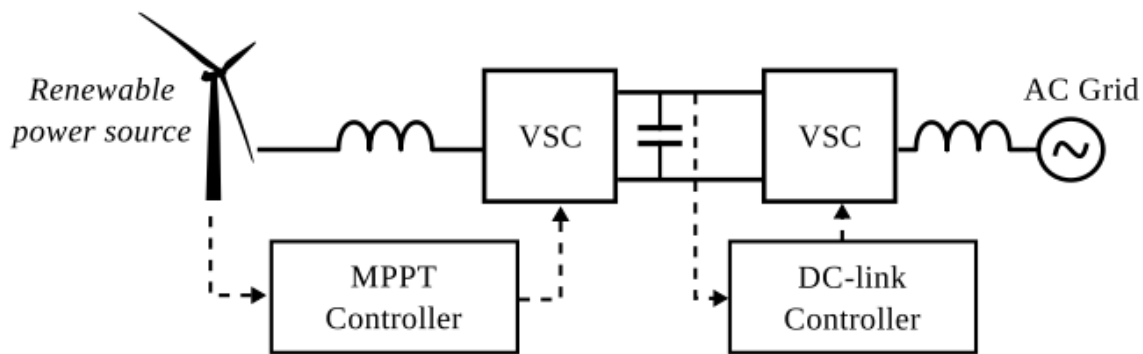


Figure 3.1 Grid feeding power source with the grid side converter controlling grid voltage [76].

Grid Forming VSC is controlled as voltage sources establishing the phase angle and magnitude of its output voltage. The VSC is usually fed by a DC power source with energy buffering capabilities, as it is the case of batteries. It can also incorporate grid supporting functionalities for voltage and frequency regulation. They are used to set the voltage and frequency in case of islanded operation of the MG. When a grid forming power source, such as the one in Figure 3.2, is connected to the grid, it can be arbitrarily commanded to exchange active and reactive power. In the islanded mode, all grid forming DG units will exchange the required amount of active and reactive power to guarantee the electrical stability of the islanded MG [76].

## VOLTAGE SOURCE CONVERTER AND ITS CONTROL

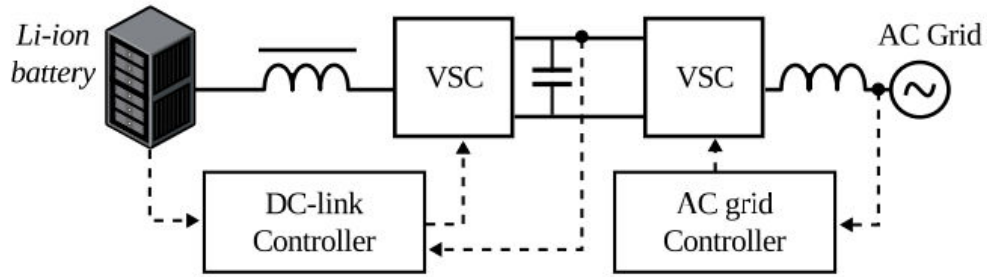


Figure 3.2 Grid forming power source with the grid side converter controlling grid voltage [76].

Grid-Supporting VSC can be represented either as an ideal ac-controlled current source in parallel with a shunt impedance or as an ideal ac voltage source in series with a link impedance, as shown in Figure 3.3. These converters regulate their output current/voltage to keep the value of the grid frequency and voltage amplitude close to the rated value [79]. The Figure 3.3 shows grid supporting VSC among which one is current source based and other is voltage source based.

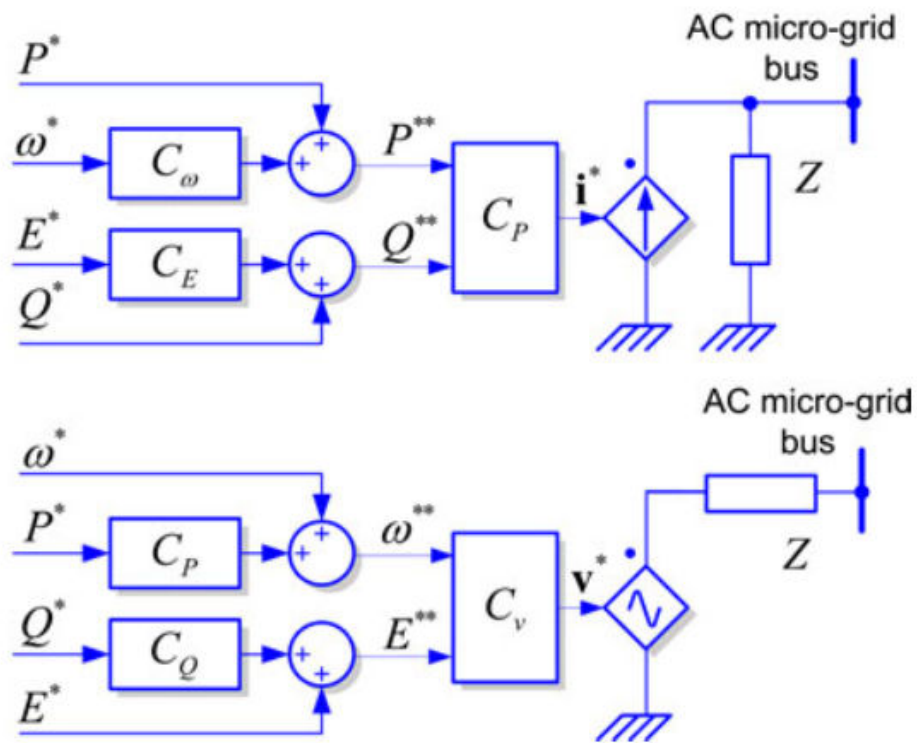


Figure 3.3 Grid Supporting VSC [79] (Current Source based and Voltage source Based).

The modeling in this chapter is for the VSC connected with the grid. The notation adopted is the one established when interfacing VSCs with the grid. In this notation, the grid voltage vector  $E$  is collinear with the d-axis in the dq frame as the modeling is done in dq frame.

## VOLTAGE SOURCE CONVERTER AND ITS CONTROL

The Laplace model of the VSC is also developed in this section which serves as a window through which it is possible to observe what is going on inside the “VSC black-box”. These models facilitate the comprehension of VSCs’ dynamics and allow at developing appropriate current controllers. The Laplace models help to find the following information of the VSC:

- ✚ The mathematical relationship between AC and DC voltages and currents of the VSC.
- ✚ The amount of power flow and its directions.
- ✚ Mathematical expressions for the dynamic behavior of the VSC and associated AC and DC
- ✚ Source /load operation.
- ✚ Control parameters of the VSC.

The VSC Laplace model described in this chapter excludes the converter’s frequency carrier signal which makes the design of the controller quite simple. Precise VSC models can be found in the specialized literature [80]-[81] but they are rather complex. Most of the complexity is due to the high-frequency carrier related to the power electronics switches operation in the VSC modeling process.

The Laplace model is important as it highlights VSC cross-couplings, helping to develop more efficient VSC controllers. Based on the VSC Laplace model, a suitable vector current controller is proposed. Results show that the VSC Laplace model has a good dynamic behavior when compared to a time-domain electrical model. Figure 3.4 shows a VSC connected to an ideal grid which can supply or consume any electrical load at any point of time. The internal equivalent inductances of the grid can be considered as negligible in comparison to the circuit inductance which is in the order of some hundreds of  $\mu\text{H}$  to few  $\text{mH}$ . The DC source can be a battery, capacitor bank, any other DC voltage source.

## VOLTAGE SOURCE CONVERTER AND ITS CONTROL

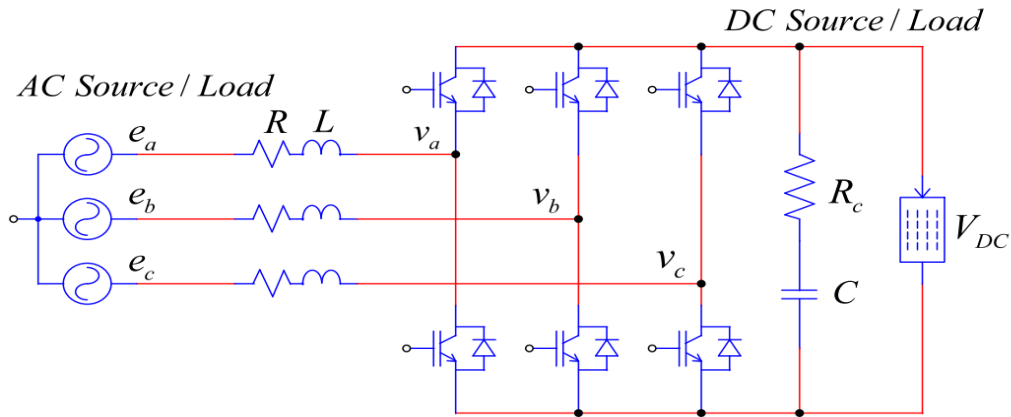


Figure 3.4 Three-phase VSC with AC and DC sources/loads.

The capacitor and inductor connected to the circuit is responsible for the dynamic operation of the converter. Inductor helps in reducing the harmonics by limiting the line current ripple magnitude and acts as energy-storage devices needed for PWM boost rectifier operation. The capacitor connected to the DC side helps to stabilize the DC voltage, particularly after a DC source/load step change. The capacitor ESR (Equivalent Series Resistor), represented by  $R_c$  in Figure 3.4 must be included in this analysis since a low capacitor ESR reduces the high frequencies generated by the converter around and above the carrier frequency signal, improving the DC voltage quality. The controller of the VSC determines the power flow between the grid and the VSC. The active and reactive power exchange between the grid and the VSC depends upon the magnitude and phase angle between the  $e_a$ ,  $e_b$ ,  $e_c$  and  $v_a$ ,  $v_b$ ,  $v_c$ . The main goal of the controller of the VSC is to generate appropriate signal  $v_a$ ,  $v_b$ ,  $v_c$  which finally determines the amount of active or reactive power to flow from the VSC to the grid or vice versa. To explain the VSC in a better way it is described in three parts as i) The VSC ac side modelling ii) The VSC dc side modelling and iii) The complete model of the VSC. The assumptions made for the modelling purpose are i) the ac side voltages  $V_a$ ,  $V_b$ ,  $V_c$  represents only the fundamental frequency and ii) the converter switches are ideal.

### 3.1.1 AC side model of the VSC

The ac side of the VSC can be described as two three phase ac sources connected through inductor and resistor in between as shown in Figure 3.5. [9, 10]. The voltage source  $e_a$ ,  $e_b$ , and  $e_c$

## VOLTAGE SOURCE CONVERTER AND ITS CONTROL

represent the grid side voltages whereas the voltages  $V_a$ ,  $V_b$ , and  $V_c$  represent the VSC side voltage.

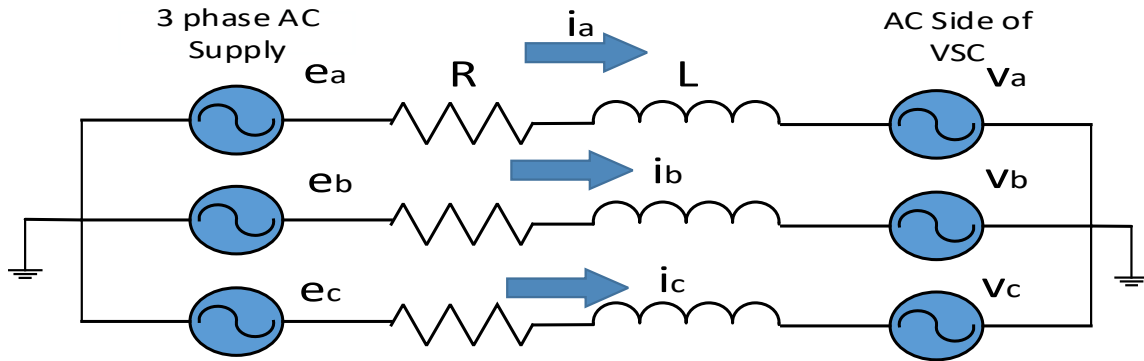


Figure 3.5 Three-phase VSC AC side model.

The voltages of ac side can be written as 3.1

$$\begin{cases} e_a = E \cos(\theta_e) \\ e_b = E \cos(\theta_e - 2\pi/3) \\ e_c = E \cos(\theta_e - 4\pi/3) \end{cases} \dots\dots\dots (3.1)$$

Similarly, the circuit equations can be written as 3.2

$$\begin{cases} e_a = Ri_a + L \frac{di_a}{dt} + V_a \\ e_b = Ri_b + L \frac{di_b}{dt} + V_b \\ e_c = Ri_c + L \frac{di_c}{dt} + V_c \end{cases} \dots\dots\dots (3.2)$$

The above equations are simplified through a three phase transformation. Three phases to dq transformations are employed to simplify the analysis of three phase circuit. They are often used to decouple variables in order to facilitate the solution of difficult equations with time varying variables. Moreover, the complexity of differential equations is often reduced due to change of variables. The three phase stationary frame regulators are regarded as being unsatisfactory for ac current regulation since a conventional PI regulator in this reference frame suffers from the significant steady-state amplitude and phase errors [82]. Rotating reference frame is considered as a superior technique to stationary frame as it achieves zero steady-state

error by acting on dc signals. Using abc to dq transformation allows simple PI structures that will be used for the power and current controllers since they operate on “dc” converter variables in the synchronous frame. Therefore, here also the control system is designed in dq frame. The transformation techniques generally used are Clarke’s and Park’s transformation. The vector representation of three phase a, b, c quantities with alpha, beta and d, q component is shown in Figure 3.6.

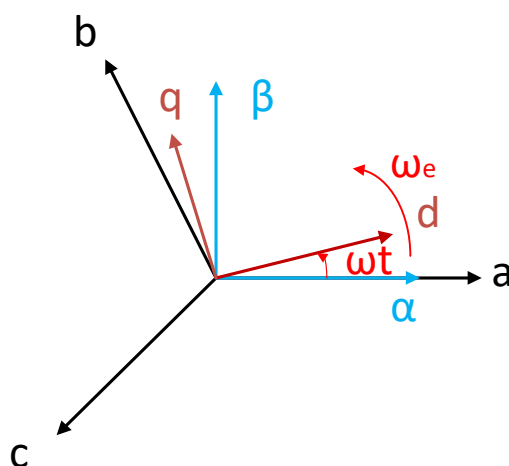


Figure 3.6 abc,  $\alpha\beta$  and dq reference frame.

Clarke’s transformation is a stationary frame transformation technique which converts time domain signals (e.g. voltage, current, flux, etc.) from three-phase coordinates ( $abc$ ) into two-phase orthogonal stationary coordinates ( $\alpha\beta$ ). Consider a three phase rotating vector which consists of a, b and c axis components. These three axis components can be represented in the two  $\alpha\beta$  coordinates using Clarke’s transformation as shown in Figure 3.6.

The dq reference frame is a synchronous one got by Park’s transformation. It rotates synchronously with the angular frequency or electric speed  $\omega_e$ . So,  $\alpha$  and  $\beta$  component of the voltage E can be written as  $e_\alpha$  and  $e_\beta$  as in equation 3.3.

$$\begin{cases} e_\alpha = E \cos \theta_e \\ e_\beta = E \sin \theta_e \end{cases} \dots\dots\dots (3.3)$$

The three phase equations in 3.2 can be written in two components i.e  $e_\alpha$  and  $e_\beta$  as in equation 3.3.

$$\begin{cases} e_\alpha = Ri_\alpha + L \frac{di_\alpha}{dt} + V_\alpha \\ e_\beta = Ri_\beta + L \frac{di_\beta}{dt} + V_\beta \end{cases} \dots\dots\dots (3.4)$$

The equations in the  $\alpha$  and  $\beta$  component written in 3.4 can be written in dq synchronous rotating frame using Park's transformation as in equation 3.5.

$$\begin{bmatrix} e_d \\ e_q \end{bmatrix} = \begin{bmatrix} \cos\theta_e & \sin\theta_e \\ -\sin\theta_e & \cos\theta_e \end{bmatrix} \begin{bmatrix} e_\alpha \\ e_\beta \end{bmatrix} \dots\dots\dots (3.5)$$

The equation 3.5 can be further simplified to 3.6 as

$$\begin{cases} e_d = E \\ e_q = 0 \end{cases} \dots\dots\dots (3.6)$$

Similarly, the current component can be written as equation 3.7.

$$\begin{bmatrix} i_d \\ i_q \end{bmatrix} = \begin{bmatrix} \cos\theta_e & \sin\theta_e \\ -\sin\theta_e & \cos\theta_e \end{bmatrix} \begin{bmatrix} i_\alpha \\ i_\beta \end{bmatrix} \dots\dots\dots (3.7)$$

Finally, the  $e_\alpha$  and  $e_\beta$  component can be written in dq component as in equation 3.8.

$$\begin{bmatrix} e_d \\ e_q \end{bmatrix} = \begin{bmatrix} \cos\theta_e & \sin\theta_e \\ -\sin\theta_e & \cos\theta_e \end{bmatrix} \begin{bmatrix} Ri_\alpha + L \frac{di_\alpha}{dt} + V_\alpha \\ Ri_\beta + L \frac{di_\beta}{dt} + V_\beta \end{bmatrix} \dots\dots\dots (3.8)$$

The mathematical simplification can be done as in equations 3.9 to 3.14

$$\begin{bmatrix} e_d \\ e_q \end{bmatrix} = \begin{bmatrix} \cos\theta_e & \sin\theta_e \\ -\sin\theta_e & \cos\theta_e \end{bmatrix} L \frac{d}{dt} \begin{bmatrix} i_\alpha \\ i_\beta \end{bmatrix} + R \begin{bmatrix} \cos\theta_e & \sin\theta_e \\ -\sin\theta_e & \cos\theta_e \end{bmatrix} \begin{bmatrix} i_\alpha \\ i_\beta \end{bmatrix} + \begin{bmatrix} \cos\theta_e & \sin\theta_e \\ -\sin\theta_e & \cos\theta_e \end{bmatrix} \begin{bmatrix} V_\alpha \\ V_\beta \end{bmatrix} \dots\dots\dots (3.9)$$

$$\begin{bmatrix} e_d \\ e_q \end{bmatrix} = \begin{bmatrix} \cos\theta_e & \sin\theta_e \\ -\sin\theta_e & \cos\theta_e \end{bmatrix} L \frac{d}{dt} \begin{bmatrix} i_\alpha \\ i_\beta \end{bmatrix} + R \begin{bmatrix} i_d \\ i_q \end{bmatrix} + \begin{bmatrix} V_d \\ V_q \end{bmatrix} \dots\dots\dots (3.10)$$

$$\begin{bmatrix} e_d \\ e_q \end{bmatrix} = \begin{bmatrix} \cos\theta_e & \sin\theta_e \\ -\sin\theta_e & \cos\theta_e \end{bmatrix} L \frac{d}{dt} \left( \begin{bmatrix} \cos\theta_e & -\sin\theta_e \\ \sin\theta_e & \cos\theta_e \end{bmatrix} \begin{bmatrix} i_d \\ i_q \end{bmatrix} \right) + R \begin{bmatrix} i_d \\ i_q \end{bmatrix} + \begin{bmatrix} V_d \\ V_q \end{bmatrix} \dots (3.11)$$

Since  $\begin{bmatrix} \cos\theta_e & \sin\theta_e \\ -\sin\theta_e & \cos\theta_e \end{bmatrix} = \begin{bmatrix} \cos\theta_e & -\sin\theta_e \\ \sin\theta_e & \cos\theta_e \end{bmatrix}^{-1}$  and  $\theta_e = \omega_e t$  &  $\omega_e = \frac{d\theta_e}{dt}$

$$\begin{bmatrix} e_d \\ e_q \end{bmatrix} = \begin{bmatrix} \cos\theta_e & \sin\omega_e t \\ -\sin\theta_e & \cos\omega_e t \end{bmatrix} L \left( \begin{bmatrix} -\omega_e \sin\theta_e & -\omega_e \cos\theta_e \\ \omega_e \cos\theta_e & -\omega_e \sin\theta_e \end{bmatrix} \begin{bmatrix} i_d \\ i_q \end{bmatrix} + \begin{bmatrix} \cos\theta_e & -\sin\theta_e \\ \sin\theta_e & \cos\theta_e \end{bmatrix} \begin{bmatrix} \frac{di_d}{dt} \\ \frac{di_q}{dt} \end{bmatrix} \right) + R \begin{bmatrix} i_d \\ i_q \end{bmatrix} + \begin{bmatrix} V_d \\ V_q \end{bmatrix} \dots\dots (3.12)$$

Simplifying mathematically 3.12, 3.13 is obtained

$$\begin{bmatrix} e_d \\ e_q \end{bmatrix} = L \begin{bmatrix} 0 & -\omega_e \\ \omega_e & 0 \end{bmatrix} \begin{bmatrix} i_d \\ i_q \end{bmatrix} + L \begin{bmatrix} 1 & 0 \\ 0 & 1 \end{bmatrix} \begin{bmatrix} \frac{di_d}{dt} \\ \frac{di_q}{dt} \end{bmatrix} + R \begin{bmatrix} i_d \\ i_q \end{bmatrix} + \begin{bmatrix} V_d \\ V_q \end{bmatrix} \dots\dots\dots (3.13)$$

The equations in 3.2 can finally be written in dq frame as in equation 3.14.

$$\begin{cases} e_d = Ri_d + L \frac{di_d}{dt} - \omega_e Li_q + V_d \\ e_q = Ri_q + L \frac{di_q}{dt} + \omega_e Li_d + V_q \end{cases} \dots\dots\dots (3.14)$$

The Figure 3.6 (a) represents the converter single-phase AC side circuit. Figure 3.6 (b) shows the correspondent vector diagram. Considering that  $e$  is collinear with the  $d$  axis, the amplitude of  $v$  and its relative phase to  $e$ ,  $\varepsilon$  defines the line current  $i_L$ . In the modified application for the MG control in this thesis the  $I_d$  is kept constant and  $I_q$  is varied to contribute the reactive power. So by changing the  $I_q$  reference the new  $V_a$ ,  $V_b$  and  $V_c$  signals from the controller is generated. These control signals is used by the PWM switching to generate new magnitude and phase angle of voltage  $V$ . This new magnitude of  $V$  and phase angle finally decides the reactive power to be contributed to the MG.

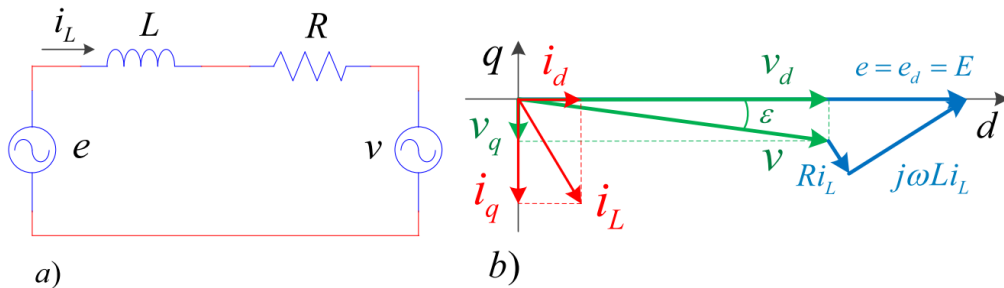


Figure 3.7 VSC single-phase and dq vector diagram.



## VOLTAGE SOURCE CONVERTER AND ITS CONTROL

The equations 3.14 can be written as 3.14 a) from the vsc's point of view

$$\begin{cases} V_d = e_d - Ri_d - L \frac{di_d}{dt} + \omega_e Li_q \\ V_q = e_q - Ri_q - L \frac{di_q}{dt} - \omega_e Li_d \end{cases} \dots\dots\dots 3.14 a)$$

The VSC can be made work either as an inverter or a rectifier. The relation between d and q component in both the cases is shown in Figure 3.7.

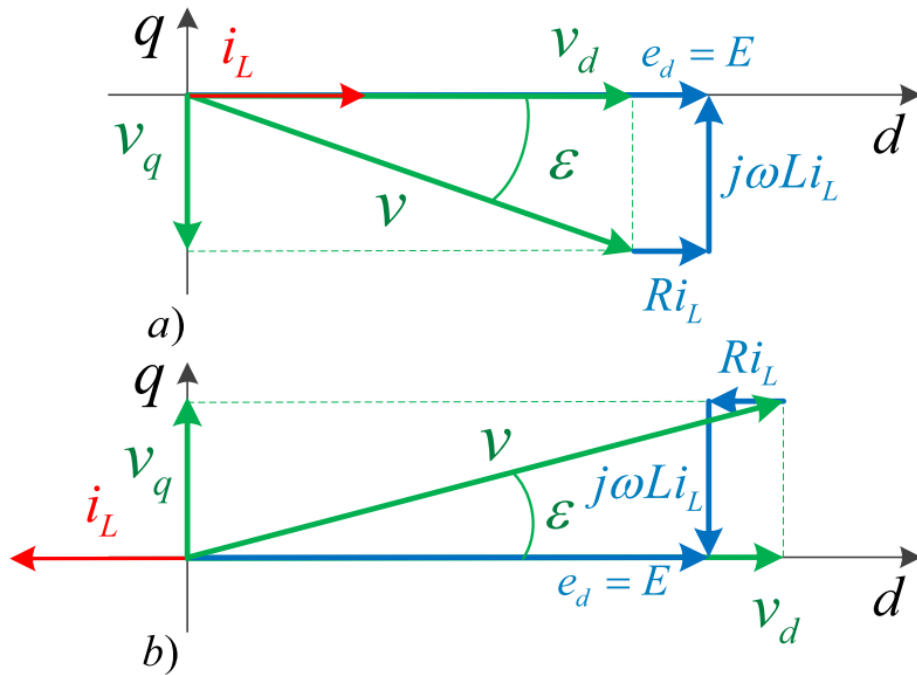


Figure 3.8 VSC's AC side - a) rectification at UPF; b) inversion at UPF.

The Figure 3.7 shows that  $i_L$  is always collinear with  $E$  (which is collinear with  $d$  axis) in both the cases of rectification and inversion as the circuit is operating in unity power factor. The current  $i_L$  is in phase with  $V_d$  in case of rectification and they are out of phase in case of inversion. The magnitude of  $E$  is greater than  $V$  in case of rectification whereas in case of inversion it is opposite.

The equation 3.14 shows that in the  $e_d$  and  $e_q$  relations we have cross coupling terms i.e.  $i_q$  term in the relation of  $e_d$  and  $i_d$  term in the relation of  $e_q$ . The circuit for the relation 3.14 can be drawn as in Figure 3.8. The  $d$  and  $q$  component of the circuit is drawn with the coupling term

## VOLTAGE SOURCE CONVERTER AND ITS CONTROL

$\omega Li_q$  and  $\omega Li_d$ . The coupling term is put in the common branch of both the circuit. The circuit is developed between the converters ac side and the ac grid.

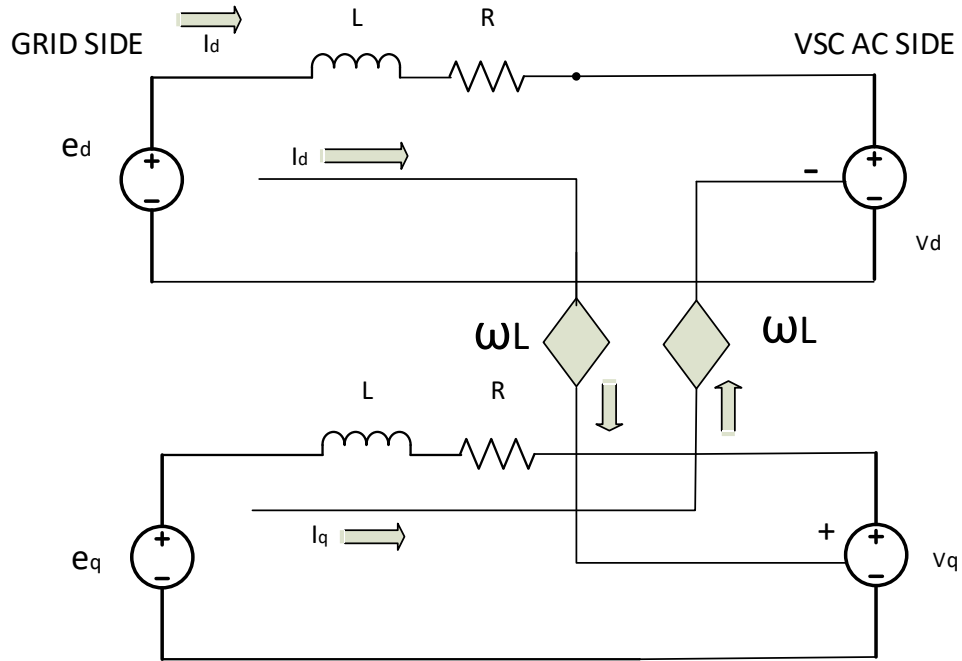


Figure 3.9 Three Phase AC model of VSC in dq.

### 3.1.2 Active and Reactive Power of the AC side

The instantaneous power at a voltage level of  $e$  can be written in Cartesian form as 3.15 [83].

$$S_e = (e_a i_a + e_b i_b + e_c i_c) + j \frac{1}{\sqrt{3}} (e_{bc} i_a + e_{ca} i_b + e_{ab} i_c) \dots\dots\dots (3.15)$$

Where first part is the active power and second part is the reactive power i.e.

$$S_e = P_e + jQ_e \dots\dots\dots (3.16)$$

The active and reactive power in alpha- beta and d-q frame can be written as in equation 3.17 and 3.18 [84].

$$S_e = (e_\alpha i_\alpha + e_\beta i_\beta) + j(e_\beta i_\alpha - e_\alpha i_\beta) \dots\dots\dots (3.17)$$

$$S_e = \frac{3}{2} \left( (e_d i_d + e_q i_q) + j(e_q i_d - e_d i_q) \right) \dots\dots\dots (3.18)$$

## VOLTAGE SOURCE CONVERTER AND ITS CONTROL

In dq frame and considering  $q=0$  and taking into account the values of (3.6), the power equation (3.18) can be simplified to (3.19) and (3.20). A positive  $P_e$  represents the active power supplied by the e source/load, while a negative one represents the power absorbed by the e source/load. The reactive power  $Q$  exists if  $i_q$  is not equal to 0.

$$S_e = \frac{3}{2}(e_d i_d - j e_d i_q) \dots\dots\dots (3.19)$$

$$= \frac{3}{2}(E i_d - j E i_q) \dots\dots\dots (3.20)$$

Finally, the active and reactive power delivered by the source can be represented in equation 3.21

$$\begin{cases} P_e = \frac{3}{2} E i_d \\ Q_e = -\frac{3}{2} E i_q \end{cases} \dots\dots\dots (3.21)$$

Now if it is considered that the Power Factor is unity i.e.  $e_d$  is in phase with  $i_d$ , in this case,  $i_d = i_L$  which is the single phase peak value. The value of  $i_q = 0$  and the rms value of current, voltage and power can be represented as 3.22 and 3.23.

$$e_{rms} = \frac{e_d}{\sqrt{2}} = \frac{E}{\sqrt{2}} \text{ and } i_{rms} = \frac{i_d}{\sqrt{2}} = \frac{I}{\sqrt{2}} \dots\dots\dots (3.22)$$

Finally leading to

$$P_e = \frac{3}{2} E i_d = \frac{3}{2} \sqrt{2} e_{rms} * \sqrt{2} i_{rms} = 3 e_{rms} * i_{rms} \dots\dots\dots (3.23)$$

### 3.1.3 DC side model of the VSC

The AC side model of the VSC has been developed in section 3.1.2. The power that crosses the DC side of the VSC and vice versa is only the active power  $P$ . It can be considered that there are no switching or conduction losses in the converter and so the power equation can be written as equation 3.24.

$$P = P_{vsc \text{ ac side}} = P_{vsc \text{ dc C side}} = P_{dc} \dots\dots\dots (3.24)$$

The voltage on the DC side of the VSC depends on the power transferred from/to the AC side of the VSC. So it is appropriate to represent the circuit in current source form  $I_0$ [85]. The DC side circuit of the VSC can be represented as in Figure 3.9.

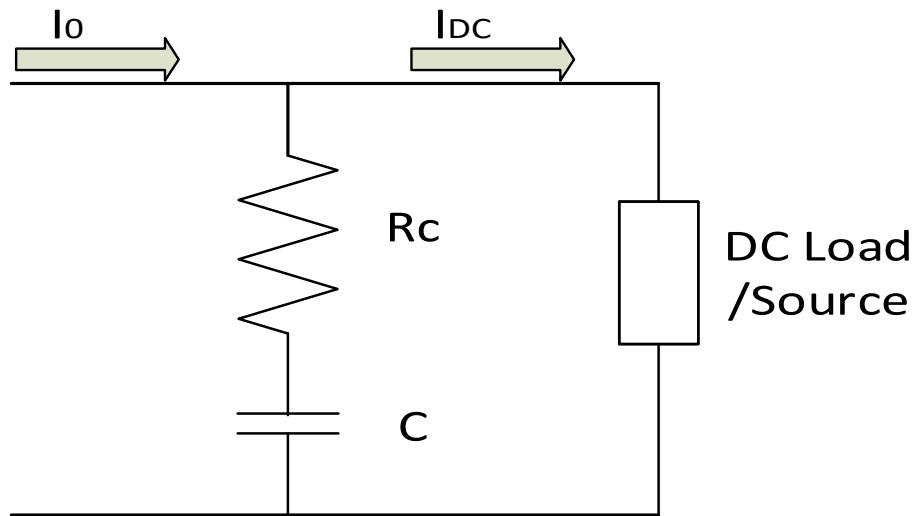


Figure 3.10 Three Phase VSC DC side.

The capacitor  $C$  connected to the DC model as shown in the Figure 3.10 helps to filter the high-frequency switching harmonics generated by the converter. It also acts as a current-to-voltage converter needed to define and stabilize the DC voltage.  $R_c$  is the ESR connected. A low capacitor ESR reduces the high frequency switching related ripple, improving the DC voltage quality. The energy stored in the capacitor can be written as 3.25.

$$E_c = \frac{1}{2} C V_{DC}^2 \quad \dots\dots\dots (3.25)$$

The instantaneous power of the capacitor can be obtained by taking the derivative of the equation 3.25 as in equation 3.26.

$$P_c = \frac{d}{dt} \left( \frac{1}{2} C V_{DC}^2 \right) = V_{DC} C \frac{dV_{DC}}{dt} \quad \dots\dots\dots (3.26)$$

Finally, the relation of power in the dc circuit  $P_{DC}$  can be written in relation to 3.27 as the power shown in 3.26 is the difference of power between instantaneous power in the capacitor and the instantaneous power in the DC source/load.

$$P_{DC} = V_{DC} C \frac{dV_{DC}}{dt} + P_{LOAD} \quad \dots\dots\dots (3.27)$$

### 3.1.4 The Complete model of the VSC

The complete model of the VSC can be developed by combining the AC and DC model discussed in section 3.1.2 and 3.1.3. The power on the AC side of the VSC can be written in dq form as in equation 3.28.

$$P_{AC} = \frac{3}{2}(v_d i_d + v_q i_q) \quad \dots\dots\dots (3.28)$$

The power in the AC and DC side must be equal so we can write a combined equation as in 3.29.

$$\frac{3}{2}(v_d i_d + v_q i_q) = V_{DC} I_0 \quad \dots\dots\dots (3.29)$$

Now the AC and DC part can be joined and represented in the form of the circuit as in the Figure 3.11. This circuit models the VSC using the power flow requested to the converter as a model parameter. In this circuit, the VSC can be analysed as a power transfer device that converts AC active power into DC power and vice-versa.

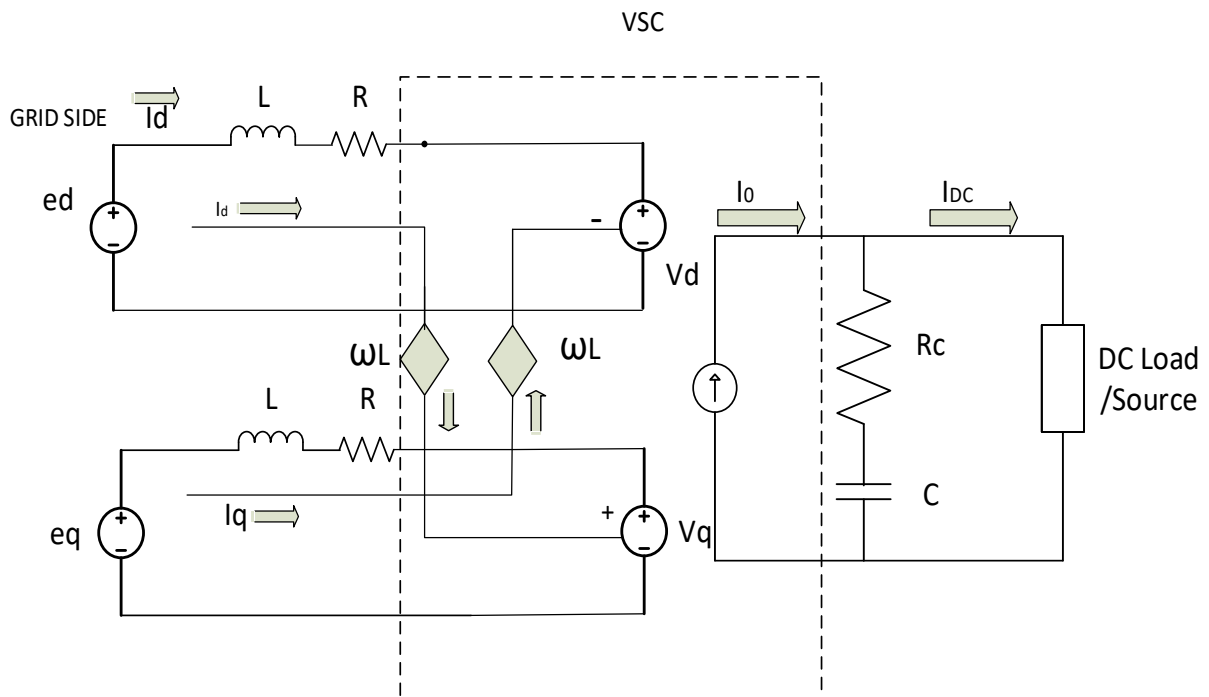


Figure 3.11 Three Phase VSC model.

## 3.2 The Laplace Model of VSC

The Laplace model of a VSC is an appropriate way to represent it because it enables to describe and expose VSC's internal cross-couplings, allowing the design of suitable VSC current controllers [86]. The modelling of the VSC is important to analyse the behaviour of VSC. The VSC dynamics is often analysed by using time-domain models (or electric models), as their representation is close to reality. Although these electrical models are appropriate to simulate, they do not provide enough information to design appropriate controllers. The Laplace-domain or frequency-domain analysis is an appropriate method to represent, simulate, design and test the VSC.

### 3.2.1 Laplace Equations of the AC side of the VSC

The equations of ac side presented in 3.14 can be written in Laplace domain as 3.30

$$\begin{cases} e_d = (R + sL)i_d - \omega_e Li_q + v_d \\ e_q = (R + sL)i_q - \omega_e Li_d + v_q \end{cases} \dots\dots\dots (3.30)$$

Simplifying equations 3.30 and writing in terms of  $i_d$  and  $i_q$  in equation 3.31

$$\begin{cases} i_d = (e_d - v_d + \omega_e Li_q) \frac{1}{R+sL} \\ i_q = (e_q - v_q + \omega_e Li_d) \frac{1}{R+sL} \end{cases} \dots\dots\dots (3.31)$$

### 3.2.2 Laplace Domain Equations of the DC side of the VSC

The DC side of the VSC is modelled considering the DC side with a battery as an assumption, as it shows Figure 3.11. The battery is modelled as a large pre-charged capacitor  $C_1$  in series with its ESR  $R_1$ . The new VSC DC side configuration is represented in Figure 3.12. The filter capacitor represented by  $C$  is typically in the order of hundreds to thousands of micro-farad, which is an insignificant capacity when compared to the battery which is modelled as a large capacitor  $C_1$  with a capacity of thousands of Farads. However, its ESR represented by  $R_c$ , is typically in the order of a few m $\Omega$ , while the battery internal resistance  $R_1$  is typically in the order

## VOLTAGE SOURCE CONVERTER AND ITS CONTROL

of hundreds of mΩ. Thus the capacitor C with low ESR is highly efficient to short-circuit the high frequency harmonics caused by power electronic switching.

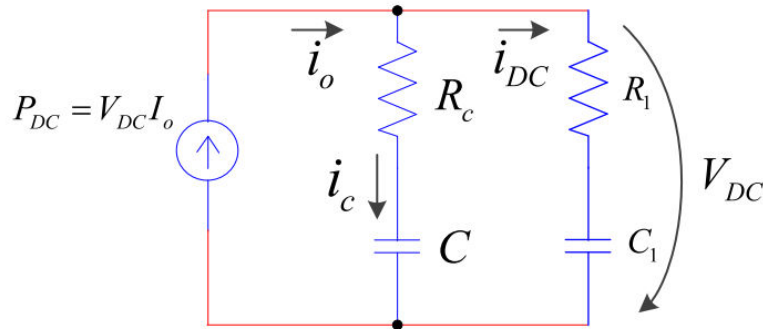


Figure 3.12 DC side of the VSC with battery modeled as a capacitor and a Resistor in series.

The time domain circuit presented in 3.12 can be represented in S domain using Laplace equations as Figure 3.13.

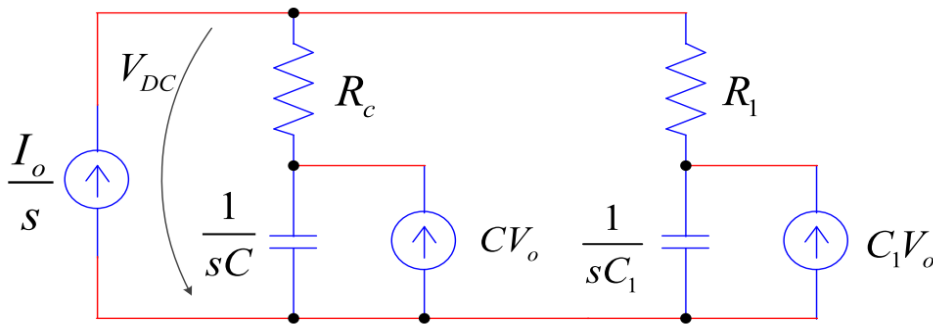


Figure 3.13 VSC DC side representation of a battery modeled as a large capacitor.

The initial voltage of the capacitor in the circuit shown in Figure 3.11 is  $V_0$ . The circuit equations can be developed as 3.32

$$\frac{I_0}{s} = \left[ \frac{R_c + R_1}{R_c R_1} - \frac{1}{R_1(sR_1 C_1 + 1)} - \frac{1}{R_c(sR_c C + 1)} \right] V_{DC} - \left[ \frac{C_1}{sR_1 C_1 + 1} - \frac{C}{sR_c C + 1} \right] V_0. \quad (3.32)$$

$\xleftarrow{\hspace{10em} A \hspace{10em}} \xrightarrow{\hspace{10em}}$

The expression A can be simplified as 3.33

$$A = \frac{s^2 C C_1 (R_c + R_1) + s(C + C_1)}{s^2 R_c R_1 C C_1 + s(R_c C + R_1 C_1) + 1} \quad \dots\dots\dots (3.33)$$

The equation of power in Laplace domain in DC side is given by

$$P_{DC} = V_{DC} \frac{I_0}{s} \quad \dots\dots\dots (3.34)$$

Putting the values of  $I_0/s$  from equation 3.34 to equation 3.32 we can re-write the equation as 3.35

$$\frac{P_{DC}}{V_{DC}} = AV_{DC} - \left[ \frac{C_1}{sR_1C_1+1} - \frac{C}{sR_cC+1} \right] V_0 \quad \dots\dots\dots (3.35)$$

Simplifying equation 3.35 as equation 3.36

$$V_{DC} = \frac{1}{A} \left[ \frac{P_{DC}}{V_{DC}} + \left[ \frac{C_1}{sR_1C_1+1} - \frac{C}{sR_cC+1} \right] V_0 \right] \dots\dots\dots (3.36)$$

Now combining equation 3.29 and 3.36, the equation can be developed as 3.37

$$V_{DC} = \frac{1}{A} \left[ \frac{\frac{3}{2}(v_d i_d + v_q i_q)}{V_{DC}} + \left[ \frac{C_1}{sR_1C_1+1} - \frac{C}{sR_cC+1} \right] V_0 \right] \quad \dots\dots\dots (3.37)$$

The AC equations on Laplace domain developed in equation 3.30 and the DC equations developed in 3.37 can be developed to a controller circuit as shown in Figure 3.13.

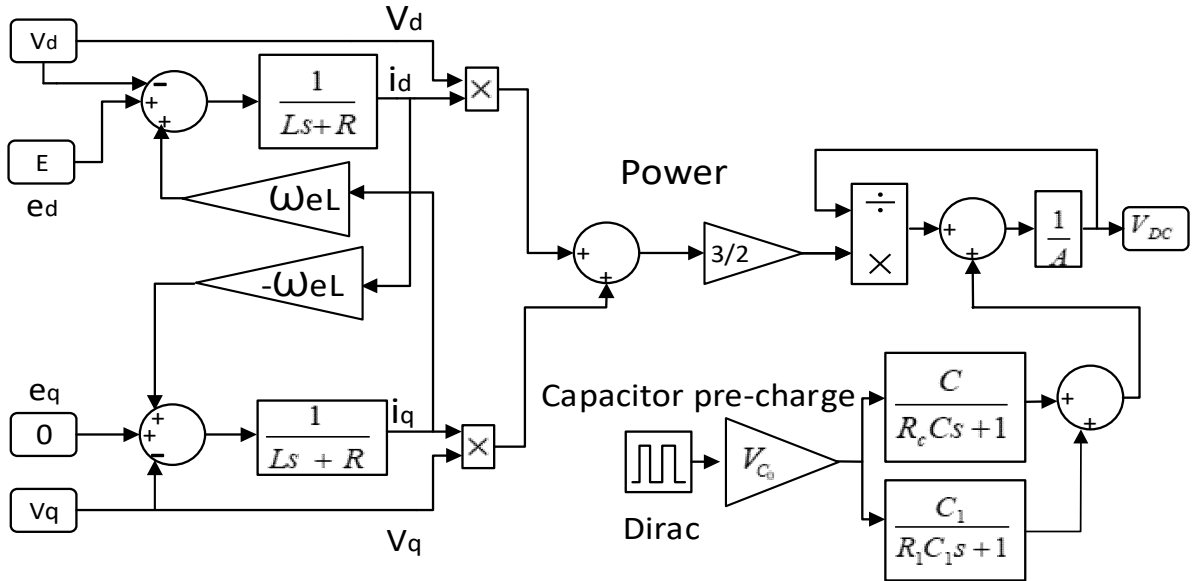


Figure 3.14 Laplace Model of VSC including a large capacitor as a battery.



### 3.3 The VSC Control Principle

The Laplace model developed in section 3.2 will be used to control the power flow through the VSC developing a controller. The controller developed will be able to

- ✚ Define the active power that flows through the VSC and its direction.
- ✚ Define the reactive power exchange between the AC source/load and the VSC which can be inductive, capacitive or null (unity power factor).

The active and reactive power, either supplied or absorbed by the VSC, are proportional to  $i_d$  and  $i_q$  currents respectively as shown in equation 3.21. The power flow through the VSC now can be controlled by making  $i_d$  and  $i_q$  to track respectively the reference currents  $i_d^*$  and  $i_q^*$ . Thus, according to (3.14 a)), to achieve  $i_d$  and  $i_q$  requested values, appropriate  $v_d$  and  $v_q$  voltages have to be built by the converter. The generation of  $v_d$  and  $v_q$  on the other hand results from VSC operation, based on a switching frequency which is generally much higher than the fundamental one, using Nyquist theorem and Fourier analysis to design appropriate waveforms which is explained in detail in the section 3.3.2 and 3.3.3.

#### 3.3.1 The VSC Current Controller

A good current controller has to produce the currents which exactly follow the current references and settle within transient period. In this work, a vector current controller for the VSC is designed in which the currents  $i_d$  and  $i_q$  follow their references  $I_d^*$  and  $I_q^*$  respectively. So the main objective of the controller is to make the line currents  $i_d$  and  $i_q$  to follow the references  $I_d^*$  and  $I_q^*$  respectively. While working in the dq reference frame it is needed to deal with the cross coupling terms so that if we want to make a change in one quantity the other quantity has to be counteracted in order to guarantee a high dynamic performance. A decoupled PI( Proportional Integrator) type controller can be used to get high performance current controller[81].

The equations developed in 3.14 a) can be written as 3.38

$$\begin{cases} V_d = e_d - Ri_d - \Delta V_d + \omega_e Li_q \\ V_q = e_q - Ri_q - \Delta V_q - \omega_e Li_d \end{cases} \dots\dots\dots (3.38)$$

## VOLTAGE SOURCE CONVERTER AND ITS CONTROL

Where  $\Delta V_d$  and  $\Delta V_q$  are the control action of the PI controller as mentioned in equation 3.39.

$$\begin{cases} \Delta V_d = k_p(I_d^* - I_d) + k_i \int (I_d^* - I_d) dt \\ \Delta V_q = k_p(I_q^* - I_q) + k_i \int (I_q^* - I_q) dt \end{cases} \dots\dots\dots (3.39)$$

As shown in the Figure 3.14 the current controller receives the current measurements  $i_d$  and  $i_q$  from the converter and generates the  $v_d$  and  $v_q$  voltages that are the final inputs to the converter. Considering the equations 3.38 and 3.39 a suitable decoupled controller is presented in Figure 3.14. It can be noticed that the current controller decoupling paths are  $-\omega L$  and  $\omega L$  are cancelled by the coupling path of the VSC model which is shown combined in Figure 3.14. The resistance  $R$  is put in the circuit to compensate the losses in the inductor.

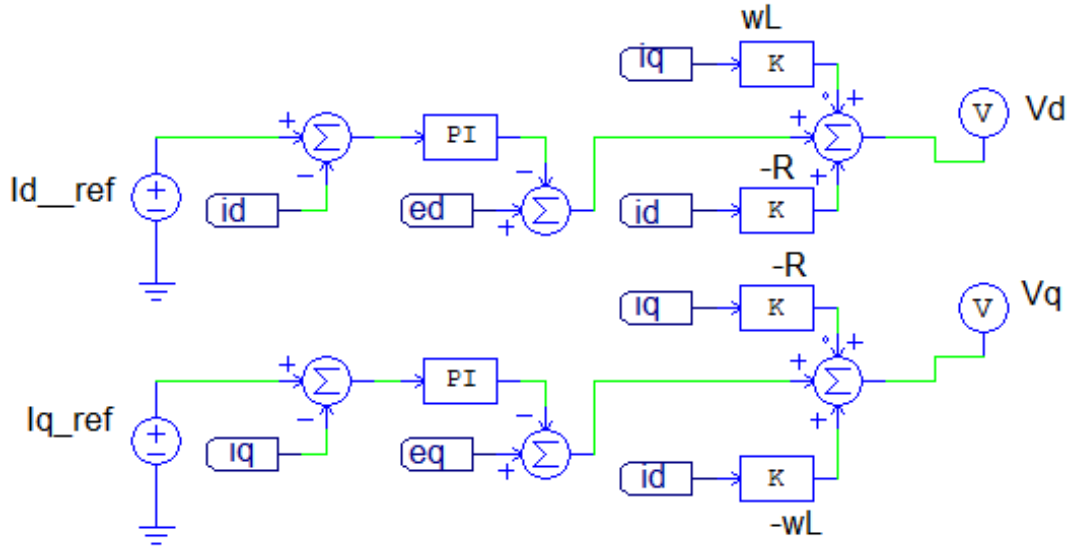


Figure 3.15 Decoupled current controller of three phase VSC.

Similarly, the complete diagram of the VSC with the controller can be presented as in Figure 3.15. As depicted the input is the  $I_d$  and  $I_q$  reference and the output of the controller is  $V_d$  and  $V_q$  which are converted in three phase quantity as  $V_a$ ,  $V_b$  and  $V_c$ . These three phase quantities are the input to the PWM switching and finally the power is contributed to the MG. The power transferred to the DC side is  $V_d I_d + V_q I_q$ .

# VOLTAGE SOURCE CONVERTER AND ITS CONTROL

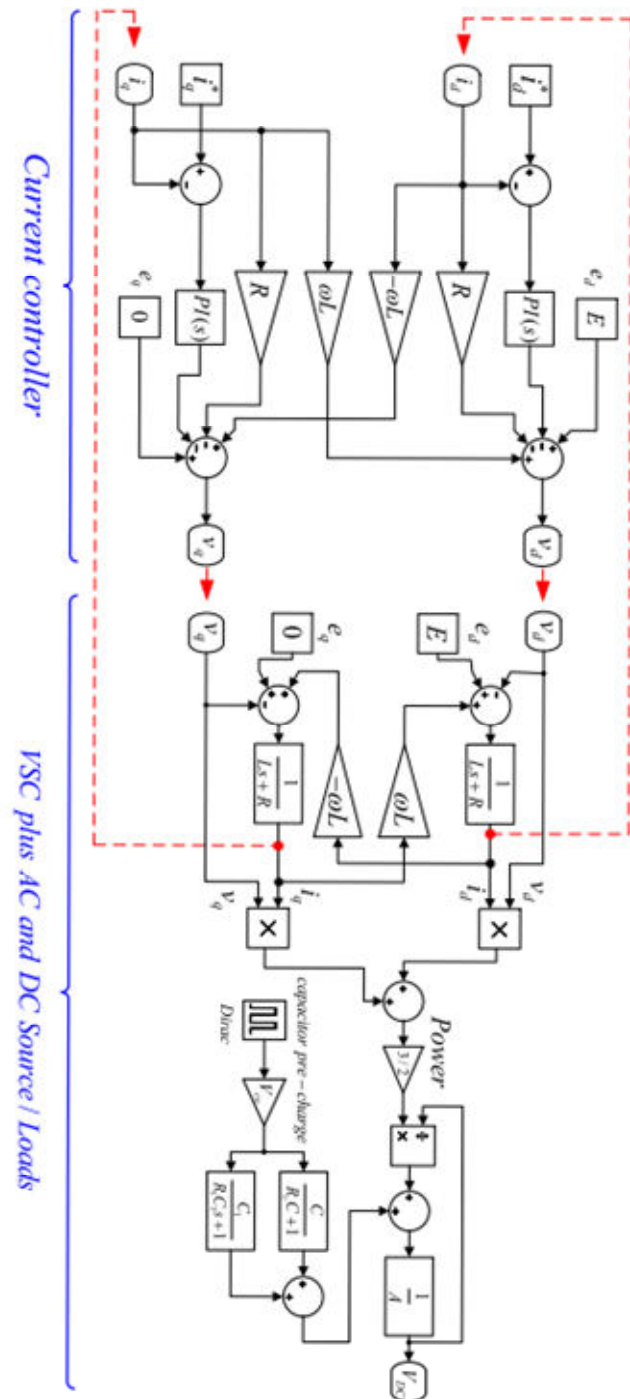


Figure 3.16 Current controller and VSC Laplace model with a battery modeled as a capacitor in the DC side.

### 3.3.2 Pulse-width Modulation Techniques for Voltage Source Converters

The main advantages of modern power electronic converters, such as high efficiency, low weight, small dimensions, fast operation, and high power densities, are being achieved through the use of the so-called switch mode operation, in which power semiconductor devices are controlled in ON=OFF way (no operation in the active region). This leads to different types of pulse width modulation[87]. This sub/section describes the needs of modulation techniques for the VSC and the type of modulation technique used in this work. Figure 3.16 shows the circuit diagram of a VSC connected with the grid. The vector voltages generated by the VSC are  $V_a$ ,  $V_b$  and  $V_c$  which interacts with  $e_a$ ,  $e_b$  and  $e_c$  voltages that define the active power flow that crosses the converter from the AC to the DC side, or vice-versa, and the reactive power that flows (only) between the AC Source/Load and the converter's AC side.

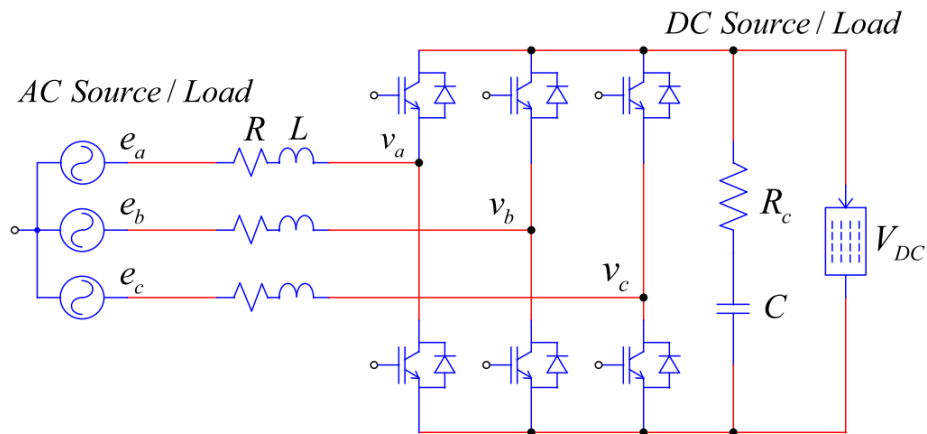


Figure 3.17 VSC connected with the grid.

The current controller of the VSC designed in the section 3.3.1 is responsible to generate the signals which after suitable amplification inside the VSC by a proper switching operation, produces the signals  $V_a$ ,  $V_b$  and  $V_c$  [88]. The switching pattern to generate the necessary signals requires a particular switching technique known as the modulation technique. The mostly used two types of the modulation techniques are the SPWM (Sinusoidal Pulse Width Modulation) and the Space Vector Pulse Width Modulation (SVM). SPWM is mostly used as it is easy to implement, on the other hand, SVM has an intensive computation time but can deliver better results like wider linear modular, lower base band harmonics and less commutation losses.

## VOLTAGE SOURCE CONVERTER AND ITS CONTROL

Ideally, it is desired that the voltages  $V_a$ ,  $V_b$  and  $V_c$  from the VSC should be sinusoidal in nature. The case is different in real operation due to the VSC's operation principle which is based on switching operation at high frequencies, the resultant  $v$  voltages exhibit complex waveforms. Apart from the fundamental frequency  $\omega$  the voltage quantities have frequency-related harmonics with modulation-frequency sidebands in the form of  $A\omega_c + B\omega$  where,  $\omega_c$  is the modulator or carrier frequency, and A and B are integers as defined in [88] for SPWM.

Harmonics are undesirable as they originate supplementary losses to the conversion process. They are limited by the line inductors in the AC side and by the capacitor attached to the DC side terminals. The line inductors act as low-pass filters limiting the amplitude of the line current harmonics while the DC side capacitor, with a low ESR, contributes to limit the harmonics present in the DC line voltage.

To reduce the amplitude of the harmonics and the size of inductances and capacitors the carrier frequency  $\omega_c$  must be set as distant as possible from the fundamental frequency  $\omega$ . But practically it is not possible to set very high frequency because switches are not ideal, taking some time to turn on and off. It causes switching losses for the duration when switches operate at non zero voltage and current. So it can be concluded that when power increases switching speed decreases, as a result, the maximum carrier frequency ends up to a compromised value and determined mainly by the available power electronic switches and their associated costs. So it is necessary to establish a compromise between the carrier frequency and the acceptable losses.

### 3.3.3 Modulation Indexes

The modulation index (MI) as a relation between the ac side and the dc side voltage of the VSC can be written as equation 3.40 [83]. The ac side voltage  $v$  is also represented as  $v_d$  and  $v_q$  component and the dc side voltage is represented as  $V_{DC}$ .

$$M = \frac{\pi}{2} \frac{v}{V_{DC}} = \frac{\pi}{2} \frac{\sqrt{v_d^2 + v_q^2}}{V_{DC}} \dots\dots\dots (3.40)$$

Theoretically, M can take any value between 0 and 1. The values of M near 0 means that  $v$  and  $V_{DC}$  have big relative voltage amplitudes. On the other hand when M is 1 means the VSC is operated in a six-step mode, resulting in square-wave  $v$  voltages. In practice, maximum values of

M are limited by the modulation technique adopted taking into account that the harmonics should be around and above the carrier frequency, i.e. the VSC should operate in the linear zone.

The equation 3.41 shows the maximum M index value for SPWM in linear operation while 3.42 shows the same limit for SVM. If the maximum value of M index is crossed the VSC operates in an over-modulation mode which causes undesirable low frequency current harmonics in ac line and there is no change in  $V_{DC}$  with the change in  $v$ .

$$M_{max} = \frac{\pi}{4} = 0.7854 \dots\dots\dots (3.41)$$

$$M_{max} = \frac{\pi}{2\sqrt{3}} = 0.9069 \dots\dots\dots (3.42)$$

The equations 3.40 show that the value of  $V_{DC}$  is always higher than the peak value of voltage  $v$ . As an example, for SVM in linear operation ( $M \leq 0.9069$ ),  $V_{DC} \geq \sqrt{3}V_{peak}$  or  $V_{DC} \geq \frac{\sqrt{3}}{2}V_{rms}$ , where  $V_{rms}$  is the single phase RMS voltage of the VSC terminal.

### 3.4 Synchronization Techniques

Rapid proliferation of DG in power grid has given rise to the proposal of numerous synchronization methods such as zero crossing detection (ZCD), Kalman Filter, Discrete Fourier transform (DFT), Nonlinear Least Square (NLS), Adaptive Notch Filtering (ANF), Artificial Intelligence (AI), Delayed Signal Cancellation (DSC) , Phase Locked Loop (PLL), and Frequency Locked Loop (FLL) [89].

Among the methods mentioned above, PLL is the most acknowledged, owing to its simplicity, effectiveness, and robustness in various grid conditions. In fact, PLL is an old technology since its concept was published in 1932. It has been used in a vast range of applications such as control systems, communications, instrumentation, and many more. It is a nonlinear closed- loop feedback control system which synchronizes its output signal with the reference input signal in frequency and phase [89].

The PLL is a closed-loop control mechanism aimed to estimate the frequency and the phase-angle of a given input signal. Figure 3.17 shows a three-block diagram that describes the PLL operation: the phase detector; the low-pass filter (LPF); and the Voltage Controlled Oscillator (VCO).

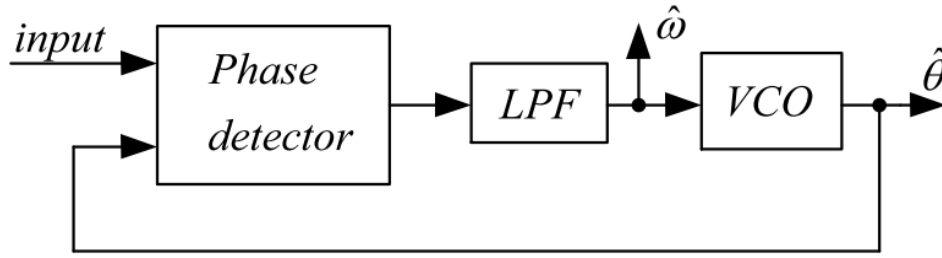


Figure 3.18 Basic structure of PLL.

The phase detector compares the input signal phase with the estimated phase and generates an error signal. The LPF guarantees the dynamic response of the PLL by removing the high-frequency components introduced by the phase detector. The LPF output gives the estimated frequency  $\hat{\omega}$ . The VCO can be seen as an integrator that determines the estimated phase-angle  $\hat{\theta}$  from the estimated frequency. Among different types of PLL synchronous reference frame PLL (SRF-PLL) is one of the simplest and robust PLL, being used in this work.

### 3.4.1 Synchronous Reference Frame PLL

Synchronous Reference Frame PLL (SRF-PLL) is widely used in three-phase grid-connected power converters for its simple implementation and fast and accurate estimation of the phase/frequency in ideal grid conditions[90]. The SRF-PLL derives the phase angle from a three-phase voltage source by completing a reference frame transformation from the stationary abc to the rotational dq. The reference frame transform can be done in two steps: applying Clarke's abc to  $\alpha\beta$  transform followed by the Park's  $\alpha\beta$  to dq reference frame transformation.

The Clarke's transform assumes that

$$\begin{aligned} V_a &= V \cos(\theta) \\ V_b &= V \cos(\theta - 2\pi/3) \\ V_c &= V \cos(\theta + 2\pi/3) \end{aligned} \quad \dots\dots\dots (3.43)$$

The Clark's transformation of  $V_{abc}$  leads to  $V_{\alpha\beta}$  which is given as 3.44

$$\begin{bmatrix} V_\alpha \\ V_\beta \end{bmatrix} = \begin{bmatrix} V \cos \theta \\ V \sin \theta \end{bmatrix} \quad \dots\dots\dots (3.44)$$

## VOLTAGE SOURCE CONVERTER AND ITS CONTROL

The phase-angle can be detected by synchronizing the voltage vector  $V_a$  with the direct or quadrature axis. By choosing the synchronization with the direct axis where  $V_d = V$  and  $V_q=0$ , the Park's transform is given by

$$[T_{DQ}] = \begin{bmatrix} \cos \hat{\theta} & -\sin \hat{\theta} \\ \sin \hat{\theta} & \cos \hat{\theta} \end{bmatrix} \dots\dots\dots (3.45)$$

Where  $\hat{\theta}$  is the estimated phase-angle that is the output of the PLL. Now multiplying  $T_{DQ}$  with  $V_{\alpha\beta}$  and representing in equation 3.46.

$$\begin{bmatrix} V_d \\ V_q \end{bmatrix} = \begin{bmatrix} \cos \hat{\theta} & -\sin \hat{\theta} \\ \sin \hat{\theta} & \cos \hat{\theta} \end{bmatrix} \begin{bmatrix} V \cos \theta \\ V \sin \theta \end{bmatrix} = \begin{bmatrix} V \cos(\hat{\theta} - \theta) \\ V \sin(\hat{\theta} - \theta) \end{bmatrix} = \begin{bmatrix} V \cos(\Delta\theta) \\ V \sin(\Delta\theta) \end{bmatrix} \quad (3.46)$$

From the synchronous referential  $V_q$  is set to be zero. When the error  $\Delta\theta$  is null the estimated dq frame is synchronized with the grid abc frame. Figure 3.18 shows the structure of the SRF-PLL method.

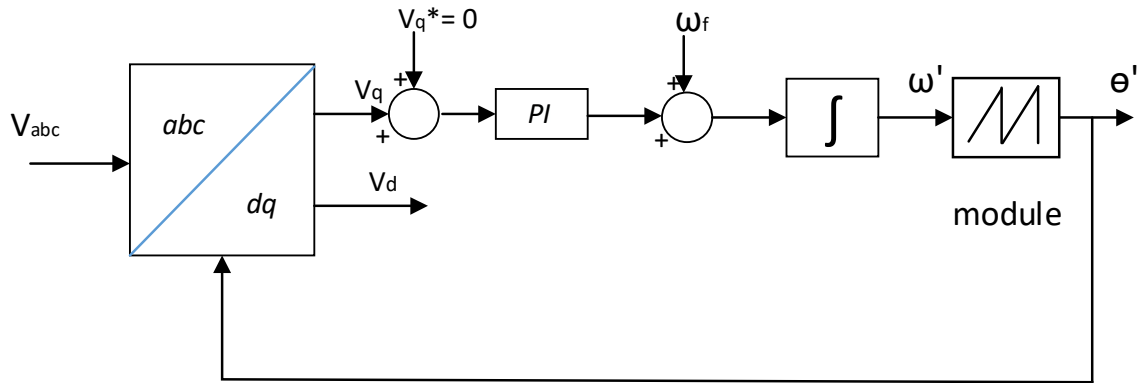


Figure 3.19 Synchronous Reference Frame PLL Model

In steady state condition  $\hat{\theta} \approx \theta$  so  $\Delta\theta$  is very small so the value of  $\sin(\Delta\theta)$  can be considered as  $\Delta\theta$ . The PLL can thus be treated as a linear control system where

$$V_q = V(\hat{\theta} - \theta) \dots\dots\dots (3.47)$$

A block diagram on equation 3.47 can be represented as in the Figure 3.19



## VOLTAGE SOURCE CONVERTER AND ITS CONTROL

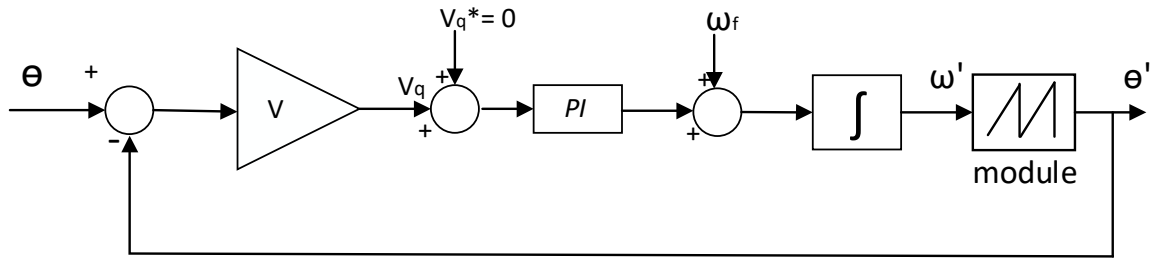


Figure 3.20 Synchronous Reference Frame PLL comprehensive Model.

The angular frequency  $\omega_f$  is the source angular frequency. For nearly constant frequency sources, like the grid frequency, it may be easily specified,  $\omega_f = 2\pi 50 \text{ rads}^{-1}$

The  $\omega_f$  speeds up the PLL synchronizing process. If unknown, it can be set to zero and the PI controller integral part will compensate its value over time. The practical consequence is that the synchronizing process will take longer time.

### 3.4.2 PSIM SRF-PLL Dynamic Evaluation

The concept discussed in section 3.4.1 is verified in this section using PSIM which will be used in further work ahead. The Figure 3.20 a) shows a PSIM implementation of the SRF-PLL. The source is a three- phase voltage system with a single-phase magnitude of 1V and a frequency of 250 Hz. The phase-angle is obtained by synchronizing the  $V_a$  voltage vector with the d axis, thus getting the  $V_q$  signal used in the close-loop control. The  $\omega_f$  angular frequency is set to zero meaning that there is not an initial estimation of the line frequency. As expected when  $\Theta = 0$   $V_a$  is at its positive maximum as shown in Figure 3.21. The “-1” multiplier is necessary to have a correct abc to dq reference frame transform in PSIM (from PSIM manual).

It is also possible to synchronize the voltage  $V_a$  vector with the q axis using the  $V_d$  signal, as represented in Figure 3.20 b). The difference is that the resulting phase-angle is now synchronized with the beginning of the sinusoid instead of with its positive maximum, as it can be observed in Figure 3.20.

# VOLTAGE SOURCE CONVERTER AND ITS CONTROL

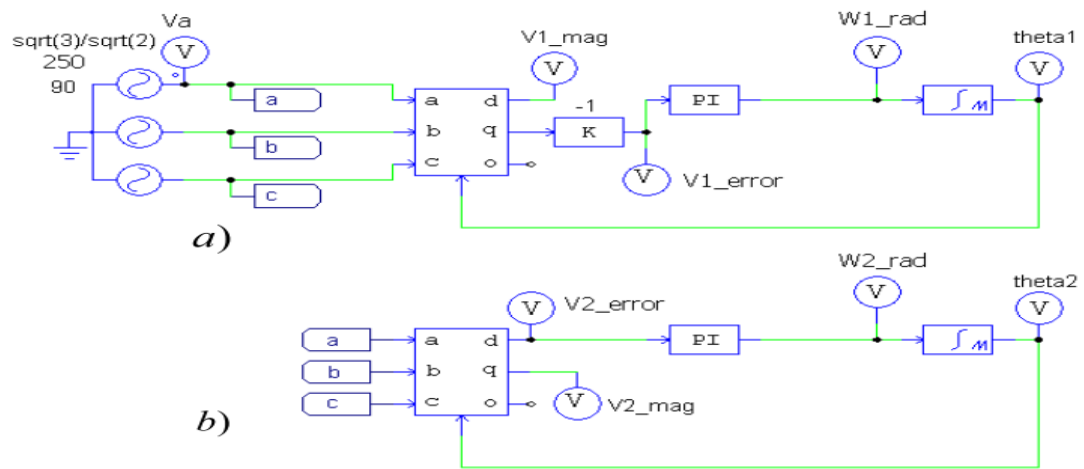


Figure 3.21 PSIM SRF-PLL synchronization test circuits using a)  $V_q$  or b)  $V_d$  as a synchronization signal.

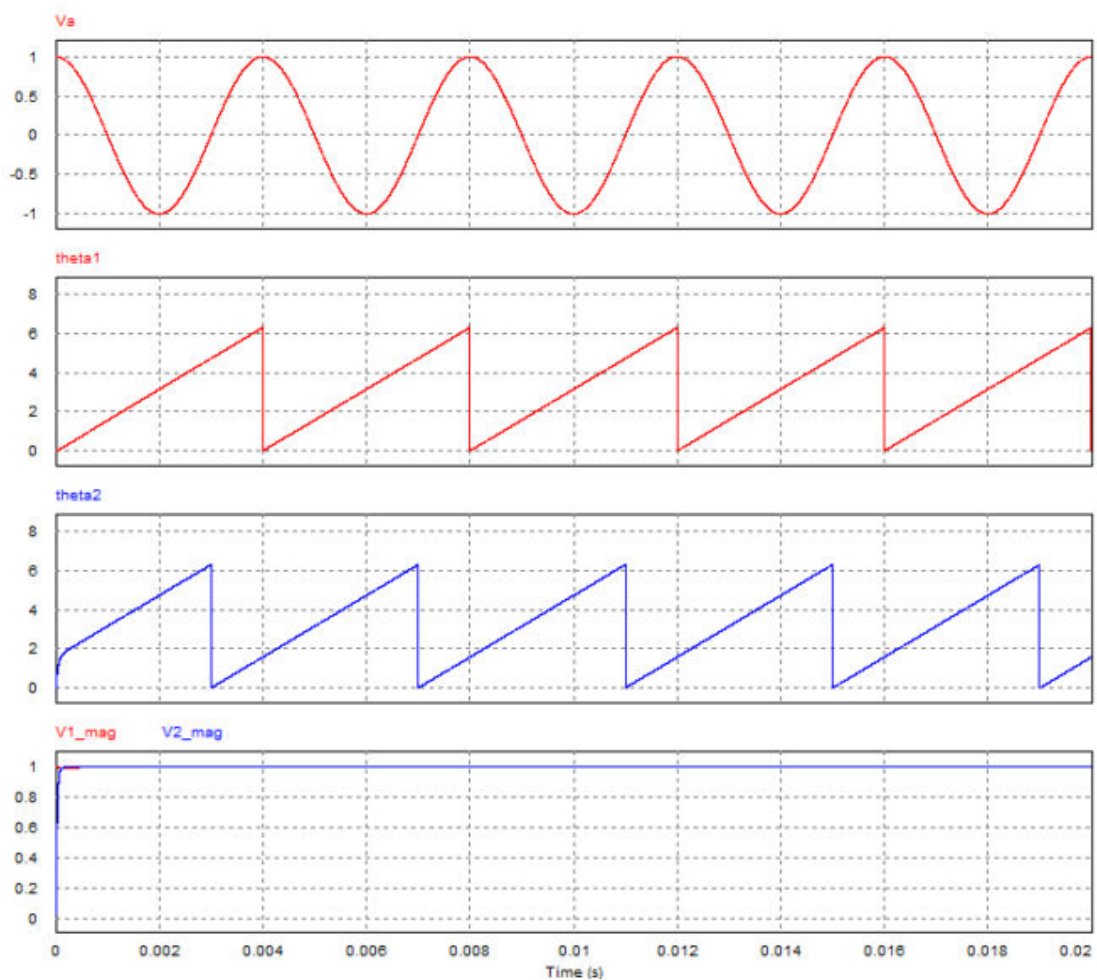


Figure 3.22 PSIM SRF-PLL synchronization test circuits waveforms.

## VOLTAGE SOURCE CONVERTER AND ITS CONTROL

The Figure 3.21 shows the output of the SRF PLL, which is equally correct for  $V_d$  and  $V_q$  references. In this way, the synchronization can be done by determining the  $\theta$  using SRF PLL.

### 3.5 VSC Working in Different Modes

This section shows the VSC working in different modes like Inverter, Rectifier, with resistive, inductive and in capacitive mode. Figure 3.22 shows VSC connected with the grid at 400 V line to line r.m.s voltages. The VSC is connected to the grid through the resistance of  $100\text{m}\Omega$  and inductance of 1 mH. The battery connected to the DC side is of 800 V. The output signals of the converter  $V_{a_c}$ ,  $V_{b_c}$  and  $V_{c_c}$  are connected to the switching circuit to generate the switching signal of the VSC. Figure 3.23 shows the VSC working as a Rectifier from 0 s to 0.1s and then as an Inverter from 0.1 s to 0.2 s. Finally, the VSC is working as a Rectifier again from 0.2s to 0.3s. The first part of the Figure 3.24 shows the phasor diagram of the output of the voltage ( $e_a$ ) and current ( $i_a$ ) waveform. It can be seen that as the VSC is working at unity power factor the voltage and current are in the same phase when working as a Rectifier and are out of phase at  $180^\circ$  when working as an Inverter. The voltage  $V_{dc}$  of the battery increases from 800 V to 825 V in case of VSC operating as rectifier i.e the battery charges when VSC is in rectifier mode.

## VOLTAGE SOURCE CONVERTER AND ITS CONTROL

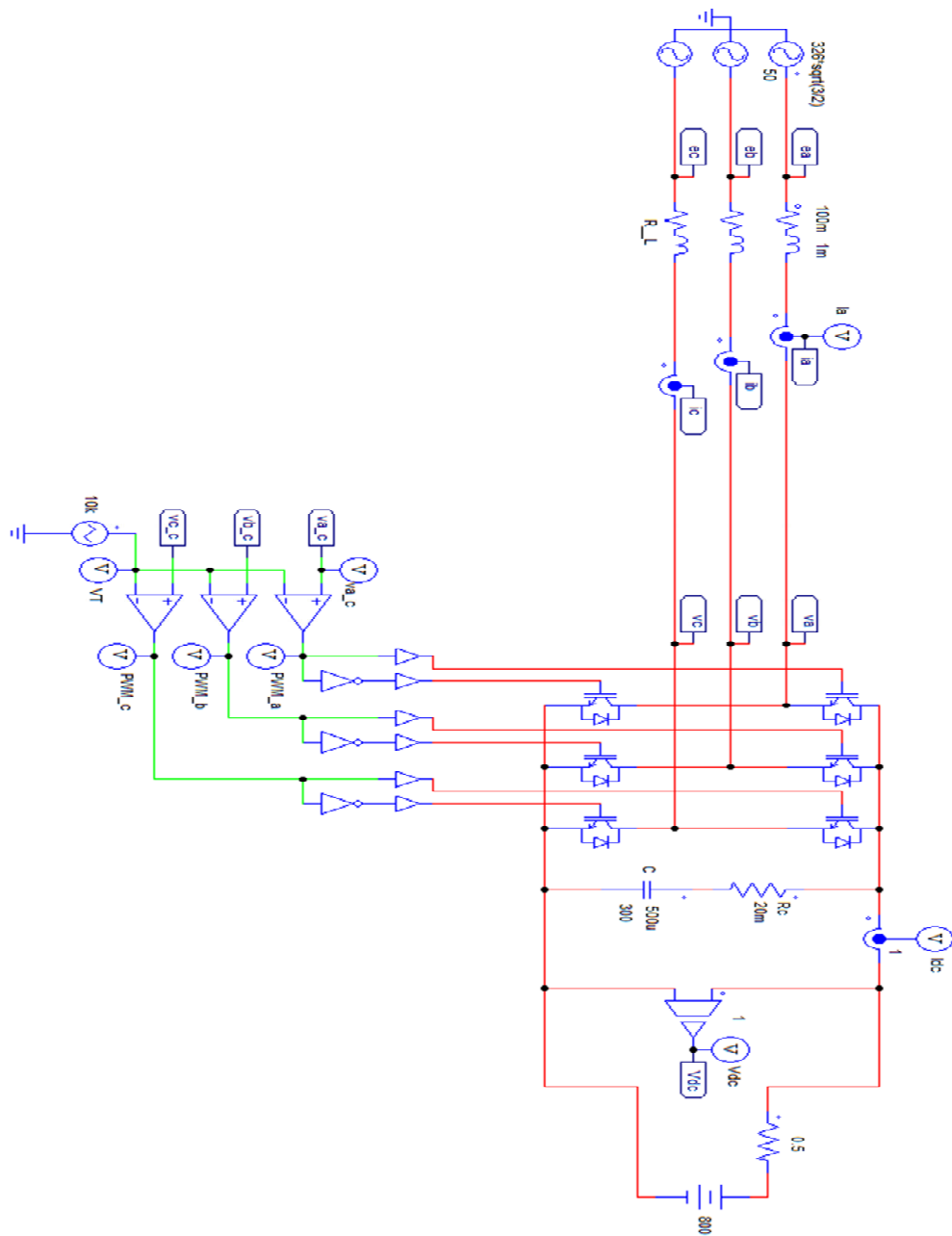


Figure 3.23 VSC connected with the Grid at 400 Line to Line (rms).

## VOLTAGE SOURCE CONVERTER AND ITS CONTROL

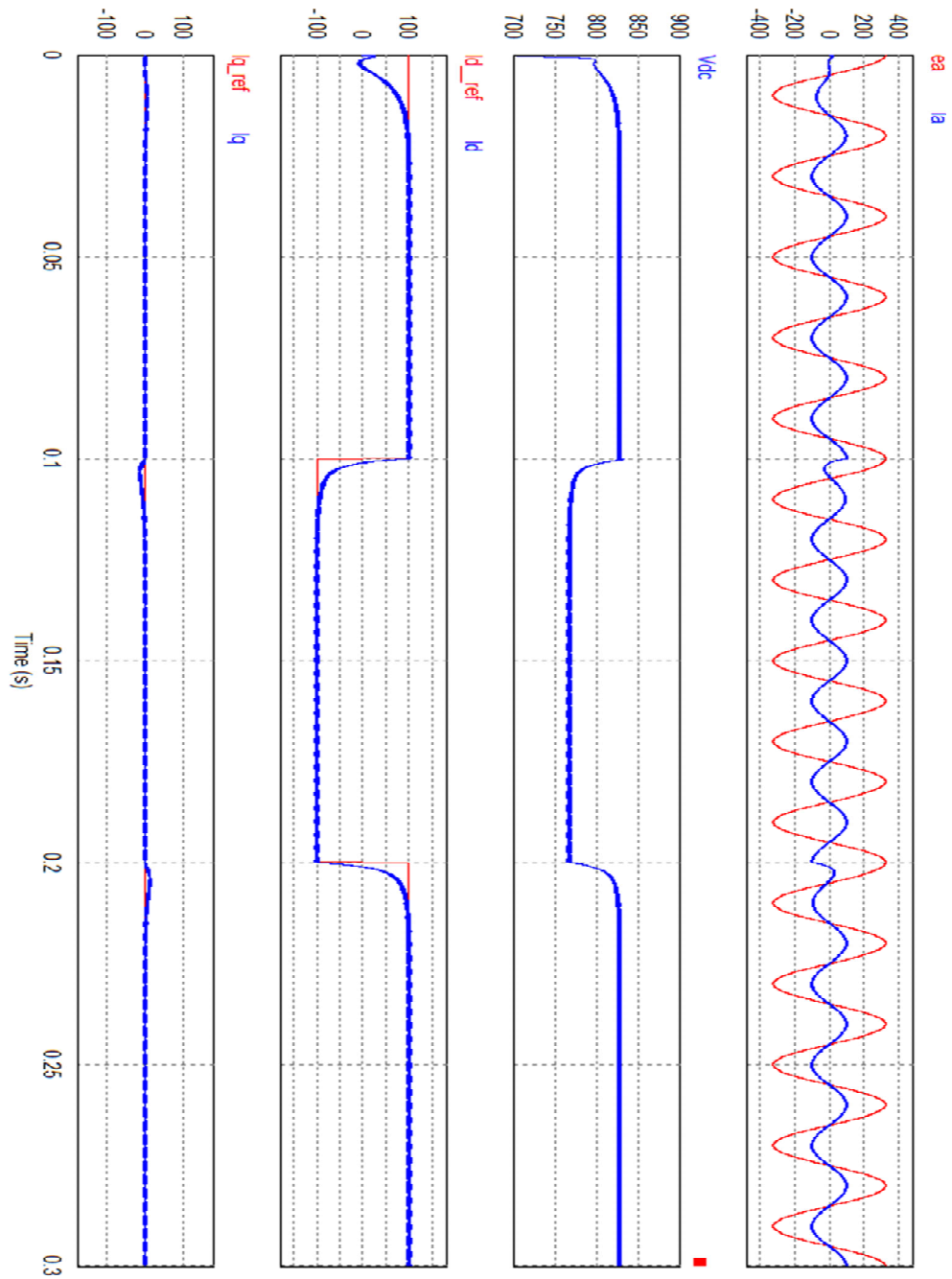


Figure 3.24 VSC working as rectifier and as inverter at UPF( Unity Power Factor);  $I_d$  = constant = 100A;  $I_d$ = single phase peak current;  $I_d$ =+100A and  $I_q$ =0 .

# VOLTAGE SOURCE CONVERTER AND ITS CONTROL

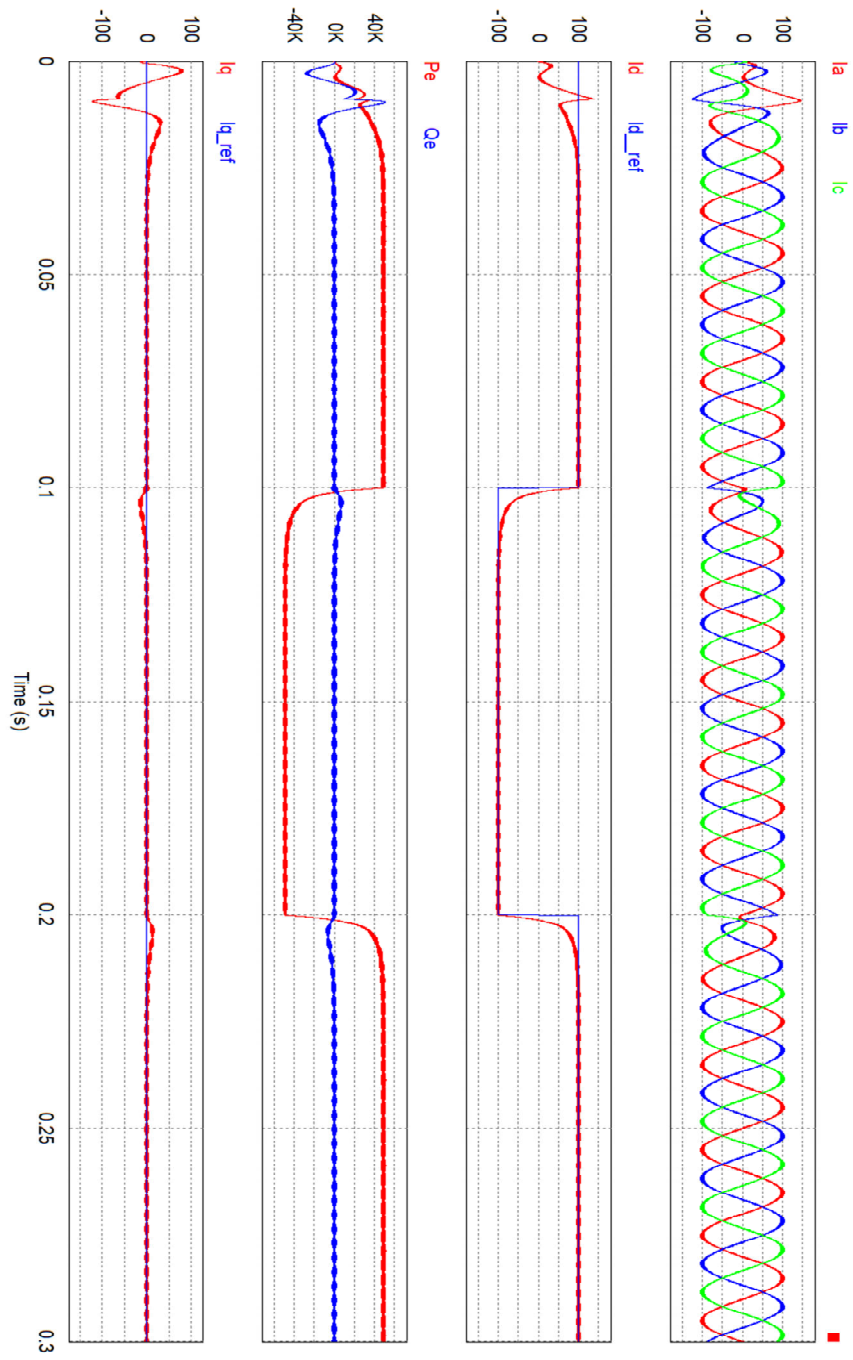


Figure 3.25 VSC working as rectifier and as inverter at UPF  $I_d = \pm 100A$  and  $I_q = 0$ .

# VOLTAGE SOURCE CONVERTER AND ITS CONTROL

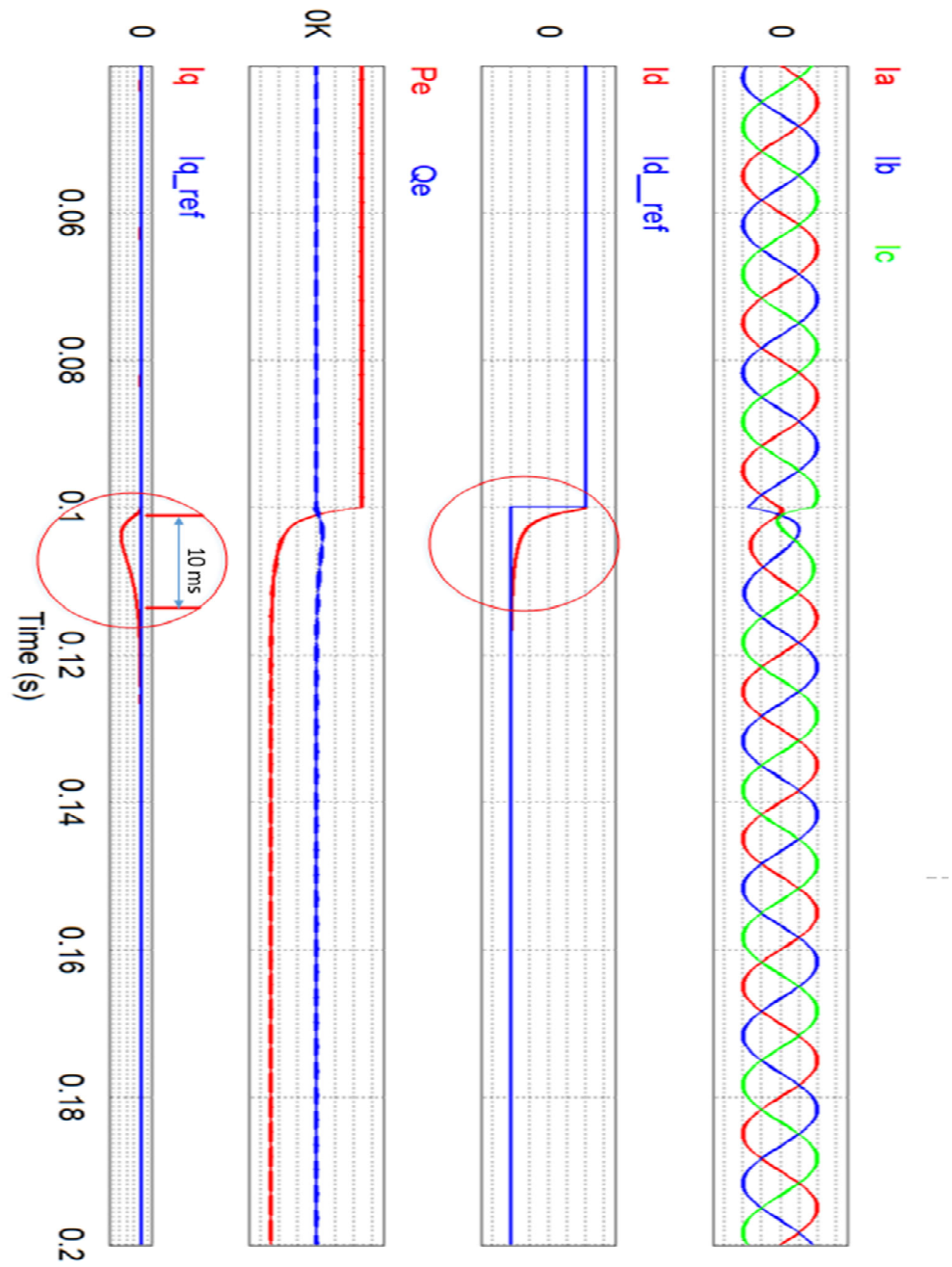


Figure 3.26 Enlarged View of  $I_d$  settling to  $I_{d\_ref}$  and the effect shown in  $I_q$ .

# VOLTAGE SOURCE CONVERTER AND ITS CONTROL

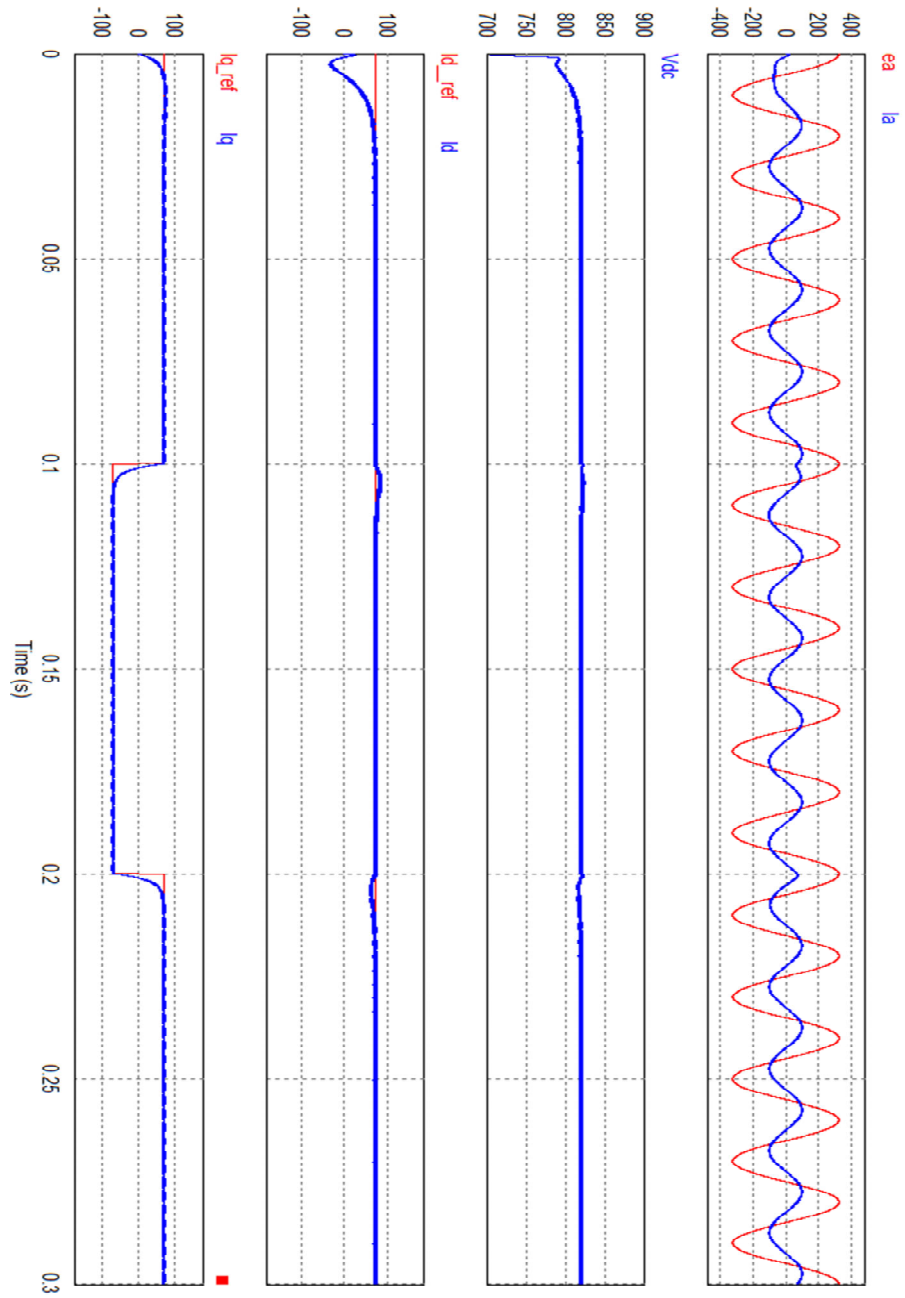


Figure 3.27  $i_a = \text{constant} = 100\text{A}$ ;  $i_d = +70.71\text{A}$  and  $i_q = +70.71\text{A}$ .



## VOLTAGE SOURCE CONVERTER AND ITS CONTROL

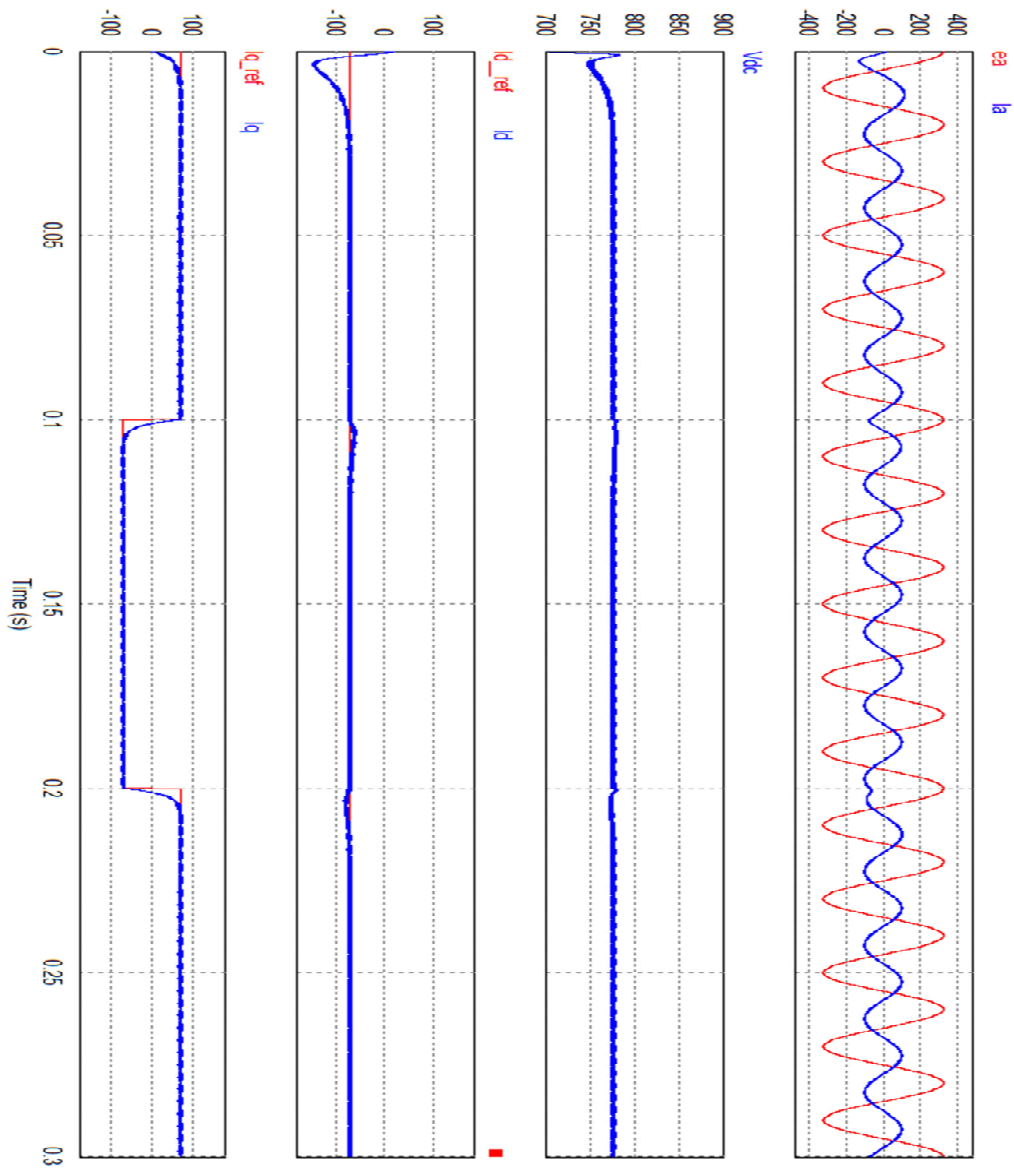


Figure 3.28 VSC working as inverter with capacitive and reactive power;  $I_a$  = constant = 100A;  $I_d$ =+70.71A and  $I_q$ =+/- 70.71A.

Similarly, when the VSC operates as an inverter the battery discharges and the terminal voltage decreases from 800 V to around 775V. The  $I_q$  reference is kept at 0 level and the  $I_d$  reference is changed from +100 to -100. It can be seen clearly that  $I_d$  and  $I_q$  follow  $I_d$  reference

and  $I_q$  reference and the changes are exactly followed within 10ms seconds. This shows that the controller designed is working properly with high dynamics.

Figure 3.25 shows the enlarged view of  $I_d$  following  $I_{d\_ref}$  which also shows that the controller is acting very fast to improve the dynamics. The red circle in the  $I_d$  reference shows that the settlement is within 10ms. Though there is decoupling done there are some transients in  $I_q$  reference also which is shown by a red circle in  $I_q$  reference. In chapter 5 it is shown that this transient in  $I_q$  axis is used to support the reactive power to the grid. The active power exchanged with the grid is around 49 kw shown as  $P_e$  in the Figure.

Figure 3.26 shows VSC working as a rectifier with the capacitive and reactive load. The references when working as a capacitive is  $I_d=+70.71A$  and  $I_q=-70.71A$  which shows that the current waveform is leading the voltage waveform. As soon as the  $I_q$  reference is changed from 70.71 A to -70.71 the mode of operation changes from capacitive to an inductive mode which can be seen from the waveform voltage and current. In case of  $I_q$  reference positive the current is leading the voltage and as soon as the reference is changed to to negative the current waveform lags the voltage waveform. The  $I_d$  reference is kept constant at +70.71 A which guarantees the rectifier operation of the VSC. As the operation is in rectifier mode the voltage of the battery is higher than 800V which shows the charging of the battery.

Figure 3.27 shows VSC working as an inverter both in capacitive and reactive mode. The value of  $I_d$  reference is always kept negative which shows it is always supplying power to the grid. When  $I_q$  is positive 70.71 A the VSC is operating in a capacitive mode in which the current waveform leads in phase angle with the voltage waveform. In this case, the inverter supplies the capacitive power to the grid. The reactive power supplied is nearly 34.5 kVAR. Similarly, when the reference of  $I_q$  is made negative the inductive power of nearly 34.5 kVAR is supplied to the grid which is shown by lagging current waveform to the voltage waveform in phase angle.

### 3.6 Conclusion

The details of VSC and its controller are discussed in this chapter. The types of VSC for the interface of DG in MG are discussed. The modeling of the VSC is done in parts as AC side, DC side and then VSC as a combined unit. The Laplace model is also developed and the advantages of

## VOLTAGE SOURCE CONVERTER AND ITS CONTROL

using Laplace model are discussed. The dq transformation to support the controller design is explained and finally, the controller in dq reference frame is developed. The modulation index necessary to use in designing the controller is explained and finally, the synchronous technique used in this work is explained with necessary diagrams. Finally, the operation of the VSC in different modes of operation is described as a method to put the VSC running in high dynamics condition able of contributing to handling the issues found in MGs.

## 4. REACTIVE POWER CONTROL USING VOLTAGE SOURCE CONVERTER

### 4.1 Introduction

The detailed model of the VSC explained in chapter three is used to contribute reactive power to the MG with fast dynamics through distributive approach in this thesis. This chapter introduces the technical problem in sharing reactive power flow in the MG. The reactive power sharing problem in this thesis is handled with a new approach in which the VSC views the rest of the MG as Thevenin's equivalent impedance (TEI). This TEI includes both line impedance and change in load. The VSC observes and acts according to the change in this TEI. The proper vector control of the VSC makes it possible to contribute desired power flow with fast dynamics. The power flow with different line parameters and different loads with the vector control designed in chapter three is carried over in this chapter.

### 4.2 The problem with reactive power sharing

The control methods to MGs are challenging as it is quite different from traditional distribution systems. The methods which are widely used for the control of the MGs are traditional droop control methods having a central control system. The reason for using the traditional droop control method is to copy the behaviour of the traditional synchronous generator and be more reliable as it has plug and play approach. It can avoid high cost, complexity, and requirements of a supervisory control. On the other hand, using traditional droop control method brings some drawbacks in the system which can be written point wise as below [91]:

- ✚ The control objectives in MG are multiple as there are many variables to be controlled simultaneously. If one variable is controlled using traditional droop control method then another variable also gets affected. For example, a design trade off needs to be considered in between the voltage  $f/V$  regulations and load P/Q sharing.
- ✚ The voltage is not a global variable as frequency so there are complications in controlling voltage in comparison to frequency. Thus, the reactive power control is difficult to share

## REACTIVE POWER CONTROL USING VOLTAGE SOURCE CONVERTER

between the renewable resources and may result in circulating reactive current[40][92].

- ✚ The lines are resistive in MG due to which the active and reactive power is highly coupled in power flow equations [3].

The problem of reactive power sharing in MG is discussed by modelling a simple circuit as shown in Figure 4.1. The figure shows the simulation of two renewable sources supplying a common load [5]. The changes in reactive power sharing are observed by changing the position of the loads, one is at point 1 and other is at point 2 as shown in Figure 4.1. There are two renewable sources connected in the MG and the load is shifted from position 1 to position 2. Two loads are connected by an automatic switch in between. One load is 25kW, 5 kVAR and other is 50 kW and 10 kVAR. The second load is put on in the circuit after 10s and the response is observed.

Furthermore, it is shown that these two loads connected are changed in two points, initially at point 1 and later at point 2. It is observed that even after keeping the same load and the same source if the position of the load is changed then there are changes in reactive power sharing which are shown in the subsequent figures. As explained above the load consists of two blocks and the second one is put on after 10 s. Figure 4.2 shows that there is an increase in active power demand from both the sources after the second load is put on at 10 s. In both the position of the load i.e. at position 1 and position 2 the load is increased after 10 s. Figures from 4.2 to 4.9 show the change in the supply pattern from both the sources with the change of load positions.

The active power supplied by DG1 when the load is at position 1 is initially 17 kW and after 10s it is 47 kW which is shown in Figure 4.2. Similarly, the active power supplied by DG2 when the load is at position 1 is 8 kW and 24 kW at position 2 respectively as shown in Figure 4.3. Figure 4.4 and Figure 4.5 show that the reactive power supplied by DG source 1 is on negative side whereas the reactive power supplied by DG source 2 is 7 and 17 kVAR respectively. The active power and the reactive power supplied by source DG1 is higher because of the fact that the connecting line resistance of source one is much lower in comparison to source DG2.

## REACTIVE POWER CONTROL USING VOLTAGE SOURCE CONVERTER

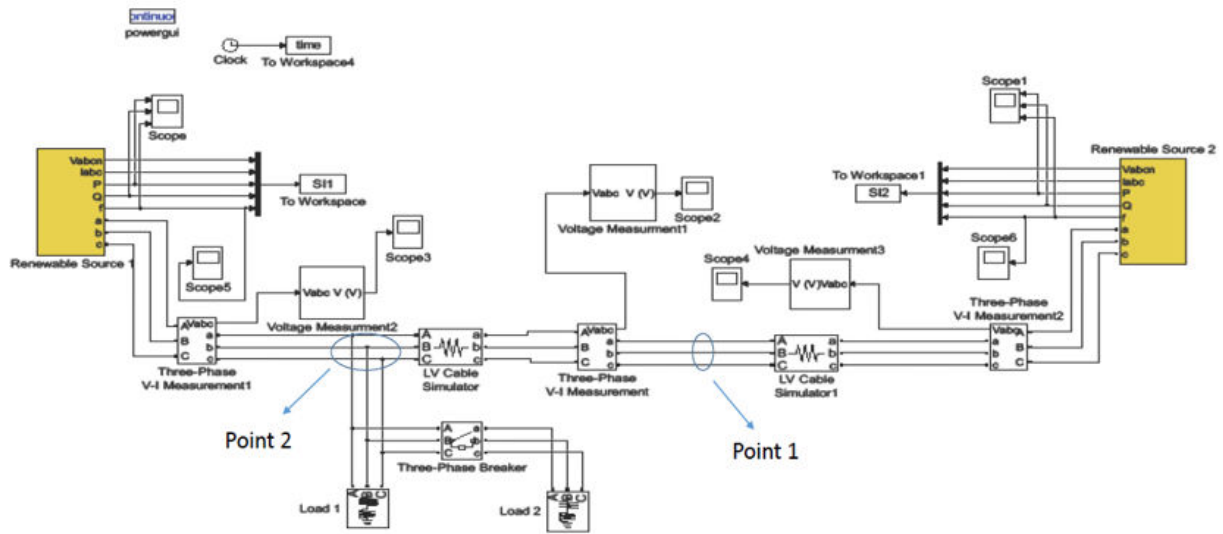


Figure 4.1 Three phase VSC model [5].

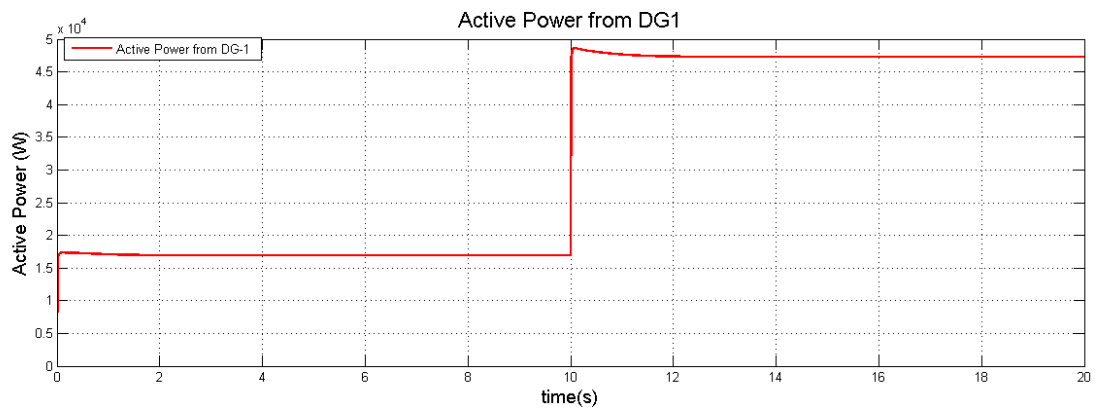


Figure 4.2 Active power supplied by the DG1 while load in point 1.

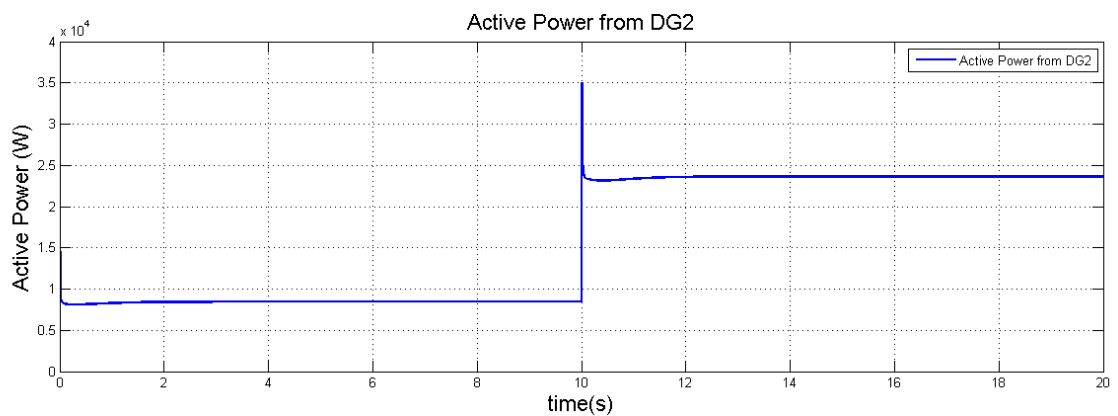


Figure 4.3 Active power supplied by DG2 while the loading is in point 1.

## REACTIVE POWER CONTROL USING VOLTAGE SOURCE CONVERTER

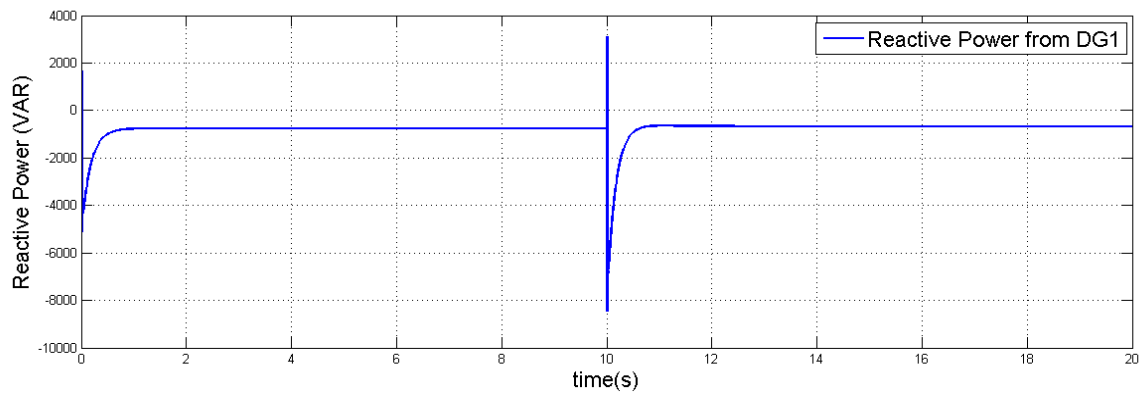


Figure 4.4 Reactive power supplied by DG1 while loading in point 1.

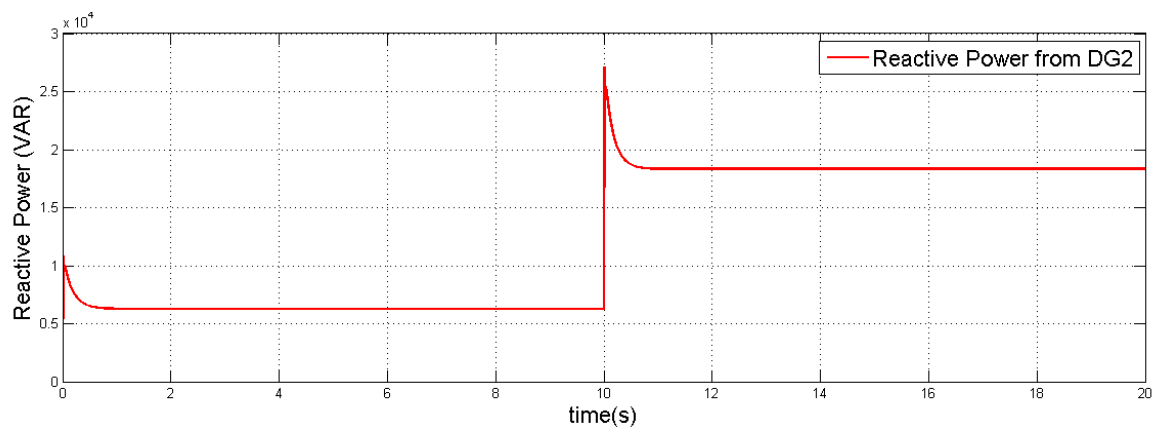


Figure 4.5 Reactive power supplied by DG2 while loading in point 1.

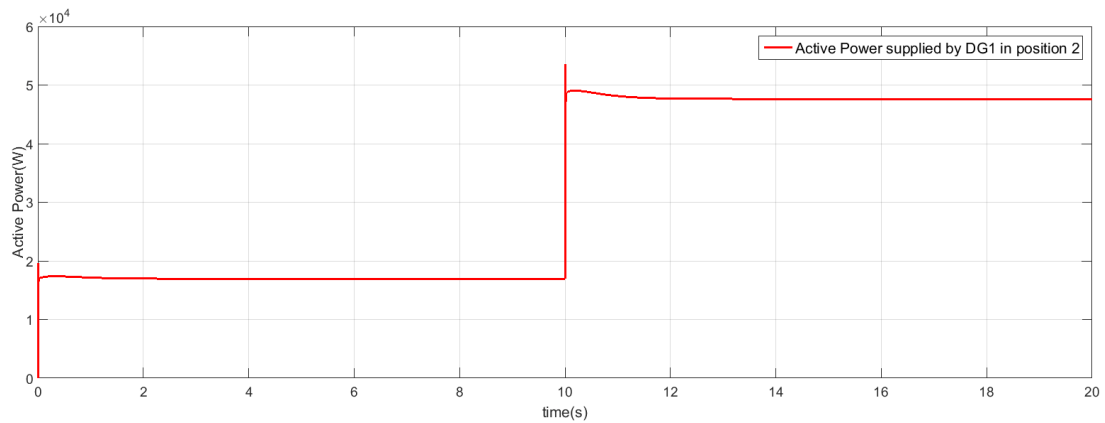


Figure 4.6 Active power supplied by DG1 while loading in point 2.

## REACTIVE POWER CONTROL USING VOLTAGE SOURCE CONVERTER

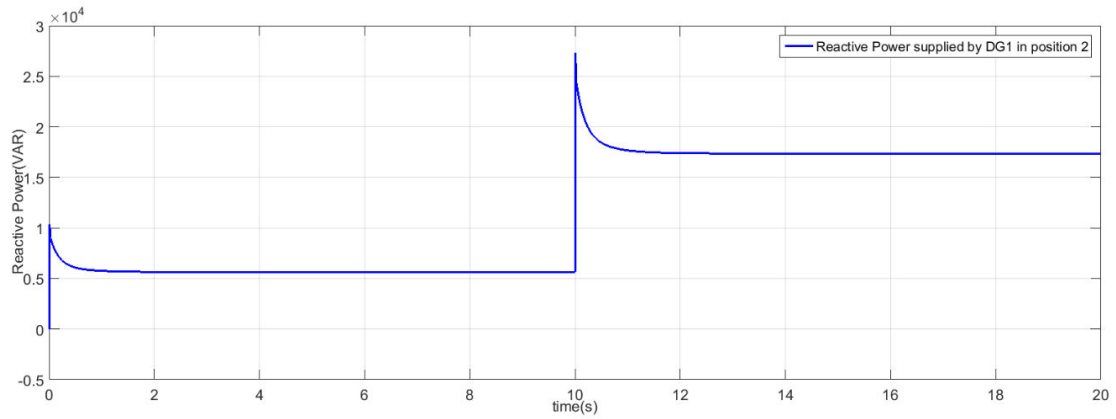


Figure 4.7 Reactive power supplied by DG1 while the loading is in point 2.

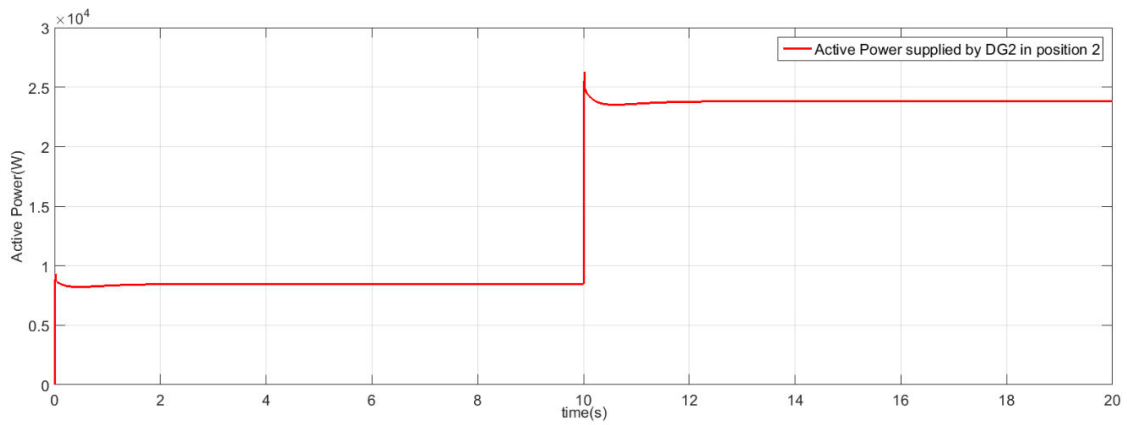


Figure 4.8 Active power supplied by DG2 while the loading is in position 2.

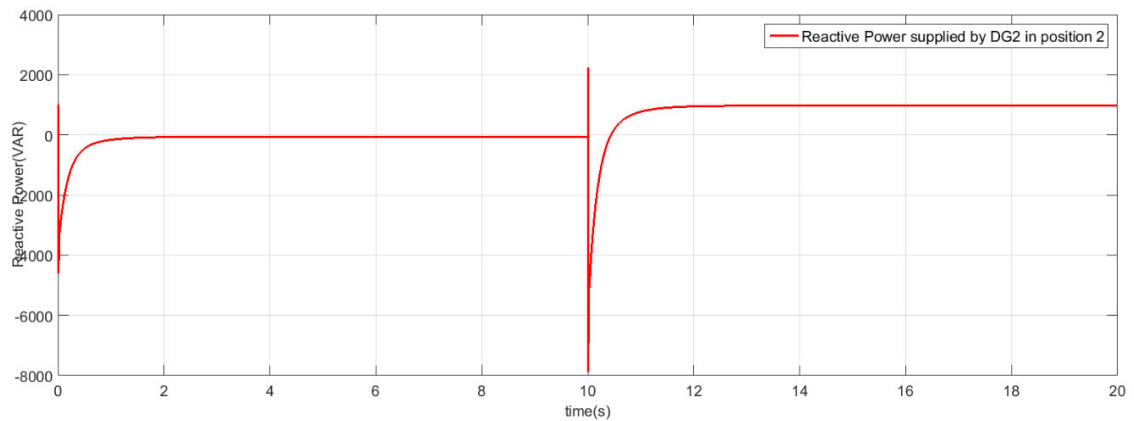


Figure 4.9 Reactive power supplied by DG2 while the loading is in position 2.

Similarly, the active power supplied by DG1 remains 17 kW and 47 kW when the load is shifted from point 1 to point 2, which is shown in figure 4.6. The active power supplied by source



## REACTIVE POWER CONTROL USING VOLTAGE SOURCE CONVERTER

DG 2 also remains same as the load was in point 1 which is shown in figure 4.8. The reactive power supplied by DG1 with the load placed in point 2 changes a lot as shown in figure 4.7. When the load is at point 1 the reactive power supplied by source 1 is negative which changes to the positive value of 5 kVAR initially and 16 kVAR after 10 seconds when the load is put in position 2. Similarly, the reactive power supplied by DG 2 changed to 0 kVAR and 0.5 kVAR respectively as shown in figure 4.9. The conclusions drawn after going through these observations are: -

- ✚ The active power sharing is independent of the position of the load changes.
- ✚ The reactive power sharing depends deeply on load changes which are also shown in the Figures 4.4, 4.5, 4.7 and 4.9.

The above observations allow at concluding that voltage cannot be considered as a global variable like frequency. As the reactive power sharing among renewable sources depends on the voltage levels, it is not easy to control as the active power which is controlled mainly by the frequency [93]. The high resistance of the MGs in comparison with the traditional grids introduces more complexity in controlling the grid [94]. As a result of high resistances of the MG lines the assumptions ( $R \ll X$ ) which is generally considered in traditional grids to make the calculations simpler cannot be assumed for the MG.

The reactive power sharing which is discussed in most of the research work are the methods which are controlled by the central supervisor and communication system. However, a new approach can be established considering the ability to use the operating characteristics of VSC with vector control. So the work of this thesis is to find a solution to this reactive power sharing. Most of the work done in research work around the world use one or other methods using a communication system which transmits the reference signals to the individual power sources. Though the use of communication system helps in maintaining the voltage level within the limit and the power sharing is also accurate, it has certain disadvantages which can be listed as below[95]: -

1. The communication lines between the different sources and equipment result in increased cost of the system.
2. The long distance communication lines will be easier to get interfered, thus reducing system reliability and expandability.

3. Another disadvantage of the central controller is that the current references are to be distributed to all converters by using high-bandwidth communication links [95], in order to achieve synchronization among the units.
4. In a microgrid, there may be many small generators available which will be far away from a common controller. In such case, it is economically not feasible to have line communication for those production units.

Considering the above points it can be concluded that the control methods which solely based on local measurements exhibit a superior redundancy, as they do not rely on a communication system for reliable operation[3][96].The main aim of this work is to develop a distributed control system in which the communication system between the DG sources has to provide data at a much less baud rate.

#### 4.3 Reactive Power Flow with different line parameters.

The problem of reactive power sharing discussed in section 4.2 is carried out considering the traditional lines in which the resistive part in the power flow equation can be neglected in comparison with the inductive part. This case cannot be considered in all the MGs as the low voltage MGs is highly resistive and in such case, the dependency just gets reversed. So it is required to develop a general relation which will be valid for every case of the line impedance values.

Figure 4.10 (a) shows power flow from point A and B in a MG and Figure 4.10 (b) shows the vector representation of the power flow. The power flow between point A and point B is described here in brief with different cases of line value. The power flow can be derived as

$$P + jQ = \underline{S} = \underline{U_1} \underline{I}^* = \underline{U_1} \left( \frac{\underline{U_1} - \underline{U_2}}{\underline{Z}} \right)^* \dots\dots\dots (4.1)$$

$$= \underline{U_1} \left( \frac{\underline{U_1} - \underline{U_2} e^{j\delta}}{\underline{Z} e^{-j\theta}} \right) \dots\dots\dots (4.2)$$

$$= \frac{U_1^2}{Z} e^{j\theta} - \frac{U_1 U_2}{Z} e^{j(\theta+\delta)} \dots\dots\dots (4.3)$$

# REACTIVE POWER CONTROL USING VOLTAGE SOURCE CONVERTER

Thus the active and reactive power flows into the line are

$$P = \frac{U_1^2}{Z} \cos \theta - \frac{U_1 U_2}{Z} \cos(\theta + \delta) \quad \dots\dots\dots (4.4)$$

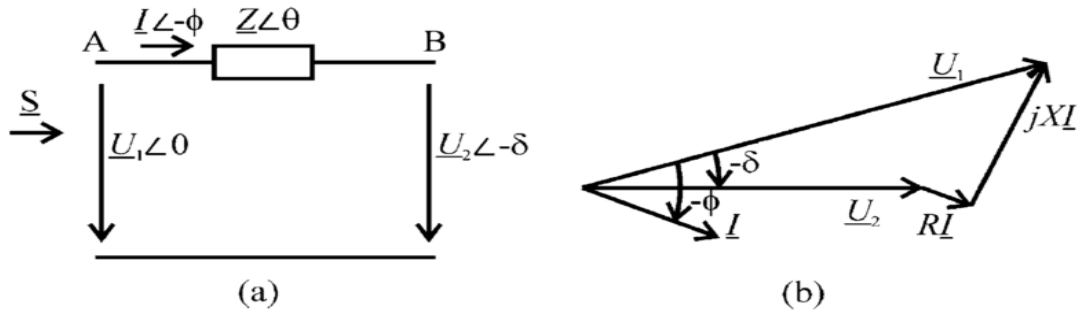


Figure 4.10 (a) Power flow through a line (b) Phasor Diagram.

$$Q = \frac{U_1^2}{Z} \sin \theta - \frac{U_1 U_2}{Z} \sin(\theta + \delta) \quad \dots\dots\dots (4.5)$$

With  $\underline{Z}e^{j\theta} = R + jX$ , equations (4.4) and (4.5) can be written as

$$P = \frac{U_1}{R^2 + X^2} [R(U_1 - U_2 \cos \delta) + XU_2 \sin \delta] \quad \dots\dots (4.6)$$

$$Q = \frac{U_1}{R^2 + X^2} [-RU_2 \sin \delta + X(U_1 - U_2 \cos \delta)] \quad \dots\dots (4.7)$$

$$U_2 \sin \delta = \frac{XP - RQ}{U_1} \quad \dots\dots\dots (4.8)$$

$$U_1 - U_2 \cos \delta = \frac{RP + XQ}{U_1} \quad \dots\dots\dots (4.9)$$

It can be assumed for overhead lines  $X \gg R$ , which means that  $R$  may be neglected. If the power angle  $\delta$  is assumed small enough, then  $\sin \delta \approx \delta$  and  $\cos \delta \approx 1$ . So equations (4.8) and (4.9) can be written (4.10) and (4.11)

$$\delta \approx \frac{XP}{U_1 U_2} \quad \dots\dots\dots (4.10)$$

$$U_1 - U_2 \approx \frac{XQ}{U_1} \quad \dots\dots\dots (4.11)$$

## REACTIVE POWER CONTROL USING VOLTAGE SOURCE CONVERTER

If the condition  $X \gg R$  is assumed the relations (4.10) and (4.11) show that the angle  $\delta$  can be controlled by controlling active power whereas the inverter voltage can be controlled by controlling the reactive power. Thus by adjusting  $P$  and  $Q$  independently, frequency and amplitude of the grid voltage are determined. Hence the well-known frequency and voltage droop regulation equations with active and reactive power can be written as (4.12) and (4.13).

$$f - f_0 = -K_p(P - P_0) \quad (4.12)$$

$$U_1 - U_0 = -K_q(Q - Q_0) \quad (4.13)$$

Where  $f_0$  and  $U_0$  are rated frequency and grid voltage respectively whereas  $P_0$  and  $Q_0$  are the active and reactive power at the rated frequency and voltage respectively.

The improvement to the control scheme is carried out considering  $R$  not to be neglected but in the general case, both  $X$  and  $R$  is considered. An orthogonal linear rotational transformation matrix  $T$  from active and reactive power  $P$  and  $Q$  to the modified active and reactive power  $P'$  and  $Q'$  can be written as 4.14.

$$\begin{bmatrix} P' \\ Q' \end{bmatrix} = T \begin{bmatrix} P \\ Q \end{bmatrix} = \begin{bmatrix} \sin \theta & -\cos \theta \\ \cos \theta & \sin \theta \end{bmatrix} \begin{bmatrix} P \\ Q \end{bmatrix} = \begin{bmatrix} \frac{X}{Z} & -\frac{R}{Z} \\ \frac{R}{Z} & \frac{X}{Z} \end{bmatrix} \begin{bmatrix} P \\ Q \end{bmatrix} \quad (4.14)$$

Applying these relations to equation (4.8) and (4.9), the equations (4.15) and equation (4.16) can be written as

$$\sin \delta = \frac{ZP'}{U_1 U_2} \quad (4.15)$$

$$U_1 - U_2 \cos \delta = \frac{ZQ'}{U_1} \quad (4.16)$$

The above relations 4.15 and 4.16 show the power flow depends on the parameters of line value. Now if the lines are assumed to be highly inductive then  $P' \cong P$  and  $Q' \cong Q$ , whereas for mainly resistive lines  $P' \cong -Q$  and  $Q' \cong P$ . Thus the frequency and voltage droop regulation can be written as (4.17) and (4.18.)

$$f - f_0 = -K_p(P' - P'_0) = -K_p \frac{X}{Z}(P - P_0) + K_p \frac{R}{Z}(Q - Q_0) \quad \dots\dots\dots (4.17)$$

$$U_1 - U_0 = -K_q(Q' - Q'_0) = -K_q \frac{R}{Z}(P - P_0) - K_q \frac{X}{Z}(Q - Q_0) \quad \dots\dots\dots (4.18)$$

## REACTIVE POWER CONTROL USING VOLTAGE SOURCE CONVERTER

It can be observed from equations 4.17 and 4.18 that the droop equations can be made to work in any case of the line impedances. The real value of the line impedances is not required but only the ratio is sufficient to work for. A partial concept of this approach has been investigated in some literature.

A step ahead to this approach has been applied in this research work in which the control circuit is made to measure the Thevenin's equivalent Impedance (ETI) connected to the VSC terminal. The VSC acts according to the value of this ETI and contributes reactive power to the MG. The ETI is measured by measuring parameters locally across the VSC terminal. Taking these variables as input the well-designed vector control of the VSC makes the VSC able to contribute reactive power with high dynamics (which is described in detail in section chapter 5. Section 4.4 describes the power flow using the VSC designed in PSIM which controls the power flow according to the demand using the controller.

### 4.4 Power Flow conducted using the designed controller in PSIM.

This section describes the power flow that can be conducted using the controller of the VSC designed in chapter 3. It is shown in this section that the active and reactive power flow can be controlled considering the variables separately with a fully decoupled design. It is also shown that the reactive power compensation can be handled by using the versatile functions of the VSC's. The work mostly carried out worldwide are the control of the MG that is done using the help of communication using MG central controller (MGCC). The work of thesis is to focus on a distributed approach in which each of the renewable resources connected with VSC will help the grid at the point of connection of renewable resources in terms of reactive power. This can be done by perfectly decoupling the active and reactive power of the grid and controlling the variables separately and using vector control of the VSC. The VSC will observe the grid connected across its terminal as an ETI whose value changes both due to position and magnitude of the load. The section below describes the basics of the VSC and its controller working using simulations on PSIM software. A brief introduction of the PSIM simulation is presented in section 4.4.1.

## 4.4.1 Description of the Simulation System

To validate the ideas of this research some of the simulations are conducted in MATLAB but most of the work is carried out in PSIM. This sub-section provides details of the simulation platforms and systems from which the simulation results have been obtained.

PSIM is software specifically designed for power electronics and electrical circuits with components like VSC, Controller etc. With fast simulation and friendly user interface, PSIM provides a powerful simulation environment for power electronics, analog and digital control, magnetics, and motor drive system studies. Powersim develops and markets leading simulation and design tools for research and product development in power supplies, motor drive, power conversion and control systems. The component models are relatively simple but sufficient for most electrical and electronics applications.

A circuit is represented in PSIM in four blocks: Power circuit, Control circuit, Sensors, and Switch controllers. The figure 4.11 shows the relationship between each block [97]. The power circuit consists of switching devices, RLC branches, transformers, and other discrete components. The control circuit is represented in the block diagram. Components in s domain and z domain, logic components (such as logic gates and flip flops), and nonlinear components (such as multipliers and dividers) can be used in the control circuit. The sensors used in the PSIM measure the voltages and currents of the power circuit and passes the values to the control circuit. Gating signals are then generated from the control circuit and sent back to the power circuit through switch controllers to control switches [97].

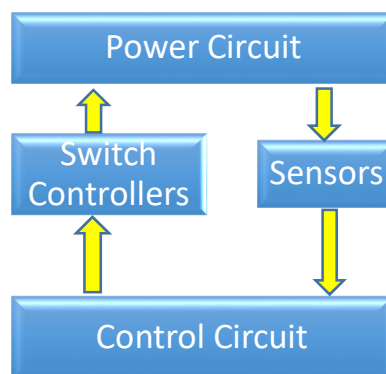


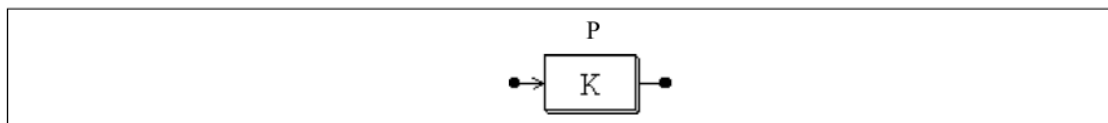
Figure 4.11 Relationship between PSIM blocks.

#### 4.4.2 Components of PSIM used in this Thesis

Some of the frequently used components in this thesis are presented in brief. The control circuit components used in this research work are: -

- **Proportional Controllers:** - The function of the proportional controller is to multiply the input with a constant. Figure 4.12 shows the image and attribute of a proportional controller.

**Image:**



**Attribute:**

Parameters	Description
Gain	Gain $k$ of the transfer function

Figure 4.12 Image and Attribute of Proportional Controller [98].

- **Integrators:** - The transfer function of an integrator is  $(s) = \frac{1}{sT}$ . There are two types of integrator. One is regular integrator (INT) and other is resettable integrator (RESETI). The output of the resettable integrator can be reset by an external control signal (at the bottom of the block). For the edge reset (reset flag = 0), the integrator output is reset to zero at the rising edge of the control signal. For the level reset (reset flag = 1), the integrator output is reset to zero as long as the control signal is high (1). The image and attribute is shown in Figure 4.13.



**Attribute:**

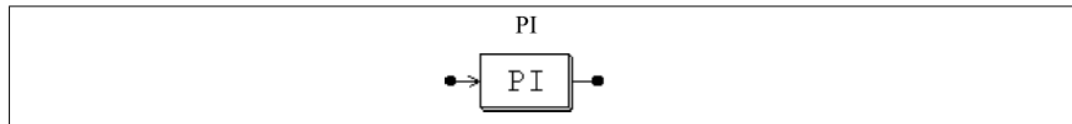
Parameters	Description
Time Constant	Time constant $T$ of the integrator, in second
Reset Flag	Reset flag (0: edge reset; 1: level reset) (for RESETI only)

Figure 4.13 Image and Attribute of Integrator [98].

## REACTIVE POWER CONTROL USING VOLTAGE SOURCE CONVERTER

➤ **Proportional-Integral Controllers:** - The transfer function of a proportional-integral (PI) controller written as  $G(s) = k \cdot \frac{1+ST}{ST}$ . The image and attributes of PI controller is shown in Figure 4.14.

**Image:**



**Attributes:**

Parameters	Description
Gain	Gain $k$ of the PI controller
Time Constant	Time constant $T$ of the PI controller

Figure 4.14 Image and attribute of PI controller [98].

➤ **Fast Fourier Transform Blocks:** - A Fast Fourier Transform block calculates the fundamental component of the input signal. The FFT algorithm is based on the radix-2/decomposition-in-frequency method. The number of the sampling points within one fundamental period should be  $2N$  (where  $N$  is an integer). The maximum number of sampling points allowed is 1024. The output gives the amplitude (peak) and the phase angle of the input fundamental component. The output voltage (in complex form) is defined as

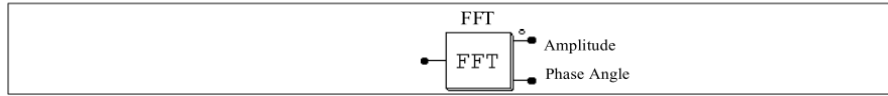
$$V_0 = \frac{2}{N} \sum_{n=0}^{n=\frac{N}{2}-1} \left[ \left\{ V_{in}(n) - V_{in} \left( n + \frac{N}{2} \right) \right\} \cdot e^{-j \frac{2\pi n}{N}} \right] \quad \dots\dots\dots (4.19)$$

The image and the attributes of Fast Fourier Transform Block are shown in Figure 4.15. This block can also be used to find the magnitude and angle of an alternating quantity. For e.g. If the input is  $100\sin(\omega t)$ , the output will be: Amplitude = 100; Angle = 0. Similarly, if the input is  $100\sin(\omega t + \pi/6)$ , the output will be: Amplitude = 100; Angle = 30. deg.



## REACTIVE POWER CONTROL USING VOLTAGE SOURCE CONVERTER

**Image:**



**Attributes:**

Parameters	Description
No. of Sampling Points	No. of sampling points $N$
Fundamental Frequency	Fundamental frequency $f_b$ , in Hz.

Figure 4.15 Image and attribute of FFT.

➤ **THD (Total Harmonic Distortion) Blocks:** - The total harmonic content of the ac wave which has distorted wave can be given as

$$THD = \frac{V_h}{V_1} = \frac{\sqrt{V_{rms}^2 - V_1^2}}{V_1} \dots\dots\dots (4.20)$$

Where,  $V_1$  is the fundamental component (RMS),  $V_h$  is the harmonic RMS value, and  $V_{rms}$  is the overall rms value of the waveform. The block diagram of the THD block is shown in Figure 4.16.

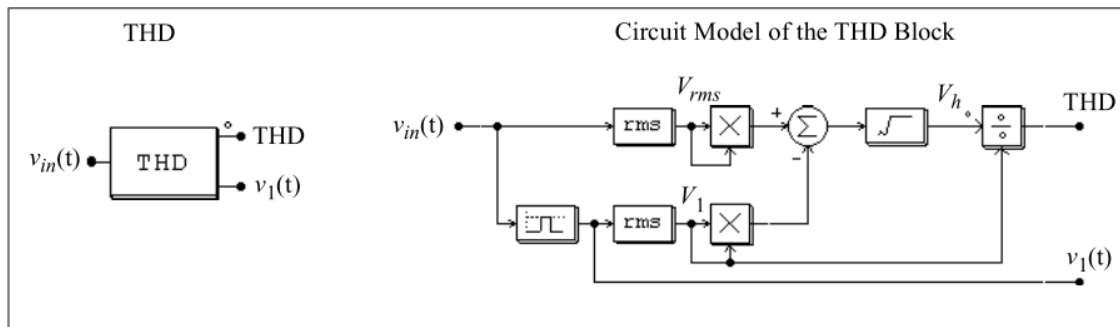


Figure 4.16 Image and circuit model of the THD block [98].

➤ **Voltage and Current Sensors:** -Voltage and current sensors measure the voltages and currents of the power circuit and send the value to the control circuit. The current sensor has an internal resistance of  $1 \mu\Omega$ . The image of voltage sensor (VSEN) and current sensor (ISEN) is shown in Figure 4.17.

**Images:**


Figure 4.17 Voltage and Current Sensor.

➤ **ABC to DQ Transformation Blocks:** - There are functional blocks which convert the abc three phase quantity to dq reference frame. Similarly, dq to abc transformation block is also there in PSIM. These blocks can be used in either the power circuit or the control circuit. It should be noted that, in the power circuit, currents must first be converted into voltage quantities (using current-controlled voltage sources) before they can be transformed. The transformation equation from abc to dq is represented in equation 4.3.

$$\begin{bmatrix} V_d \\ V_q \\ V_0 \end{bmatrix} = \frac{2}{3} \begin{bmatrix} \cos \theta & \cos \left( \theta - \frac{2\pi}{3} \right) & \cos \left( \theta + \frac{2\pi}{3} \right) \\ \sin \theta & \sin \left( \theta - \frac{2\pi}{3} \right) & \sin \left( \theta + \frac{2\pi}{3} \right) \\ \frac{1}{2} & \frac{1}{2} & \frac{1}{2} \end{bmatrix} * \begin{bmatrix} V_a \\ V_b \\ V_c \end{bmatrix} \quad \dots\dots\dots (4.21)$$

Similarly, the transformation from dq to abc is given in equation 4.4. The images of both the transformation are shown in Figure 4.18.

$$\begin{bmatrix} V_a \\ V_b \\ V_c \end{bmatrix} = \begin{bmatrix} \cos \theta & \sin \theta & 1 \\ \cos \left( \theta - \frac{2\pi}{3} \right) & \sin \left( \theta - \frac{2\pi}{3} \right) & 1 \\ \cos \left( \theta + \frac{2\pi}{3} \right) & \sin \left( \theta + \frac{2\pi}{3} \right) & 1 \end{bmatrix} * \begin{bmatrix} V_d \\ V_q \\ V_0 \end{bmatrix} \quad \dots\dots\dots (4.22)$$

## REACTIVE POWER CONTROL USING VOLTAGE SOURCE CONVERTER



Figure 4.18 abc to dq0 and dq0 to abc transformation block.

### 4.4.3 PSIM Block to measure phase angle between voltage and current

The two major measurement required in measuring an electrical quantity is the magnitude and phase angle. The measurement of the phase angle cannot be made directly with inbuilt PSIM block. The arrangement made to measure the phase angle is presented in Figure 4.19.

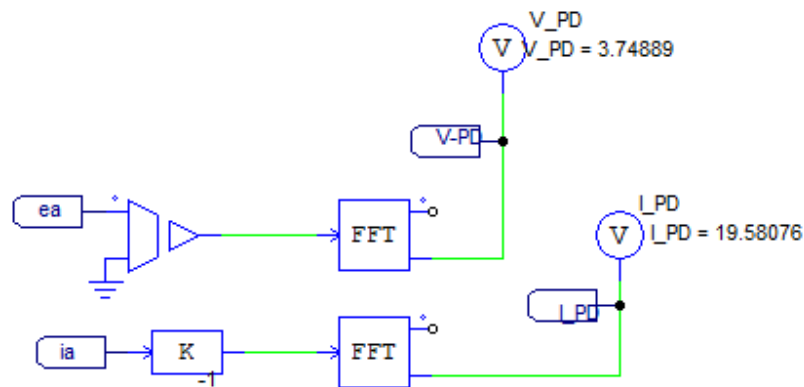


Figure 4.19 Phase angle measurement between voltage and current.

Figure 4.19 shows that FFT block has been used. The FFT block calculates the fundamental component of the input. The FFT algorithm is based on the radix-2/decimation-in-frequency method. The number of the samples in one fundamental period should be where  $N$  is an integer. The maximum number of sampling points allowed is 1024. The output gives the amplitude (peak) and the phase angle (in deg.) of the input fundamental component[98]. The output of this block is used to measure the phase difference between voltage and current.  $ea$  and  $ia$  are the instantaneous values of voltage and current of the VSC.  $V\_PD$  is the phase angle of the voltage and  $I\_PD$  is the phase angle of the current supplied by the VSC.

#### 4.4.4 PSIM Block to measure the inductive or capacitive part of the impedance.

The VSC has to estimate the exact value of impedance (both line and load) to support the grid in reactive power. The controller of the VSC measures the inductive or capacitive value of the impedance using the PSIM block shown in the Figure 4.20.

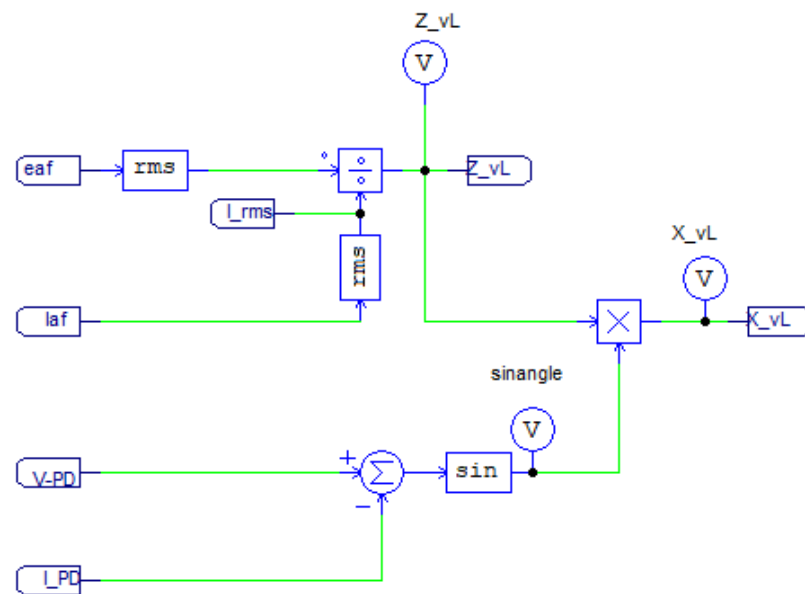


Figure 4.20 Measurement of equivalent impedance (Inductive or Capacitive).

Figure 5.20 shows the calculation of equivalent inductive or capacitive reactance across the VSC. It can be observed that it considers both the phase angle and magnitude of the voltage and current of the VSC. Using the block shown in Figure 4.19 the phase angle is measured and it is used to calculate the reactance of the circuit across the VSC. The inductive reactance is measured by multiplying impedance with sine of the angle between voltage and current.

#### 4.4.5 Power Flow using the designed controller in PSIM

VSC is a bidirectional converter which can convert the ac power from DC to AC and vice versa [99]. The VSC can control the active power that crosses the converter from the DC side to the AC side and vice-versa. Similarly, it can control the reactive power that is exchanged between the AC source and the AC side of the VSC. If properly controlled VSC can set reactive power as

## REACTIVE POWER CONTROL USING VOLTAGE SOURCE CONVERTER

inductive, capacitive or null independently of the active power [99]. This characteristic of the VSC is further described using the simple circuit of the VSC and its working principle as shown in Figure 4.19 [77].

VSC is modelled in PSIM software and the controller which is discussed in section 3.3 is used implementing in PSIM software. Figure 4.21 shows the VSC connected to the grid having a line to line RMS value of voltage is equal to  $200 \cdot \sqrt{3/2}$ . The voltage source converter and the grid can be drawn in a simplified diagram to analyze the power flow as shown in Figure 4.22. Taking this figure into account the analysis is done on the power flow between the VSC and the grid. The dc side voltage of the VSC is considered 600V.

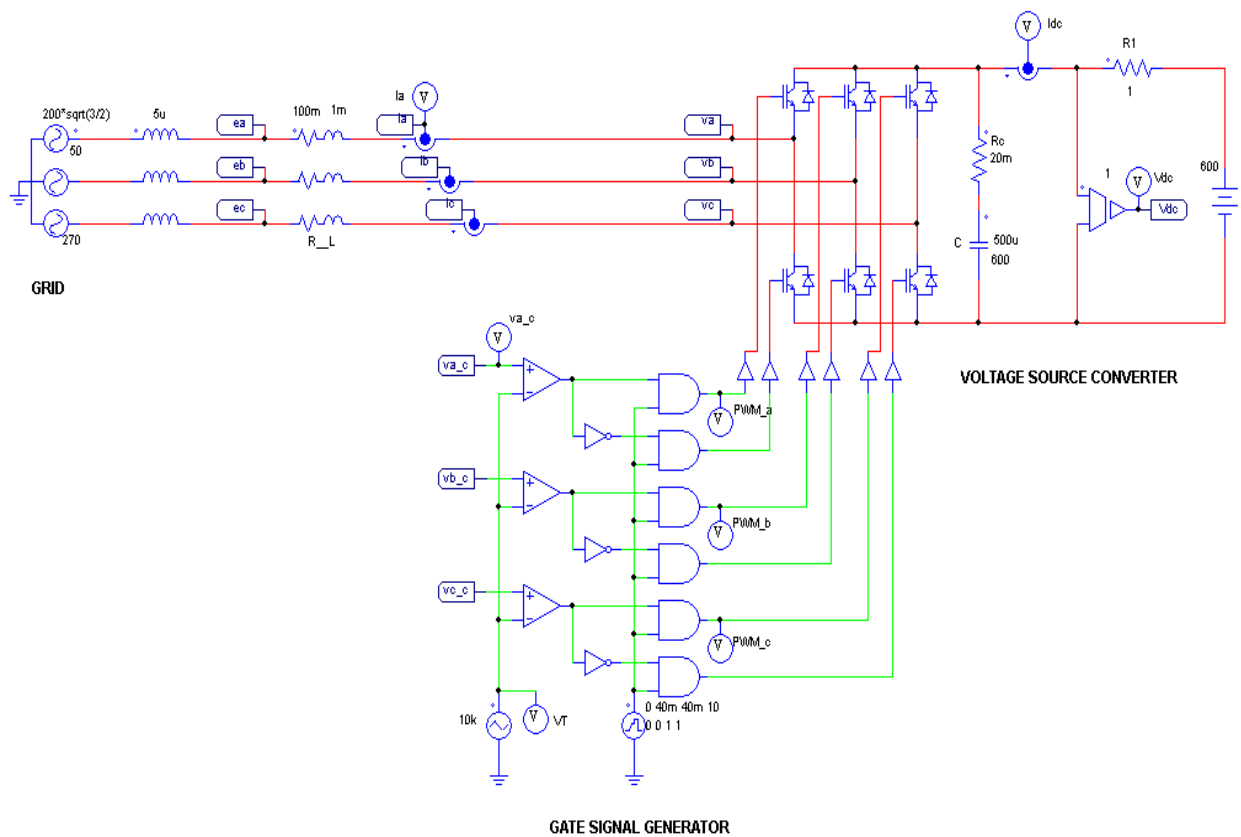


Figure 4.21 VSC connected to a grid through a line having an inductance of 100 m H and resistance of 1 m-ohm.

# REACTIVE POWER CONTROL USING VOLTAGE SOURCE CONVERTER

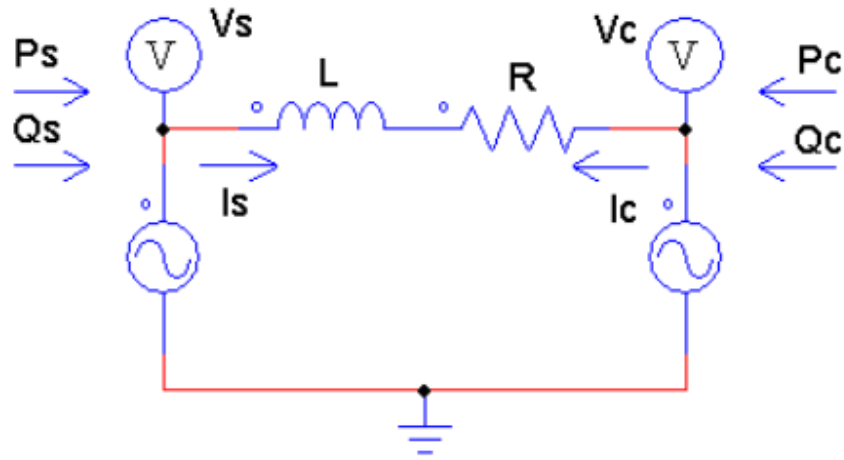


Figure 4.22 Single line diagram of VSC connected to a grid.

As shown in Figure 4.22  $V_s$  represents the grid as one of the source and  $V_c$  represents the voltage of the VSC. The active and reactive power flow between Grid and the VSC is denoted by  $P_s$ ,  $Q_s$  and  $P_c$ ,  $Q_c$  respectively. In time domain the voltage equations of voltage source converter and the grid can be represented as

$$V_s(t) = \sqrt{2}V_{s\text{rms}} \sin(\omega t) \quad \text{where } \omega t = \theta_1$$

$$V_c(t) = \sqrt{2}V_{c\text{rms}} \sin(\omega t + \delta) \quad \dots (4.23)$$

where  $\theta_2 - \theta_1 = \delta$

In complex or frequency domain the above equations can be written as

$$\vec{V}_s = |V_s| e^{-i\theta_1} \text{ and } \vec{V}_c = |V_c| e^{-i\theta_2} \quad \dots (4.24)$$

$$\text{Where } |V_s| = V_{s\text{rms}} = V_s \text{ and } |V_c| = V_{c\text{rms}} = V_c$$

Power viewed from  $V_s$  can be written as  $S_s = P_s + jQ_s = VI^*$  where  $I^* = \frac{\vec{V}_s^* - \vec{V}_c^*}{\vec{Z}}$ , Now

simplifying the equation of power  $S_s$  by putting the value of  $I^*$  we get

$$S_s = \vec{V}_s^* \frac{\vec{V}_s^* - \vec{V}_c^*}{\vec{Z}} = \frac{V_s^2 - V_s V_c e^{j(\theta_1 - \theta_2)}}{R - jX} = \frac{V_s^2 - V_s V_c e^{j\delta}}{R - jX} \quad \dots (4.25)$$

Now the power viewed from  $V_s$  the equation can be written as

# REACTIVE POWER CONTROL USING VOLTAGE SOURCE CONVERTER

$$S_s = P_s + jQ_s = \frac{RV_s^2 - RV_sV_c \cos \partial - XV_sV_c \sin \partial}{R^2 + X^2} + j \frac{XV_s^2 - XV_sV_c \cos \partial - RV_sV_c \sin \partial}{R^2 + X^2} \dots\dots\dots (4.26)$$

Similarly, the power viewed Vc the equation can be written as

$$S_c = P_c + jQ_c = \frac{RV_c^2 - RV_sV_c \cos \partial - XV_sV_c \sin \partial}{R^2 + X^2} + j \frac{XV_c^2 - XV_sV_c \cos \partial - RV_sV_c \sin \partial}{R^2 + X^2} \dots (4.27)$$

Now assuming  $R \ll X$  and neglecting R the above equations can be simplified as

Power viewed from Vs

$$S_s = P_s + jQ_s = \frac{-V_sV_c \sin \partial}{X} + j \frac{V_s^2 - V_sV_c \cos \partial}{X} \dots\dots\dots (4.28)$$

And power viewed from Vc

$$S_c = P_c + jQ_c = \frac{V_sV_c \sin \partial}{X} + j \frac{V_c^2 - V_sV_c \cos \partial}{X} \dots\dots\dots (4.29)$$

The mathematical formulation and the power transfer can be shown in a tabular form as Table 4.1.  $P_s$  is the active power from the grid and  $Q_s$  is the reactive power from the grid. Similarly,  $P_c$  and  $Q_c$  are the active and reactive power from the VSC.

Table 4.1 Active and reactive power between VSC and Grid.

	Source $V_s$	Source $V_c$	
$P_s$	$\frac{-V_sV_c \sin \partial}{X}$	$\frac{V_sV_c \sin \partial}{X}$	$P_c$
$Q_s$	$\frac{V_s^2 - V_sV_c \cos \partial}{X}$	$\frac{V_c^2 - V_sV_c \cos \partial}{X}$	$Q_c$

The power transfer shown in Table 4.1, which is from sources  $V_s$ , and  $V_c$  is verified using PSIM simulation and the simulation result is presented in tabular form as below. The values considered for the line inductance is 1 mH and the voltage of the VSC is considered 230 V. The real values of active and reactive power transfer are depicted in tabular form as Table 4.2.

## REACTIVE POWER CONTROL USING VOLTAGE SOURCE CONVERTER

Table 4.2 Actual values of active and reactive power flow between VSC and Grid.

		Ps	
		+8kW	-8kW
Qs	+3kVAR	$\delta = -2.769^\circ$ Vc= 226.2 V	$\delta = +2.769^\circ$ Vc= 226.2 V
	0 kVAR	$\delta = -2.720^\circ$ Vc= 230.3 V	$\delta = +2.720^\circ$ Vc= 230.3 V
	-3kVAR	$\delta = -2.673^\circ$ Vc= 234.4 V	$\delta = +2.673^\circ$ Vc= 234.4 V

The active power is positive when the angle ( $\delta$ ) is negative i.e. active power,  $P_s$  is positive. Similarly, when angle  $\delta$  is positive the active power,  $P_s$  is negative. The actual values are used to transfer the active power of + 8kW and -8kW. The reactive power ( $Q_s$ ) from VSC is positive when  $V_s$  is greater than  $V_c$ . The reactive power from the VSC is negative when  $V_s$  is less than  $V_c$ . The three cases of reactive power flow are considered for three different voltage differences. The reactive power flows are + 3kVAR for  $V_c = 226.2$  V, 0 kVAR for  $V_c = 230.3$  V and -3 kVAR for  $V_c = 234.4$  V. These relations show that VSC can be used to control the flow of both the active and reactive power to the grid in both the directions if properly implemented.

In order to analyse the above idea further, a circuit is considered in which two three-phase sources are considered with the first one being a normal three-phase source (Grid) and another is a renewable source connected through VSC. The circuit diagram is shown in the Figure 4.23.

In the circuit shown in Figure 4.23, the power flow between the grid and the VSC is analyzed by varying the parameters of the VSC. The power flow as shown in the previous section depends on two variables i.e. phase angle and voltage magnitude. It is shown through this circuit that how VSC can be used to change the variables i.e. the angle and voltage magnitude to control the power flow. Figure 4.24 shows the graphical representation of the active power variation with the change in phase angle



## REACTIVE POWER CONTROL USING VOLTAGE SOURCE CONVERTER

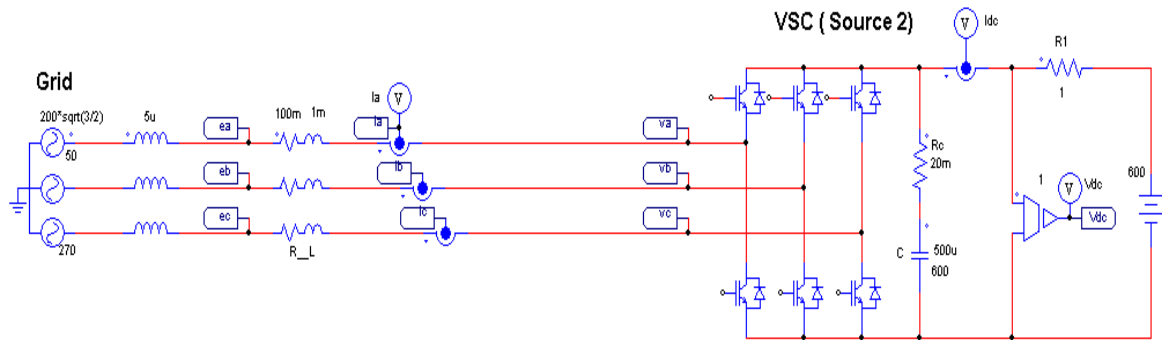


Figure 4.23 Power transfer between Grid and Voltage Source Converter.

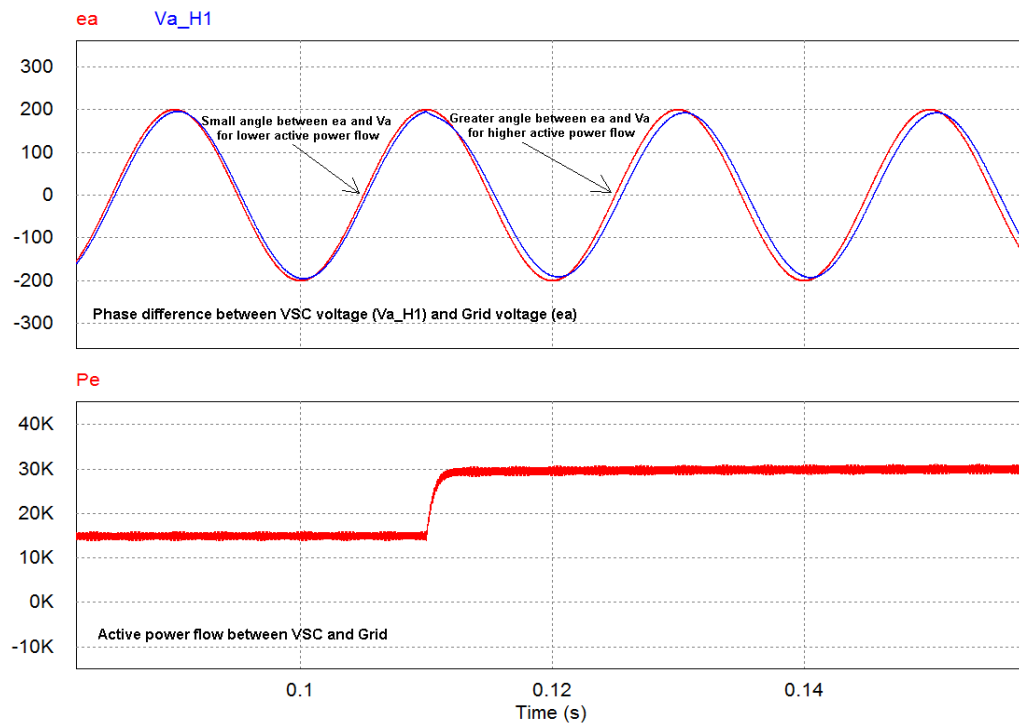


Figure 4.24 Variation of active power flow (kw) with the variation of the phase angle between VSC and GRID.

In Figure 4.24,  $ea$  is the voltage waveform of the grid in volts and  $V_{a\_H1}$  is the voltage waveform of the VSC in volts. The figure shows that the active power flow can be varied by changing the phase angle difference between the VSC voltage and that of the grid voltage. As shown in the figure the active power flow is increased from 15 kW to 30 kW by increasing the phase angle difference between the two voltages  $ea$  and  $V_{a\_H1}$ .

## REACTIVE POWER CONTROL USING VOLTAGE SOURCE CONVERTER

Similarly, the change in reactive power flow can be varied by changing the voltage difference between the VSC voltage and the grid voltage as shown in the figure below. In the following figure,  $e_a$  represents the voltage of the grid whereas  $V_{a\_H1}$  represents the voltage of the VSC.

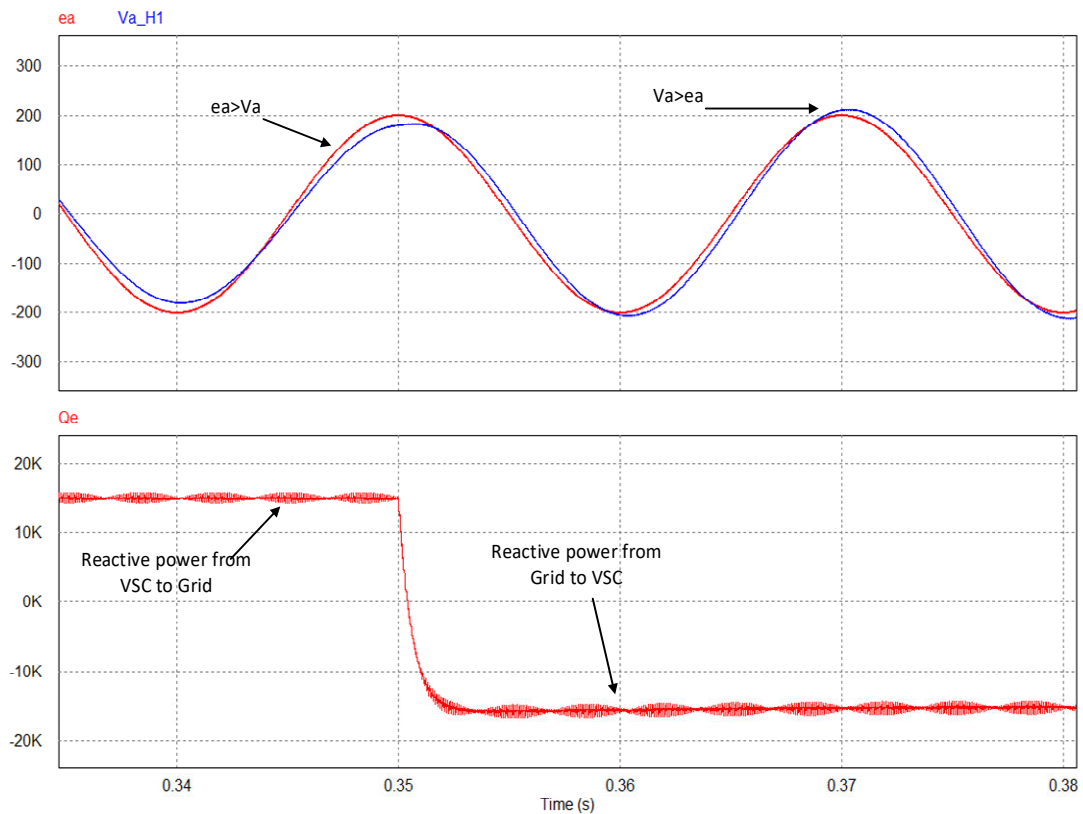


Figure 4.25 Variation of reactive power with the variation of voltage magnitude.

The Figure 4.25 shows the reactive power flow between the VSC and the grid, which can be increased or decreased by changing the voltage, difference fo magnitude between them. The reactive power is positive for  $e_a > v_a$  i.e. the flow of reactive power is from VSC to the grid. Similarly, the flow of the reactive power is negative for  $v_a > e_a$  which means the reactive power flows from the grid to the vsc. In this way, the active and reactive power can be made to flow with a separate vector control to each variable using the control of the VSC.

Most of the works done in MGs are done considering average model converters in which the transients are neglected. Using the VSCs with local control distributed approach will allow analyzing the actual scenario. In MG and other small-scale distribution, the load has power factor

## REACTIVE POWER CONTROL USING VOLTAGE SOURCE CONVERTER

usually less than one due to more inductive load. It is desired to have some loads which will help to improve the power factor. VSC can also help the grid in this respect by supporting the grid by acting as leading power factor load. Therefore, if the controller of the individual renewable sources is designed with VSC using the dq transformation there will be more control on the MG. The active power can be controlled by changing the reference value of  $I_d$  in the switching circuit whereas the reactive power can be controlled by changing the reference value of  $I_q$ . In this research work, the terminal voltage of the VSCs and the phase angle is analysed with the change in load.

Using this characteristic, as an indicator, VSC can be used to control the reactive power. The upcoming renewable source with VSC control will view the remaining grid as a Thevenin's equivalent circuit and supply the grid according to the requirement of the grid. If all the upcoming renewable resources are connected with this approach in the existing MG, the problem of reactive power control can be solved which will finally help to maintain the voltage level and reactive power demand. The idea will be discussed in detail with results of simulations in chapter five.

### 4.5 Conclusion

This chapter discusses the problem in reactive power flow and possible solutions, which will be solved further in chapter five. The issues in reactive power sharing are discussed with Matlab simulations in section 4.1. The effect of line impedances and influence the power flow equations is described in section 4.2. Section 4.3 shows how the controller designed in chapter 3 can be used to share the power flow according to the MG requirements. The VSC along with the controller is very much efficient to supply the load with required active or reactive power. The approach if used with proper application can contribute to the requirement of the reactive power with high dynamics until central action comes in action in the steady state. The idea is further discussed and evaluated in detail considering the renewable sources connected to the grid in chapter five.

## 5 REACTIVE POWER CONTRIBUTION BY RENEWABLE SOURCES

### 5.1 Introduction

The higher demand for renewable resources to be incorporated into the traditional power system has compelled the power system planner and researchers to go for alternate options in order to keep the MG as a performant grid. Along with the solutions, challenges and the challenges in MG are still there to be solved. Many research works are being carried out worldwide to solve the issues but still there are some limitations, which were discussed in detail in chapter two.

It is found that existing strategies that use voltage-controlled converters and droop control have a number of specific shortcomings, which directly affect the performance of the MG. One of the limitations is slow dynamics included due to the structure of dual-loop voltage controllers, poor performance of voltage controllers compared to current regulators, sluggish power sharing response as a result of feeding back the measurement of the generated powers in the droop function, and significant sensitivity to the MG structure and impedance of the distribution lines [100].

According to the analysis performed in section 4.2, it was observed that the relations are quite similar to the traditional power system in which the high inductive lines were assumed neglecting the resistive part in power flow equation. Neglecting the resistive part, it was derived that the active power is directly proportional to frequency and the reactive power is directly proportional to voltage.

Considering the resistive nature of the low voltage MG lines the power flow equations are reversed. As the active power is directly proportional to voltage and reactive power is proportional to phase angle which is just opposite in case of traditional power flow equation of high voltage inductive lines .i.e. active power ( $P$ ) is directly proportional to Voltage and Reactive Power ( $Q$ ) is directly proportional to phase angle ( $\phi$ ). Therefore, it has to be concluded that the impedance of the line disturbs a lot the reactive power flow.

The approach of this work is to handle the above issues i.e. the slow nature of the dual voltage control loops by introducing current control loops to make the dynamics of the controller higher and faster. Another major problem of different line impedances in comparison to the traditional line are tried to solve with different approaches in many research work like, virtual impedance, connecting virtual inductance to make it as traditional lines, ratio resistance/inductance included in the power flow equation etc. which were discussed in state of art.

The problem of resistive low voltage MG is taken care with an approach of equivalent Thevenin's impedance (ETI), integrating line parameters and the load. The ETI is observed across the VSC terminals, which actually represents not only the resistive lines but also the change in load. The ETI is derived in section 5.2.

### 5.2 Analytical derivation of the equivalent impedance observed by the VSC

The values of line parameters of low voltage MG make a difference in power flow due to which the traditional power flow equations cannot be used directly. One of the recent approaches is discussed in section 4.3 in which only a tentative ratio of the resistance and inductance is sufficient to use the modified power flow equation of the MG. A step forward to that an exact measurement of the ETI across the terminal of the VSC is done in this thesis. The mathematical derivation of the equivalent impedance is carried out in this section. Figure 5.1 shows VSC connected to the grid at a voltage level of 400 V. The loads are connected to the AC bus and are changed in successive steps. The AC terminal of the VSC is at 400V (Line-Line) whereas the DC side of the VSC is 1000 V just to allow a complete range of power.

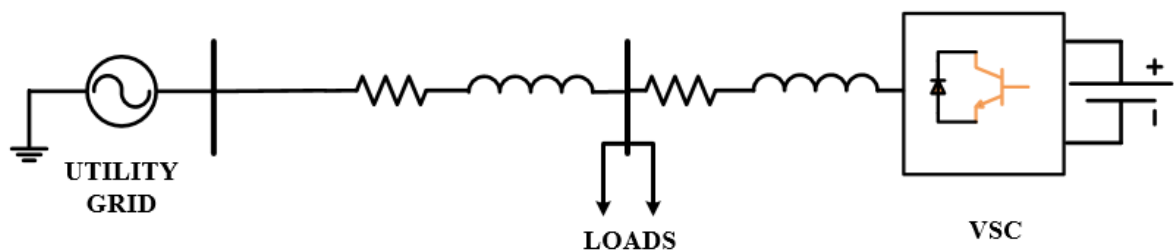


Figure 5.1 VSC connected to the grid

## REACTIVE POWER CONTRIBUTION BY RENEWABLE SOURCES

The VSC terminal observes the equivalent impedance of the MG and behaves according to the change in load at the point of connection. This allows each VSC of the MG to support the MG at the point of connection. If each VSC can contribute with reactive power in a high dynamic time, it will be a good solution to the reactive power sharing as the renewable resources are connected to the MG through a VSC. Figure 5.2 shows the circuit diagram of VSC connected to the grid to derive the equivalent impedance. The equivalent impedance seen by the VSC terminal is written as  $Z_{VL}$ . As shown in Figure  $Z_L$  is the load impedance,  $Z_1$  is the impedance of the grid side, VSC and  $V_g$  is the voltage source of the VSC and the grid respectively.

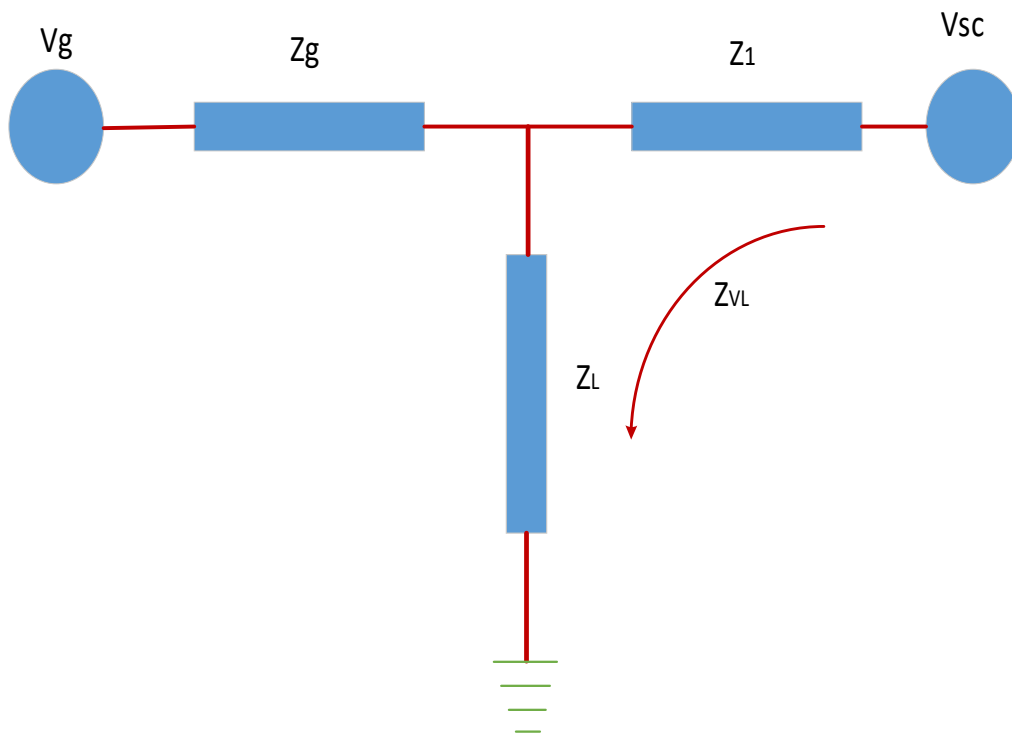


Figure 5.2 Equivalent impedance observed by the VSC

The equivalent impedance observed by the VSC can be derived as from equation 5.1 to 5.17

$$V_L = Z_L(I_1 + I_g) \quad \dots\dots\dots (5.1)$$

## REACTIVE POWER CONTRIBUTION BY RENEWABLE SOURCES

Where  $V_L$  is the voltage across the load,  $Z_L$  is the load impedance,  $I_1$  is the current from the VSC and  $I_g$  is the current from the grid. Simplifying equation 5.1 further to 5.4

$$= Z_L I_1 + Z_L I_g \quad \dots\dots\dots (5.2)$$

$$\frac{V_{sc}}{I_1} = Z_{VSC} \quad \dots\dots\dots (5.3)$$

$$Z_{VSC} = Z_1 + Z_{VL} \quad \dots\dots\dots (5.4)$$

The relations can further be written as 5.5 and derived to 5.15

$$Z_L(I_1 + I_g) = Z_{VL} I_1 \quad \dots\dots\dots (5.5)$$

$$Z_L = \frac{Z_{VL} I_1}{(I_1 + I_g)} = Z_{VL} \frac{I_1 e^{j\Phi_1}}{I_1 e^{j\Phi_1} + I_g e^{j\Phi_G}} \quad \dots\dots\dots (5.6)$$

$$= (R_{VL} + jX_{VL}) \frac{\frac{\boxed{C}}{\phantom{I_1 \cos \Phi_1}} \frac{\boxed{D}}{\phantom{I_1 \sin \Phi_1}}}{\underbrace{(I_1 \cos \Phi_1 + I_g \cos \Phi_G)}_{\phantom{I_1 \cos \Phi_1}} + j \underbrace{(I_1 \sin \Phi_1 + I_g \sin \Phi_G)}_{\phantom{I_1 \sin \Phi_1}}} \quad \dots\dots (5.7)$$

$$\begin{matrix} \boxed{A} & \boxed{B} \\ (R_{VL} + jX_{VL}) = (R_L + jX_L) \frac{A+jB}{C+jD} & \dots\dots\dots (5.8) \end{matrix}$$

$$(R_{VL} + jX_{VL}) = (R_L + jX_L) \frac{(A+jB)(C-jD)}{C^2 + D^2} \quad \dots\dots\dots (5.9)$$

$$= (R_L + jX_L) \frac{(AC+BD) + j(BC-AD)}{I_1^2} \quad \dots\dots\dots (5.10)$$

$$\begin{aligned}
 &= (R_L + jX_L) \frac{(I_1^2 \cos^2 \Phi_1 + I_1 I_G \cos \Phi_1 \cos \Phi_G + I_1^2 \sin^2 \Phi_1 + I_1 I_G \sin \Phi_1 \sin \Phi_G)}{I_1^2} \\
 &+ \frac{j((I_1^2 \sin \Phi_1 \cos \Phi_1 + I_1 I_G \cos \Phi_1 \sin \Phi_G) - (I_1^2 \sin \Phi_1 \cos \Phi_1 + I_1 I_G \sin \Phi_1 \cos \Phi_G))}{I_1^2} \dots\dots\dots (5.11)
 \end{aligned}$$

$$\begin{aligned}
 &= (R_L + jX_L) \frac{(I_1^2 (\cos^2 \Phi_1 + \sin^2 \Phi_1) + I_1 I_G (\cos \Phi_1 \cos \Phi_G + \sin \Phi_1 \sin \Phi_G))}{I_1^2} \\
 &+ \frac{j(I_1 I_G (\cos \Phi_1 \sin \Phi_G - \sin \Phi_1 \cos \Phi_G))}{I_1^2} \dots\dots\dots (5.12)
 \end{aligned}$$

$$\begin{aligned}
 &= (R_L) \frac{(I_1^2 + I_1 I_G (\cos(\Phi_1 - \Phi_G)) + j(I_1 I_G (\sin(\Phi_G - \Phi_1)))}{I_1^2} + \\
 &jX_L \frac{(I_1^2 + I_1 I_G (\cos(\Phi_1 - \Phi_G)) + j(I_1 I_G (\sin(\Phi_G - \Phi_1)))}{I_1^2} \dots\dots\dots (5.13)
 \end{aligned}$$

$$\begin{aligned}
 &= (R_L) \frac{(I_1^2 + I_1 I_G (\cos(\Phi_1 - \Phi_G))}{I_1^2} - (X_L) \frac{(I_1 I_G (\sin(\Phi_G - \Phi_1)))}{I_1^2} \\
 &+ j(R_L) \frac{(I_1 I_G (\sin(\Phi_G - \Phi_1)))}{I_1^2} + j(X_L) \frac{((I_1^2 + I_1 I_G (\cos(\Phi_1 - \Phi_G)))}{I_1^2} \dots\dots\dots (5.14)
 \end{aligned}$$

$$\begin{aligned}
 &= \frac{R_L(I_1^2 + I_1 I_G (\cos(\Phi_1 - \Phi_G)) - X_L(I_1 I_G (\sin(\Phi_G - \Phi_1)))}{I_1^2} \\
 &+ j \left( \frac{R_L(I_1 I_G (\sin(\Phi_G - \Phi_1)) + X_L(I_1^2 + I_1 I_G (\cos(\Phi_1 - \Phi_G)))}{I_1^2} \right) \dots\dots (5.15)
 \end{aligned}$$

So equating the real and imaginary component we get: -



$$R_{VL} = \frac{R_L(I_1^2 + I_1 I_G (\cos(\Phi_1 - \Phi_G)) - X_L(I_1 I_G (\sin(\Phi_G - \Phi_1)))}{I_1^2} \dots\dots\dots (5.16)$$

$$X_{VL} = \frac{R_L(I_1 I_G (\sin(\Phi_G - \Phi_1)) + X_L(I_1^2 + I_1 I_G (\cos(\Phi_1 - \Phi_G)))}{I_1^2} \dots\dots\dots (5.17)$$

The relation derived in the equation (5.15) shows that the equivalent impedance observed by the VSC can be separated into two parts i.e. resistive and inductive part in case of the inductive load. The equivalent values depend upon both the magnitude and phase angle as shown in (5.16) and (5.17). These variables are indirectly taken as an input variable for the controller of the VSC and the digital algorithm acts according to the change of load.

### 5.3 Voltage and Frequency Control

As discussed in section 5.1 the VSC can be used to control the voltage and frequency separately, this section describes how the VSC can take care of voltage and frequency when the load changes. However, the main work carried out in this thesis is to contribute to the reactive power in the MG but this section demonstrates that the VSC can be designed to contribute to both active and reactive power separately. The control is performed in an external loop, which controls the active and reactive power references. The results shown in Figure 5.3 are related to a VSC connected to the grid. The grid is considered as the synchronous machine driven by an induction motor. This arrangement is done to show that the grid is not ideal and has some limitations so that both the change in frequency and voltage can be shown.

## REACTIVE POWER CONTRIBUTION BY RENEWABLE SOURCES

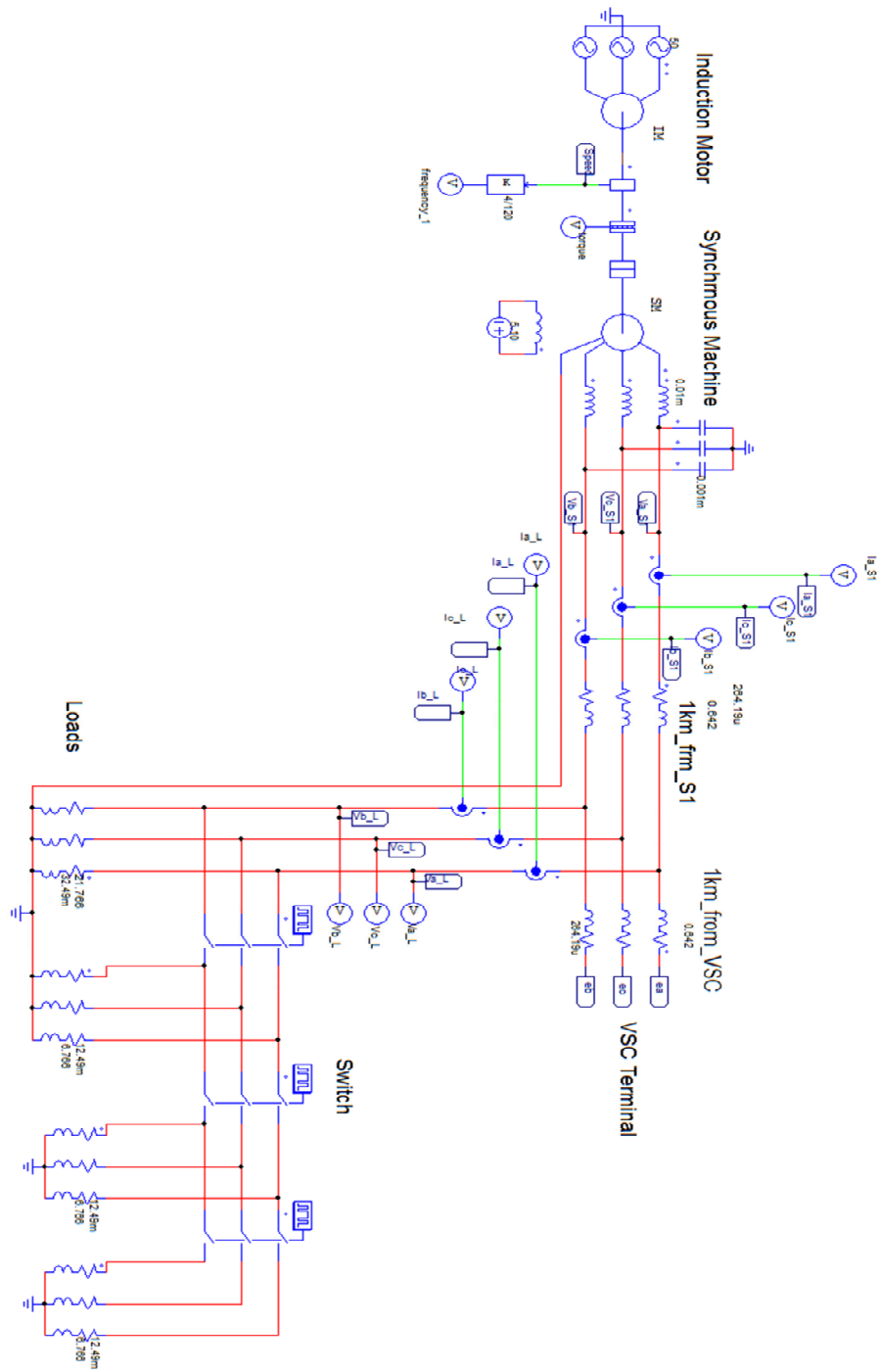


Figure 5.3 VSC connected to the grid.

Figure 5.3 show that the VSC is connected at a distance of 1 kilometre from the load as similar to the grid, which is also at a distance of 1 kilometre from the load. The load is changed in steps using the switches and the effect is observed which is presented in Figure 5.4. It can be

## REACTIVE POWER CONTRIBUTION BY RENEWABLE SOURCES

seen from the Figure 5.4 that with the increase in load the frequency and the terminal voltage across the load goes on decreasing. The load is changed in three steps. Figure 5.4 shows the drop in voltage and frequency with the increase in load current.

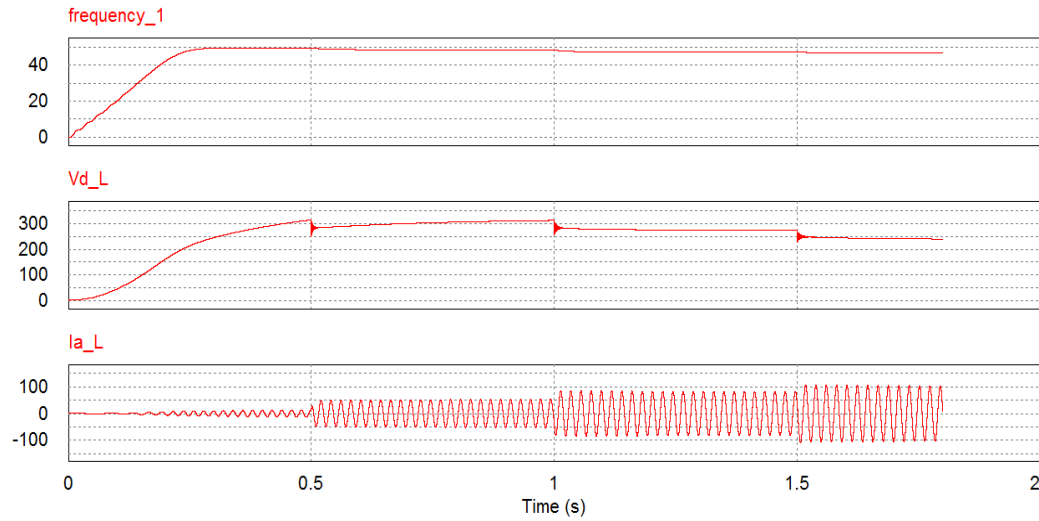


Figure 5.4 Voltage and frequency drops with the increase in load current.

As the load is inductive, the voltage and frequency both are affected by the change in load. This decrease in frequency is taken care by the VSC, which is shown in Figure 5.5. As the frequency decreases, the  $I_d$  component of the current is increased by increasing the  $I_{d\_ref}$ . It can be seen from the figure that  $I_{d\_ref}$  is followed by  $I_d$  exactly which shows the correct functioning of the controller of the VSC. As load, current is increased in steps the  $I_{d\_ref}$  is also increased in steps, which makes the  $I_d$  component to increase which finally stabilises the frequency.

## REACTIVE POWER CONTRIBUTION BY RENEWABLE SOURCES

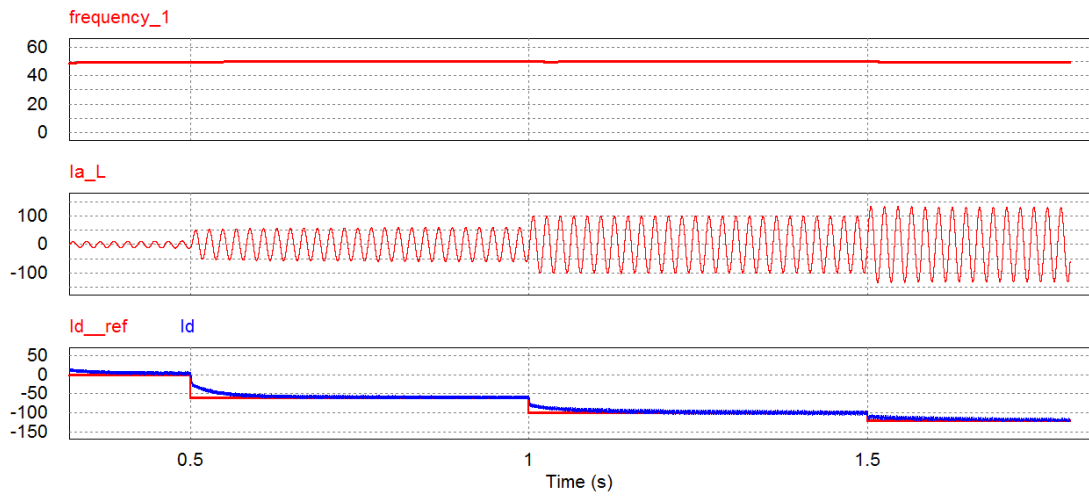


Figure 5.5 Improvement of frequency with the injection of active power from the VSC.

The Figure 5.6 below shows that the voltage drop can be improved by using the VSC. The quadrature component of the current is increased to adjust the voltage drop. It also depicts the contribution from the VSC as  $I_q$ .

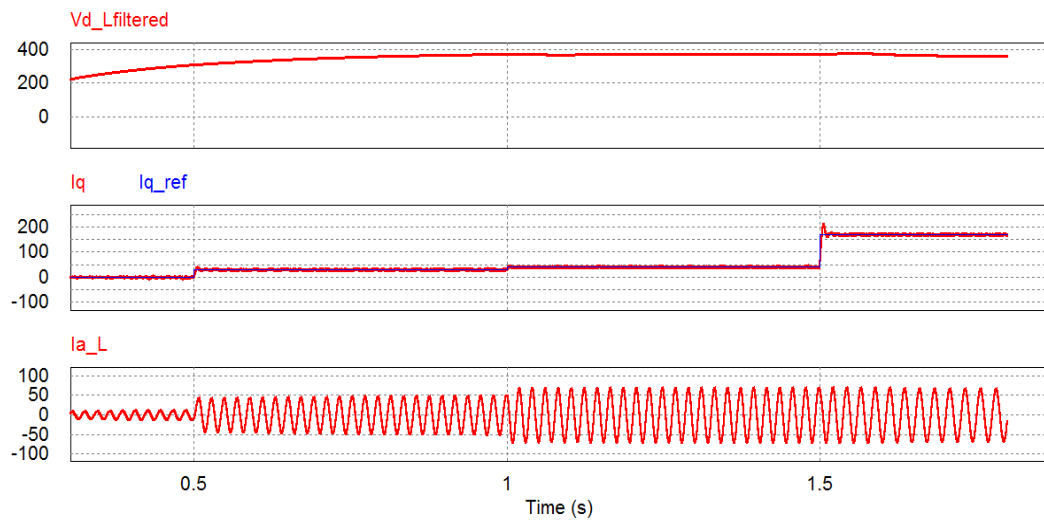


Figure 5.6 Voltage improvement by the increment of the reactive power from the VSC.

Figure 5.6 show that the voltage is improved by increasing the  $I_{q\_ref}$ , which in turn the  $I_q$  increases. The increase in  $I_q$  finally increases the reactive power to compensate for the voltage drop. The simulations show that both the  $I_{q\_ref}$  and  $I_{d\_ref}$  (reference current) are exactly followed by  $I_q$  and  $I_d$  respectively which ensures the correct functioning of the VSC.

## REACTIVE POWER CONTRIBUTION BY RENEWABLE SOURCES

These simulations shown in Figure 5.3 to 5.6 shows that the active and reactive power can be controlled separately using the VSC. The decoupling is perfectly done and the dynamic response is quite good in comparison to the initial simulations shown in MATLAB in section 4.1 in which the response was very slow. The current control loops in this method have good dynamics and the controlling process is achieved very fast.

### 5.4 Reactive Power Sharing in Microgrids

MGs are emergent grids integrating a large number of renewable power sources, interconnected by VSCs.

The reactive power supplied by the VSC in section 5.3 was through a loop control which shows that the VSC can be used to contribute to both active and reactive powers. The work is further carried forward by using closed loop control so that the reactive power is contributed automatically by the VSC as required. The contribution of the reactive power is carried out using the ETI across the terminals of the VSC. This is made possible by using a functional block of electronic algorithm implemented in C-language, which performs the computation of needed reactive power. A brief description of the controller, this algorithm and its flowchart is presented in sections 5.4.1, 5.4.2 and 5.4.3 respectively.

#### 5.4.1 Role of the Controller

The equivalent reactance derived in section 5.2 is used in a functional block through digital algorithm in the controller of the VSC to generate the  $I_q$  component. This  $I_q$  component is processed with primary  $i_q$  reference used and the result is adopted as  $i_q$  new reference. Figure 5.7 shows the controller used to generate the required signals  $V_{a\_C}$ ,  $V_{b\_C}$ , and  $V_{c\_C}$ . These ones are applied to the PWM switching block. The signals  $V_{a\_C}$ ,  $V_{b\_c}$ , and  $V_{c\_C}$  are generated according to the input signals  $I_q$  and  $I_d$  where  $I_d$  is responsible for active power and  $I_q$  is responsible for reactive power. The enlarged view of the input of the controller is shown in Figure 5.8. This Figure shows that  $I_{q\_Reference}$  is the reference given to generate the reactive power support to be contributed by the VSC. Zero is kept in the addition of  $I_{q\_Reference}$  for initializing.

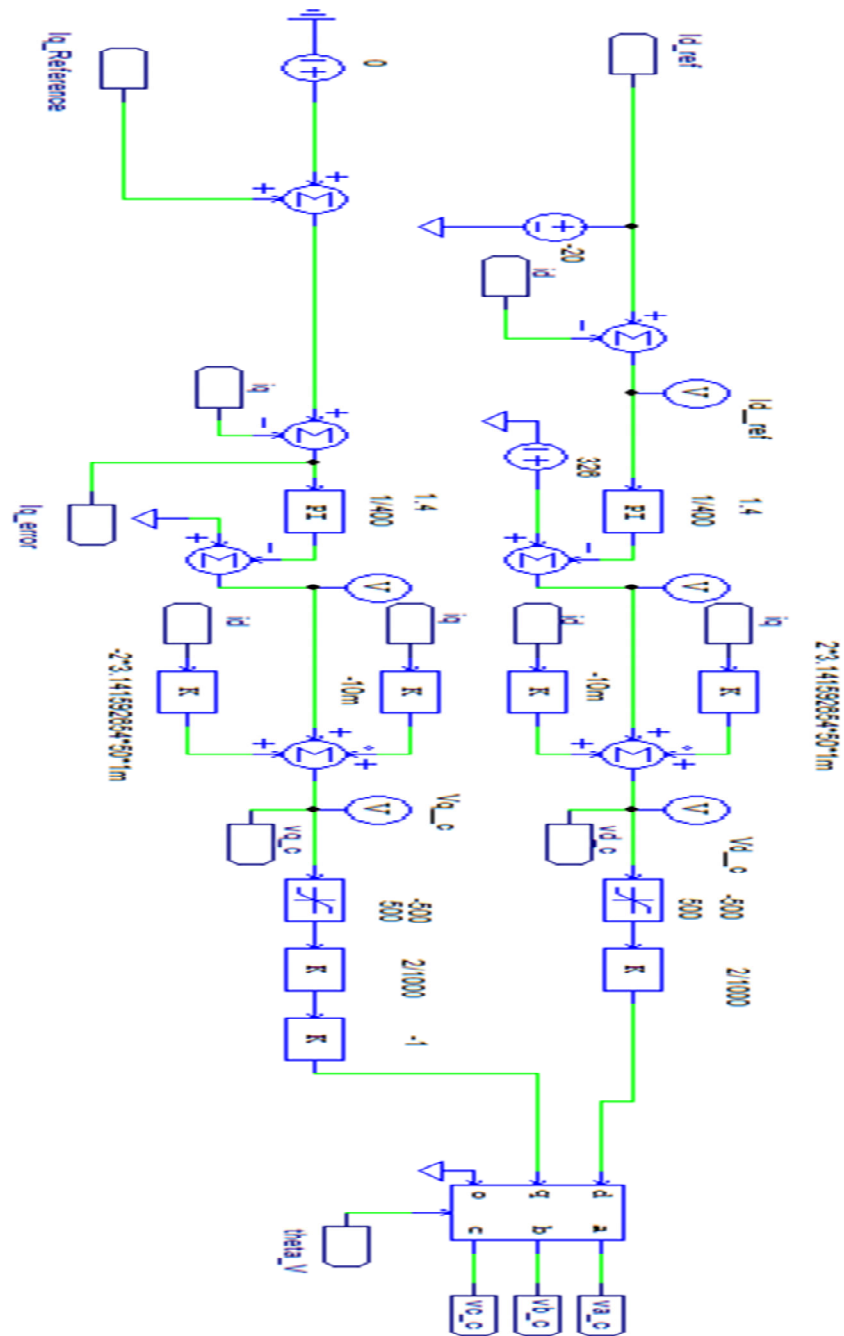


Figure 5.7 Controller used to generate the signals for the VSC to control reactive power.

The gain of the PI block is kept 1.4 and the time constant is 1/400 as shown in Figure 5.8. The  $I_d$  is kept constant as -20 so that a constant active power support is provided to the grid, which can be considered as the active power generated at the MPPT of the renewable source.

## REACTIVE POWER CONTRIBUTION BY RENEWABLE SOURCES

After the PI block there is the decoupling block placed in the controller circuit, which is responsible for the decoupling of the active and reactive power. At last, there is the dq to abc conversion block in which the angle for synchronization is obtained from the PLL as  $\Theta_{\text{theta\_V}}$ .

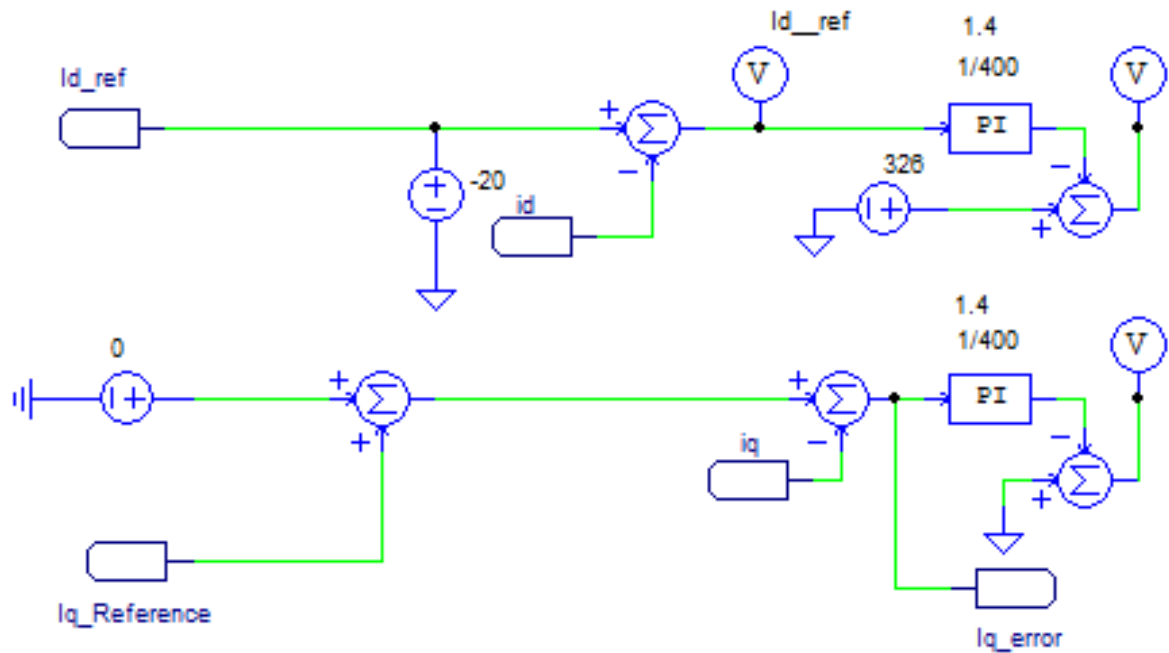


Figure 5.8 Enlarged view of one of the section of the controller

### 5.4.2 Digital Algorithm for Reactive Power Contribution

The digital algorithm performs a function added to the VSC operation at managing its contribution to reactive power needs. It is implemented through an additional functional block. The VSC together with this additional block works to share the reactive power with the MG. Figure 5.9 shows the flowchart of the algorithm used to generate the  $I_{q\_Reference}$  using the digital algorithm.

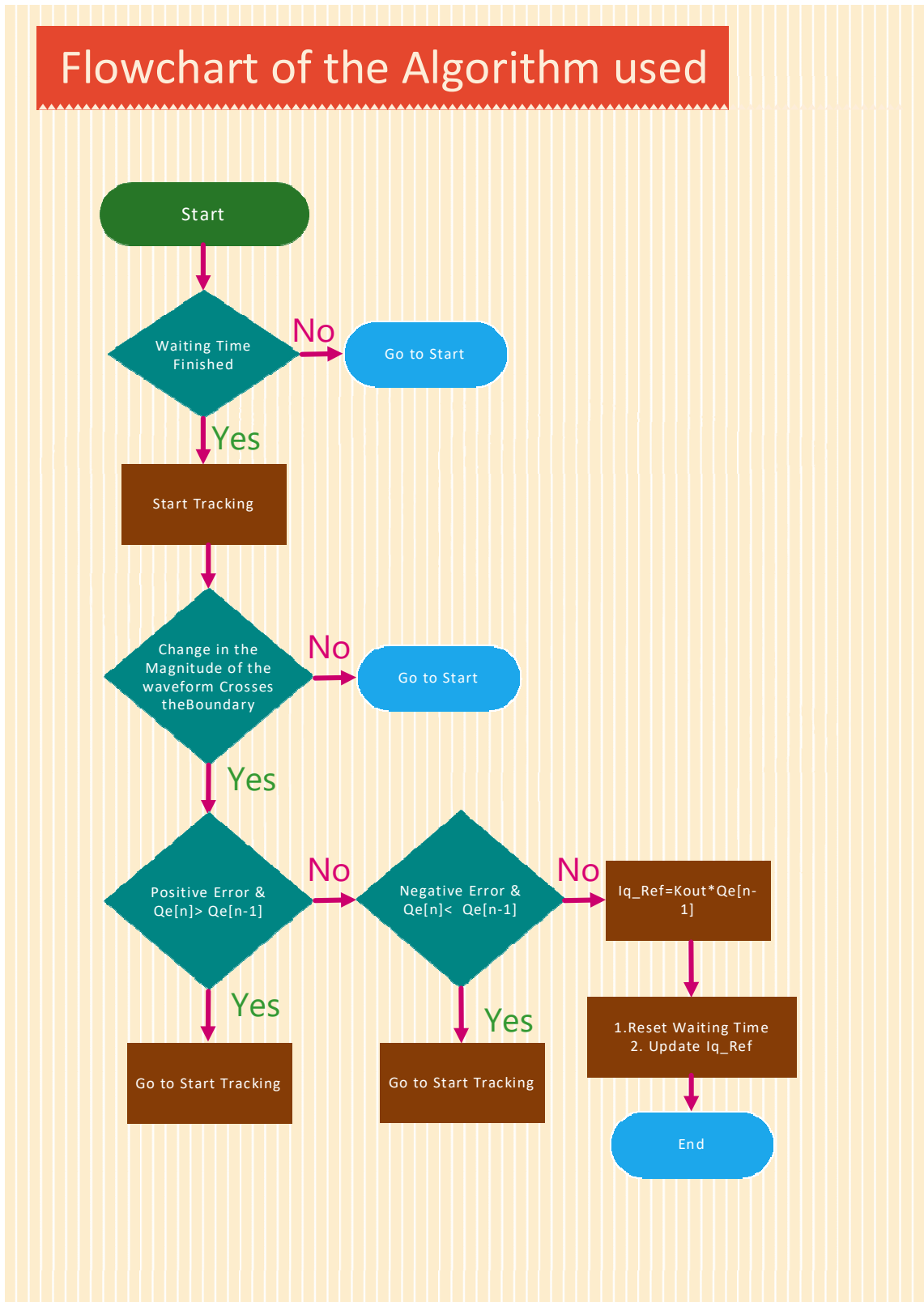


Figure 5.9 Flowchart of the algorithm used in C-Block



Similarly, Figure 5.10 shows the C-block used to implement the digital Algorithm. The algorithm works taking change in the reactive power as the input, which is in this case, is the difference of  $Q_e$  and  $Q_{e\_reference}$  ( $Q_{e\_error}$ ).

It is based on the operation of the VSC as a current controlled converter. Therefore, the converter output voltage evolves according to the ETI impedance, and the transient generated reactive power evolves according to. At measuring with high dynamics this evolution of the controller can take care properly of the load changes. Then the algorithm has to react by taking care of the changes faster than the current controller at stabilizing the generated currents, active and reactive ones.

This input is processed through the digital algorithm using the C-block. The program in C language is launched continuously in the background and is activated after certain set waiting time. If the change in reactive power ( $Q_{e\_error}$ ) is within the set range, then there is no action taken. If the change in  $Q_{e\_error}$  crosses certain set limit then the change is categorized whether it is a positive change or the negative change. After the separation of the type of change, the compensation for the reactive power is generated as  $I_{q\_Reference}$ . After a certain change made the value is stored in the buffer so that next time the change is compared with the stored value. The  $I_{q\_Reference}$  generated is used in the controller of the VSC to contribute the reactive power to the MG. The algorithm can be described in following steps: -

- ✚ Initialize the amplifying error signal  $K_{in}$ .
- ✚ Initialize  $K_{out}$ , which is the factor that is used to convert the reactive power error to quadrature component of the current ( $I_q$ ).
- ✚  $hys\_error$  is the band within which the controller does not generate any compensation signal.
- ✚ Wait Time is initialized to set the cycle time.
- ✚ The algorithm waits for set waiting time.
- ✚ If the change in the  $Q_{e\_error}$  exceeds than the band initialized than it enters the next level.
- ✚ The positivity or negativity of the change is categorized and peak reached is guaranteed as  $Q_e[n] > Q_e[n-1]$  for positive change.

## REACTIVE POWER CONTRIBUTION BY RENEWABLE SOURCES

- ✚ If change is negative and the peak is checked confirming  $Q_e[n] < Q_e[n-1]$ .
- ✚ After the change is categorized the compensation is generated as  $I_{q\_Reference} = K_{out} * Q_e[n-1]$
- ✚ After this change, this new value is kept in buffer and the waiting time is reset.

The algorithm is implemented as a functional block using C-block as shown in Figure 5.10.

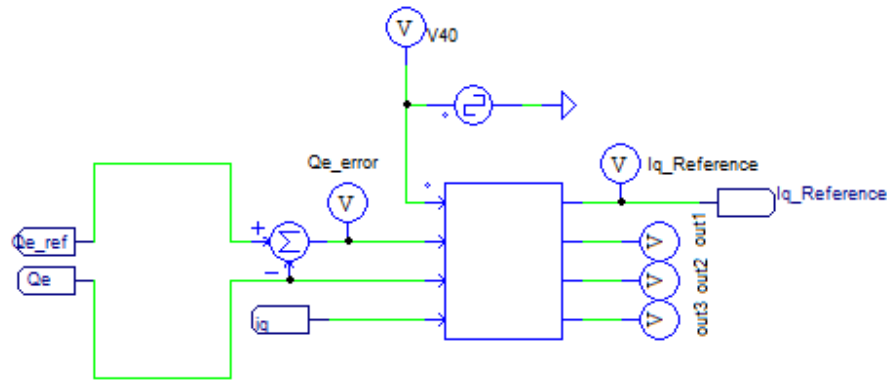


Figure 5.10 C-Block used for implementation of digital algorithm

Figure 5.10 shows the C- block used in the PSIM software. As shown the difference of the reference reactive power and the current reactive power is given as the input ( $Q_{e\_error}$ ) to the block. The input is fed as a digital input to the C-block and the output is the  $I_{q\_Reference}$ , which is used to contribute the reactive power to the MG as it is added to previous  $I_{q\_Referece}$ . As shown in the flowchart the change in the reactive power is firstly classified according to being within the permissible band or not. If it crosses the band then it is classified weather it is a positive or negative change. Once the positivity or negativity is classified then the peak of the change is identified. Once the peak of the change is identified then the  $I_{q\_reference}$  is generated for the compensation. Using this  $I_{q\_Reference}$  the reactive power is compensated by the VSC within one cycle of the normal grid frequency.

### 5.4.3 Reactive Power sharing with Renewable energy using VSC

The contribution made from the renewable resources based on a VSC and performed by the algorithm analyzed above is discussed in this section.

## REACTIVE POWER CONTRIBUTION BY RENEWABLE SOURCES

Figure 5.11 shows the connection of VSC with the grid, which is at 400V line to line (RMS). The current, voltage and power are measured at the grid terminal, VSC terminal, and the load terminal. The load is connected in between the grid and the VSC. The VSC is connected through the terminal  $e_a$ ,  $e_b$ , and  $e_c$  as shown. The load is varied in two steps at 0.1s and 0.15s. The voltages of the grid side are measured as  $V_{a1}$ ,  $V_{b1}$ , and  $V_{c1}$ . Similarly,  $V_{a\_L}$ ,  $V_{b\_L}$ ,  $V_{c\_L}$  and  $V_a$ ,  $V_b$  and  $V_c$  are the voltages across the load and the VSC respectively.  $I_{a1}$ ,  $I_{b1}$ , and  $I_{c1}$  are the currents through the grid.  $I_{a\_L}$ ,  $I_{b\_L}$ , and  $I_{c\_L}$  are the total currents through the load. Similarly,  $I_{a2}$ ,  $I_{b2}$ , and  $I_{c2}$  are the currents through the VSC. The loads are varied in two steps, which are changed at 0.1s and 0.15s.

Figure 5.12 shows the circuit diagram of the VSC. The output of the controller  $V_{a\_c}$ ,  $V_{b\_c}$  and  $V_{c\_c}$  as shown in Figure 5.7 is fed to the switching unit of the VSC. The DC side of the VSC is connected with 1000 V dc. The switching frequency of the VSC is 10 KHz. The voltmeter  $V_{dc}$  measures the voltage of the dc side, which changes according to the mode of operation of the VSC. The VSC is connected to the grid with 1-ohm resistance and 1mH inductance per phase as shown in the Figure 5.12.

Figure 5.13 shows the reactive power change in the load and the support provided by the grid and the VSC respectively. It is shown that there is increase of the reactive load to nearly 60 kVAR at 0.1s and to nearly 80 kVAR at 0.15s. At these changes, the VSC support changes from zero to nearly 4 kVAR and 6 kVAR respectively. Along with the change in the reactive load, there is change in the dynamics of the  $Q_e$  error, which is noted by the digital algorithm as a change in the ETI. The functional block along with the controller of the VSC produces the new  $I_{q\_Reference}$  and feeds to the controller of the VSC. According to the new  $I_{q\_Reference}$  the controller produces the new switching signal which makes the VSC to contribute the reactive power. This percentage of share can be increased with the change in the magnitude of the  $I_q$  compensation.

It can be seen from Figure 5.13 that the dynamics of the system is very fast and the support is provided within half cycle of the normal grid frequency i.e 10ms. There is some transient condition in this half cycle but the contribution is settled very fast.

One point to validate is the robustness of the algorithm – dedicated to VSC contribution for reactive power sharing – to changes in the active power needs. This is shown in Figure 5.14.

## REACTIVE POWER CONTRIBUTION BY RENEWABLE SOURCES

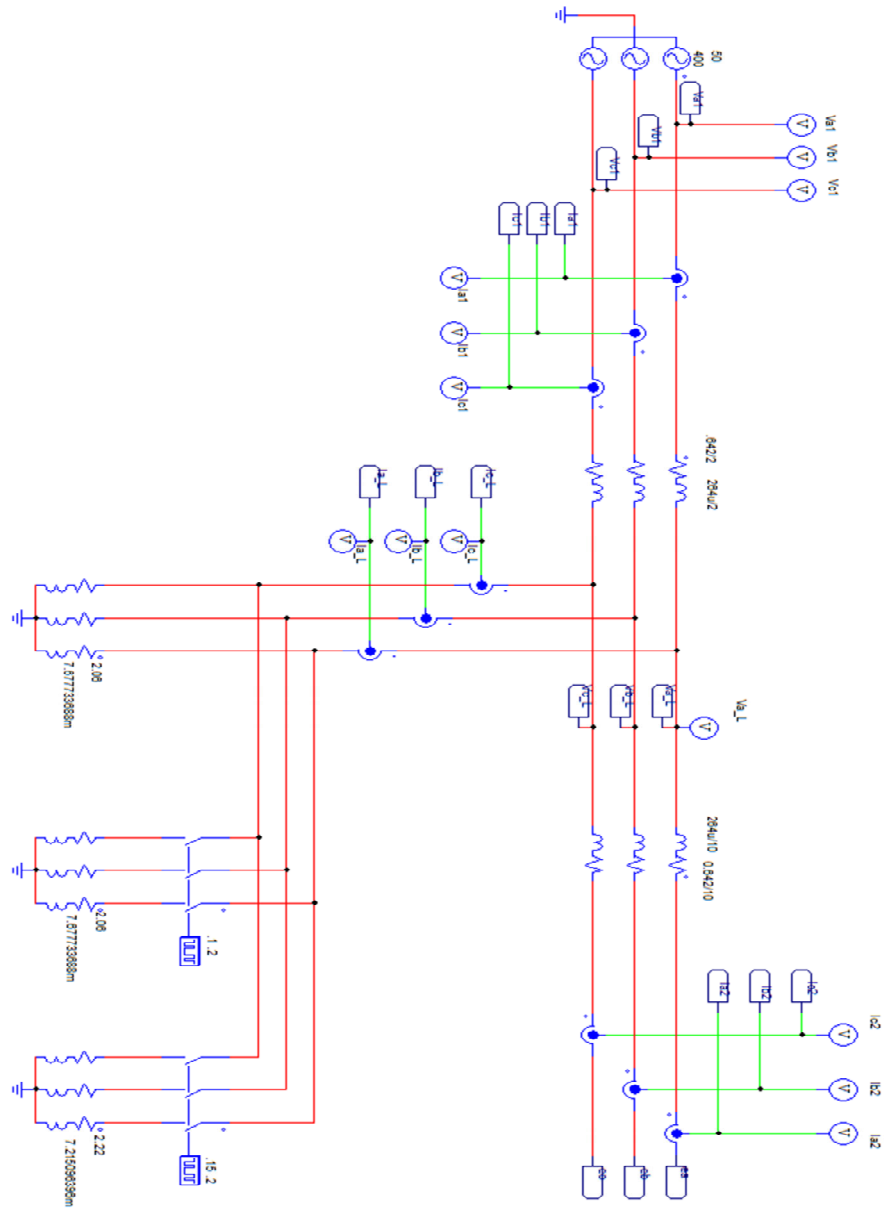


Figure 5.11 VSC connected to the grid.

112

## REACTIVE POWER CONTRIBUTION BY RENEWABLE SOURCES

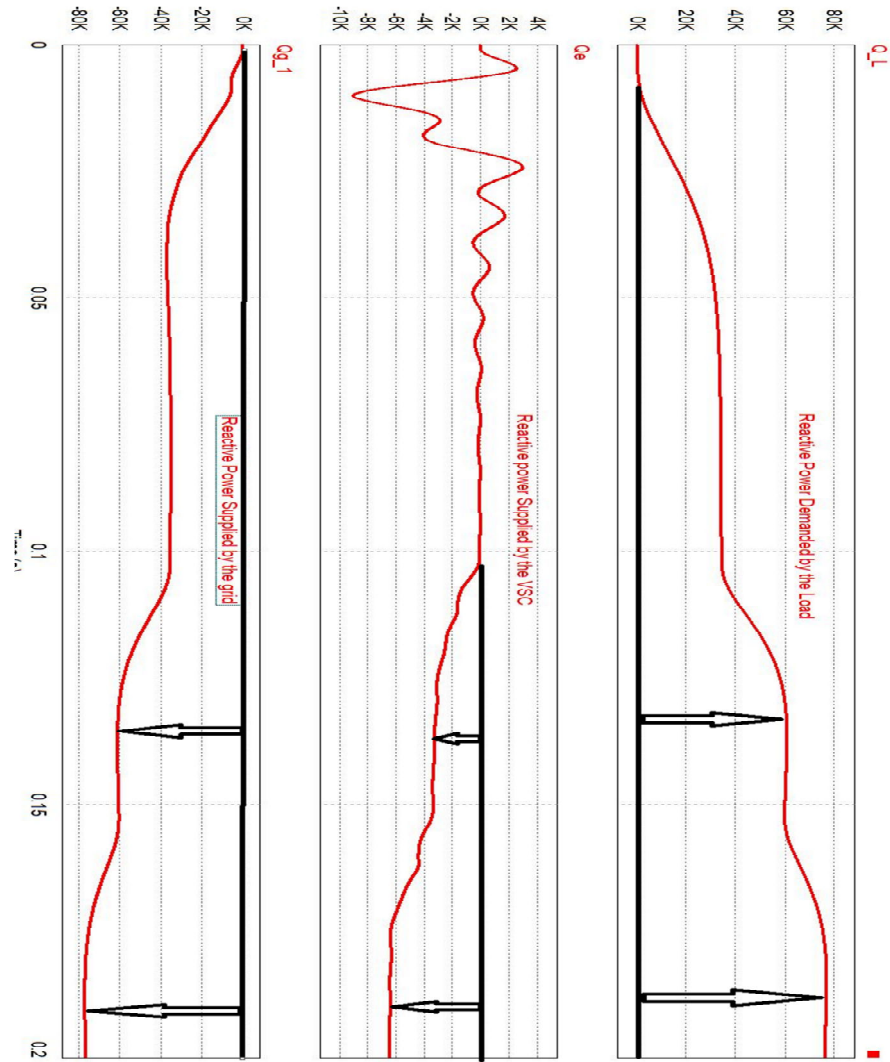


Figure 5.13 Reactive power support by the VSC

Figure 5.14 shows change in active power of the load and the active power supplied by the grid and the VSC. The active power is changed along with the reactive power at 0.1s and 0.15s. As the VSC is supposed to contribute only to the reactive power the reference of the active power is kept constant (according to power source MPPT) in the VSC and it supplies a constant active power. However, there is a certain transient at the time of load change but it settles very

quickly. Therefore, it can be seen that the reactive power support can be made by the VSC keeping the active power constant. The grid supplies all the increase in active power demand.

The behavior of the current controlled VSC must be analyzed in terms of keeping the output voltage within the range of standard quality of service. The essay for it is planned in the same operating conditions shown in previous analysis.

Figure 5.15 shows the dq component of the voltage of the VSC as  $e_d$  and  $e_q$ . It can be seen that the  $e_q$  is maintained constant at zero and the value of  $e_d$  changes with the change in the load but it is maintained within permissible range after some transients with the change in load. The contribution from the VSC limits the  $e_d$  component within the standard range.

The reactive power is supplied to the MG based on the  $I_q\_Reference$  generated by the controller. As shown in the Figure 5.16, there are four plots.  $Q_e$  is the reactive power support by the VSC,  $I_q\_Reference$  which is an input to the controller to make reactive power contribution is the outcome of the external functional block prepared using the digital algorithm in C block.  $I_q$  is the q component of the controller which actually determines the reactive power to be contributed by the VSC. It can be observed from the Figure 5.16 that  $I_q$  follows  $I_q\_Reference$  which guarantees the correct functioning of the controller. The load is changed in two steps at 0.1s and 0.15 second. When the reactive power demand in the load is changed, the VSC acts instantly and supports the grid with a certain percentage of the reactive power. The controller helps to generate the  $I_q\_reference$  by observing the transients as  $Q\_e$  error.

The reference is already ready in the half cycle of the full transient wave, which can be seen, in the first plot ( $Q\_e$  error) of the Figure 5.16. The transients can be seen while changing the loads, which can be measured, and accordingly the  $I_q\_reference$  is generated. The transients are marked with black circles in Figure 5.16. The transients in the  $Q\_e$  error plot is the input to the algorithm, which is sensed by the functional block and the compensation, provided is the  $I_q\_Reference$ , which is shown inside the black circles in the  $I_q\_Reference$  plot. Similarly, the  $I_q$  is shown in the next plot which exactly follows the  $I_q\_Reference$ . The black circles are the initial transients as soon as the load is changed. The red circles following the black circles shows the

## REACTIVE POWER CONTRIBUTION BY RENEWABLE SOURCES

equivalent compensation generated according to the  $I_{q\_Reference}$ . The reference is generated observing the positive error of the change in the  $Q_e$  error as the load is increasing. As described in the algorithm the functional block works for positive error for increase in load and negative error for decrease in load.

It can be observed from Figure 5.16 that within half cycle of the normal grid cycle  $I_{q\_Reference}$  already generates the required level of the compensation  $I_q$  current. This  $I_{q\_Reference}$  is fed to the controller. Using this  $I_{q\_Reference}$  input and a fixed  $I_d$  reference the switching signal is produced.

Similarly, Figure 5.17 shows the reactive power being reduced from the load. The digital algorithm works for the negative error in this case. The four plots shown in the figure are just opposite to that of positive error shown in Figure 5.16. The  $I_{q\_Reference}$  is generated for the negative error and the acting on this negative reference the reactive power  $Q_e$  flows in the opposite direction as depicted in the fourth plot of the Figure. This shows that the controller along with the additional functional block is quite capable of contributing reactive power in both the cases.



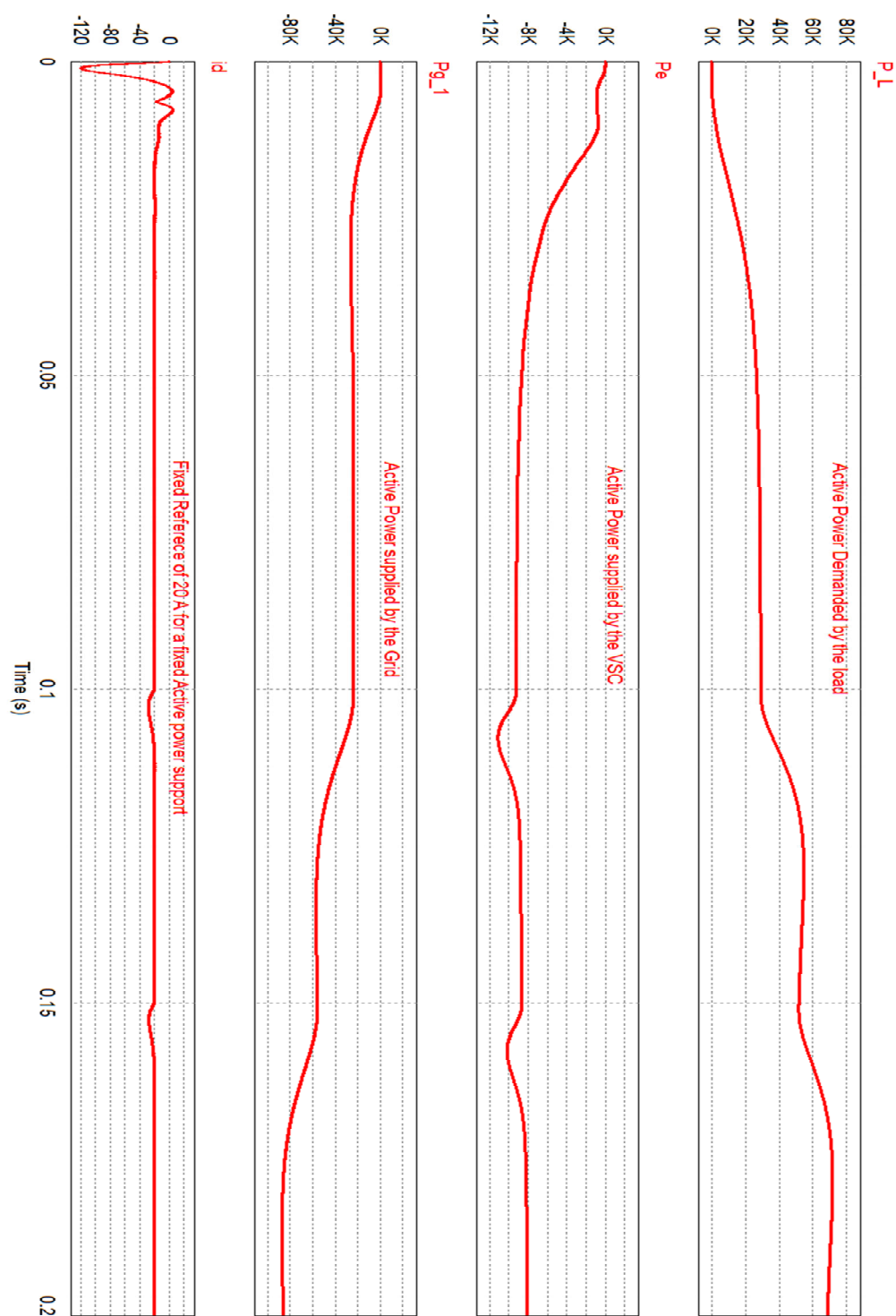


Figure 5.14 Active power supplied by the VSC.

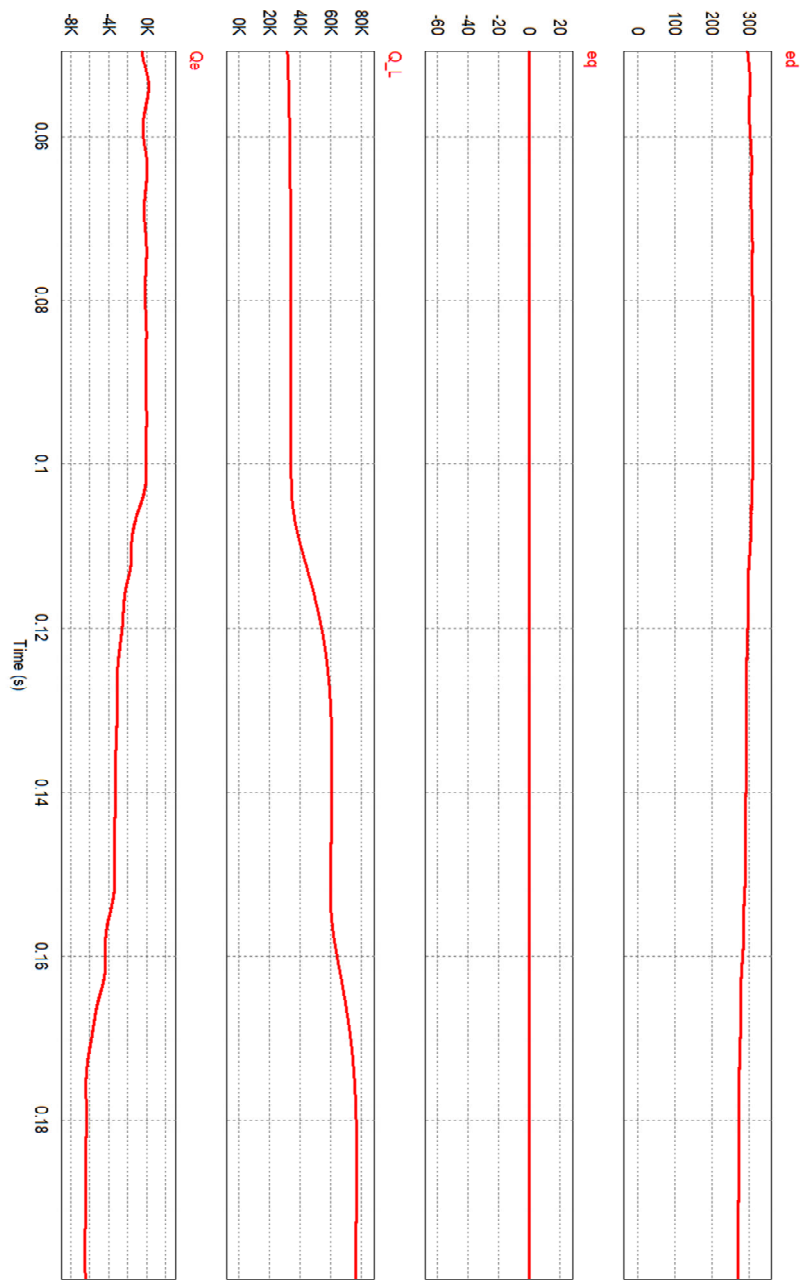


Figure 5.15 Change in ed and eq components of the voltage with the change in load.

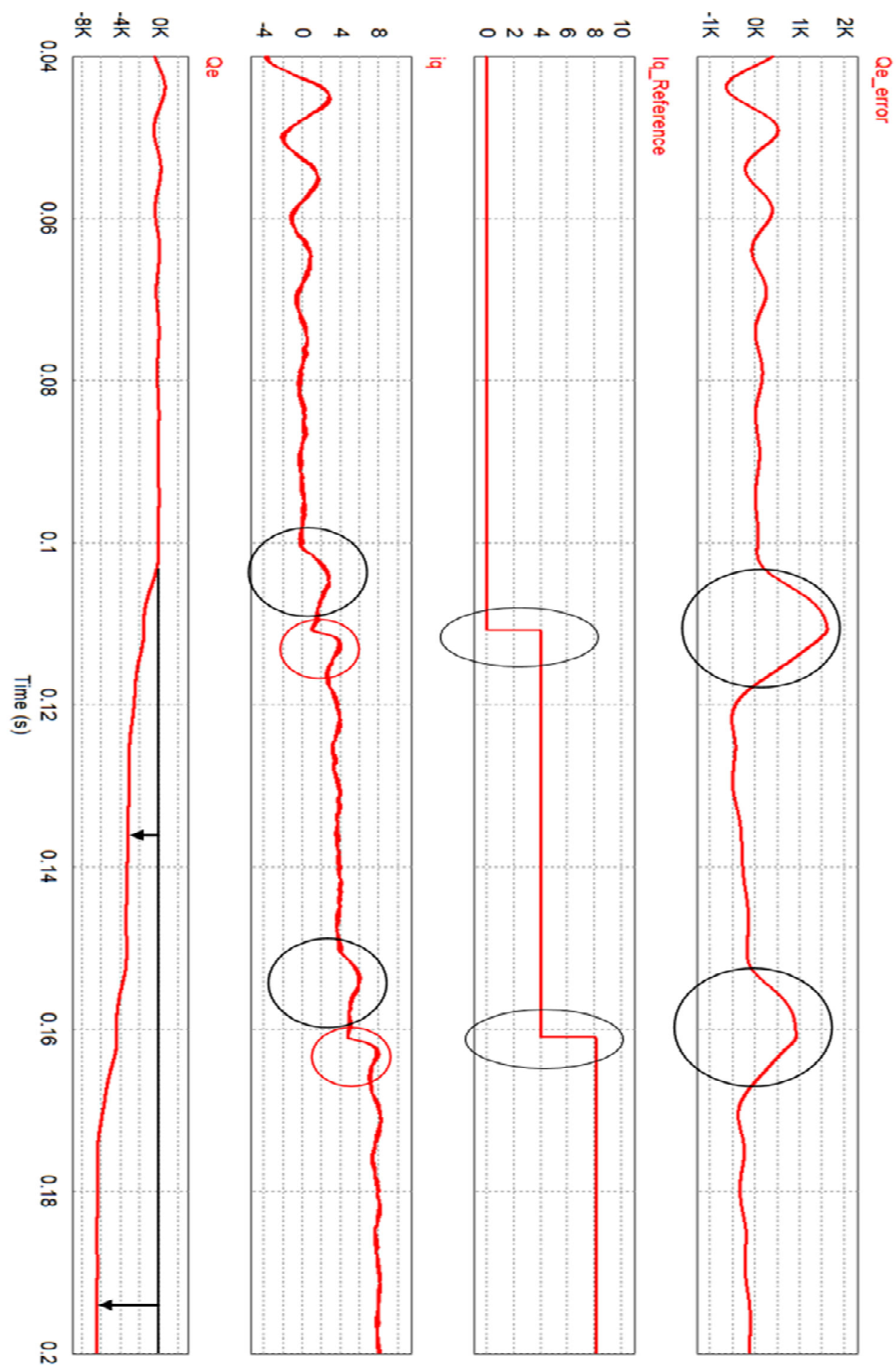


Figure 5.16 Generation of the  $I_q\_Reference$  for the positive error.

# REACTIVE POWER CONTRIBUTION BY RENEWABLE SOURCES

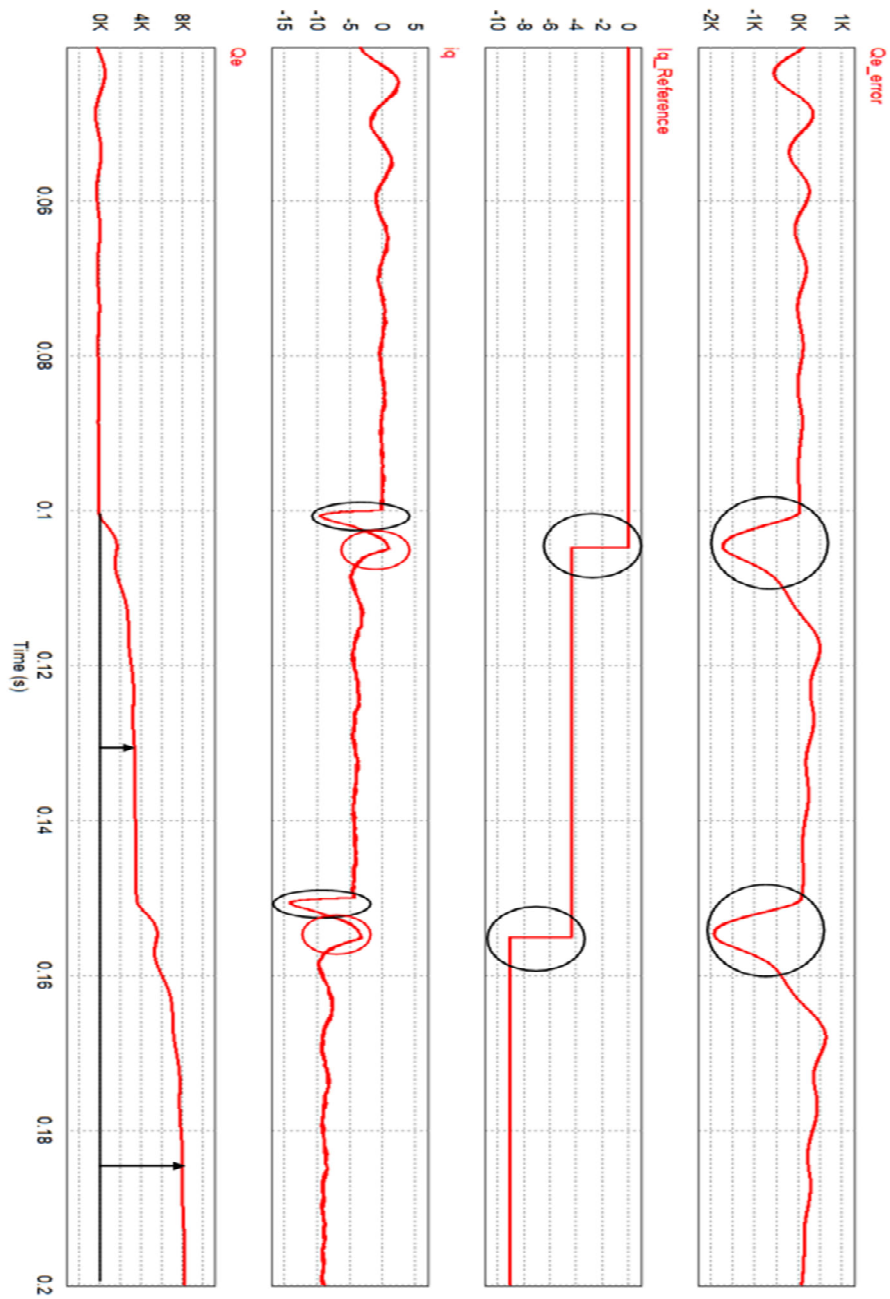


Figure 5.17 Generation of the  $I_{q\_Reference}$  for the negative error.

# REACTIVE POWER CONTRIBUTION BY RENEWABLE SOURCES

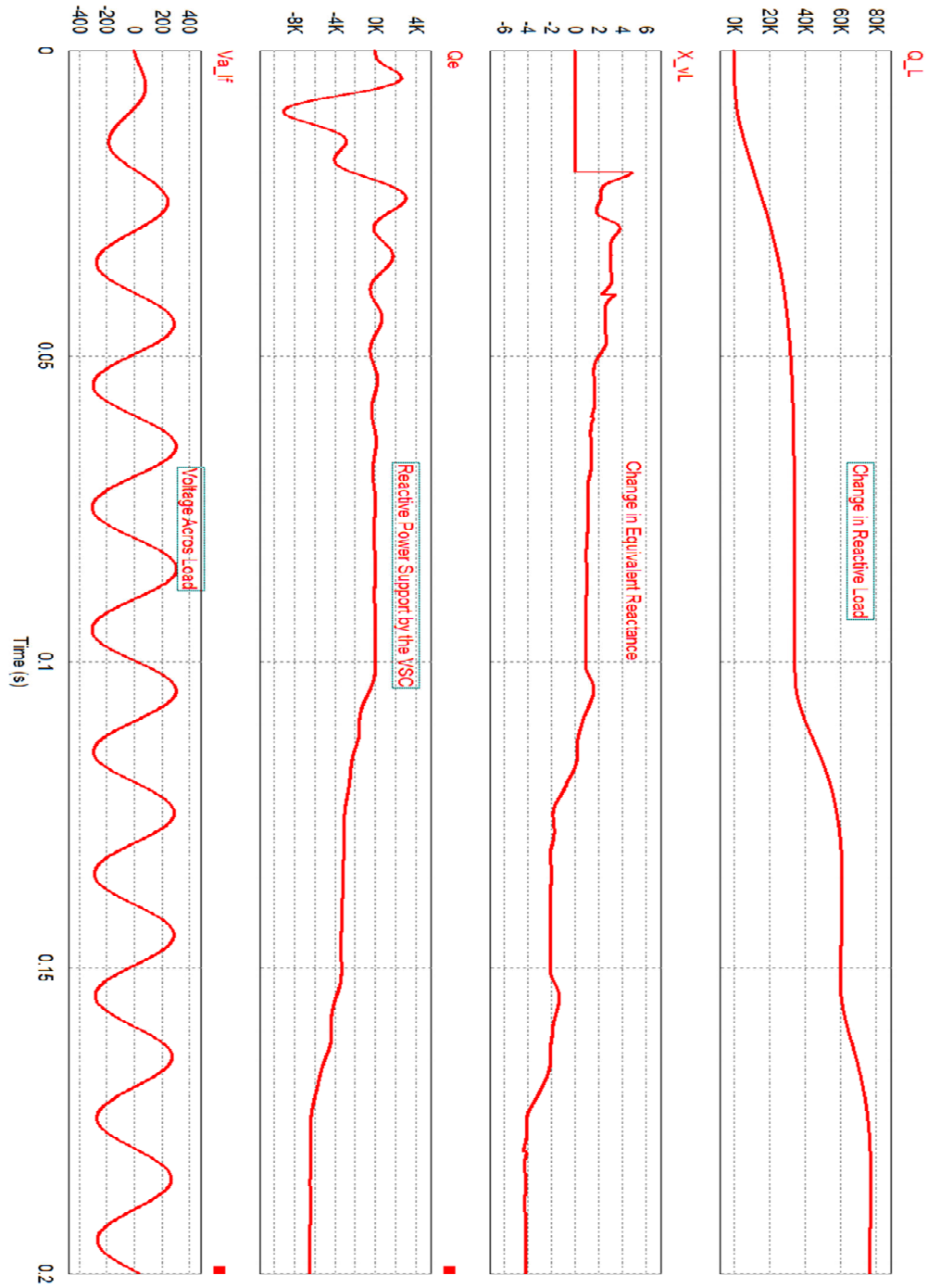


Figure 5.18 Change in equivalent reactance and voltage across the load.

Figure 5.18 depicts the change in equivalent reactance  $X_{vL}$  across the terminal of the VSC. It can be seen that the equivalent  $X_{vL}$  decreases with the increase in the reactive power load. This  $X_{vL}$  is actually taken as an indication in the generation in the compensation of the

reactive power using the external functional block. With the decrease in the  $X_{v\_L}$  the reactive power support from the VSC increases and the voltage change is kept within range which is shown in Figure 5.18.

### 5.5 Conclusion

This chapter discusses about the main results of the thesis. The researched and designed VSC controller is able of decoupling the two control variables,  $I_d$  and  $I_q$ , reacting very fast and precisely to changes in the MG, either active or reactive ones.

The disruptive approach oriented to model the MG according to Thevenin's theorem and the proposed algorithm is appropriate to manage the issue behind this thesis: To put every renewable power plants contributing to share reactive power with high dynamics. In fact, the transient response at contributing to share reactive power lasts less than 10 ms, which points out to a time constant of the VSC response equivalent to 2 ms, in other performance indicator a settling time of 10 ms. These indicators are very good when one faces grid dynamics, even conventional grids supported on very large power plants based on large synchronous generators, ie, large rotating inertia.

Finally, the behavior of the VSC as element interconnecting with MG is analyzed, discussing its performance at contributing to share the reactive power as well as its robustness to changes in the demand of active power and voltage regulation as its main role is performed controlling the current.

## 6 CONCLUSION AND FUTURE WORK

### 6.1 Conclusion

The increased penetration of renewable sources with distributed generations has led to the development of idea to keep the consumers in local clusters with generation called MG. Similar to the conventional grid the main requirement of the MG is also to keep the voltage and frequency within permissible limit. To achieve this requirement the proper power sharing is also one of the major factors. The power sharing is generally conducted using droop mechanism which is an imitation of the behavior of synchronous generators. However, this thesis has demonstrated that there are certain disadvantages in this approach that encourage investigating alternative control strategies.

The work of this thesis started with the detailed state of the art of the research and development work going on in the field of MG. It is shown that there are still a lot of challenges to be solved in the field of MG like proper and fast reactive power sharing, absence of inertia in renewable resources with electronics interface. Much latest work going on around the world is presented in chapter two as state of art. Among the many work done it is found that although a lot has been done in solving the problems yet many more has to be done. To solve the issue of power sharing much of the work is to mimic the behavior of synchronous generator using droop equations. The use of virtual impedance is also adopted in a lot of research work to solve the problem of line drop. Complex circuits are used with control loops, which are used to solve the problem of sharing of reactive power. The use of many voltage control loops has ultimately made the operation slow.

Most of the works going on around the world are following the central approach to control the active and reactive power sharing for different renewable resources. This makes the operating process a bit slow and the reliability of the system also decreases. Moreover it causes the increase of the related costs. So a step towards the distributive approach is adopted by this thesis to share the reactive power using a vector control method. The MGCC used by most of the MGs worldwide will be limited to use in the steady state only if all the VSC interconnecting the renewable resources use this distributive approach.

## CONCLUSION AND FUTURE WORK

This distributive approach with current loops makes the system fast enough to handle the dynamic changes in the grid load as well as more reliable. To achieve the goal, the vector controller of the VSC interfacing the renewable source is researched and designed in chapter three. The modeling of the VSC and the controller is researched to design the controller to handle the reactive power and the voltage level across the load. The modulation and synchronization techniques, which are used in VSC operation, are also described in chapter 3. The controller designed is tested using PSIM models to supply or consume power according to the requirements of the load demand. Finally, the operation of the VSC in different modes of operation is described as a method to put the VSC running in high dynamics condition able of contributing to handling the issues found in MGs. The power exchange between VSC and MG using the designed controller is performed with high dynamics[65].

The problem of reactive power sharing is described in detail in chapter 4 based on computational analyses with Matlab. It is verified that the reactive power sharing is strongly dependent on the line parameters what points out to consider the reactive power sharing according to the relative position of the load and power source. The problem with the importance of line parameters in the power flow equation is described in the chapter four. It is shown that the complex impedance, which has to be considered in case of MG, creates a problem in which it is not possible to ignore any part of the impedance as is done in traditional power flow equation.

Finally, the reactive power contribution by each renewable power source integrated in a MG is analyzed in chapter 5. The algorithm used in controlling the VSC is presented with a flowchart. The base to support the algorithm performance is to adopt a MG model based on Thevenin's theorem. The analytical derivation of the Thevenin's equivalent impedance on which the controller acts is described. The controller generates the right compensation signal for the reactive power sharing based on the changes in equivalent impedance across the terminal of the power source VSC. This compensation signal is used to generate the reactive power support by the VSC. The new needed reactive power is supplied by the VSC within half cycle of the normal frequency of the grid. In fact, the controller dynamics is high enough, presenting a short transient



## CONCLUSION AND FUTURE WORK

associated to the load change with a settling time of 10 ms. It should be emphasized that the active power remains constant in the operation according to the framework of the thesis.

The controller is researched and worked out in dq reference frame in which the d axis represents the active power and the q axis represents the reactive power. The decoupling is done perfectly so that there is no much effect of change in one variable on the other one (active and reactive power). The contribution of the VSC in the reactive power sharing can be adjusted by setting the factor of the compensation variable within the power range of the renewable source.

### 6.2 Future Work

While this thesis has presented the fundamental characteristics and principles of reactive power sharing in a MG with higher dynamics, the capability of this new scheme still needs significant further investigation in several areas.

Firstly, the concept of reactive power sharing is applied successfully for one VSC. This concept can be implemented and tested for a real world MG like CERTS, with many VSC's. Each VSC with similar approach will be supporting the MG with reactive power dynamically. This will help the MG to act during transient period of load change.

Secondly, the work can be tested with a MG developed in RTDS (Real Time Digital Simulation).

Thirdly, while all the results presented in this thesis show extremely good robustness and resilience, there are most likely some stability limitations for the new scheme that need to be identified. A more formal control stability analysis would be very advantageous to determine the potential operating limits for this new strategy.

Fourthly, the work developed in this thesis can be tested in hardware. Initially the work can be developed with one VSC which can be further carried forward with many VSC's.

Finally, a more general investigation into the operation of more complex MG situations with various source types and load characteristics can be carried forward. The harmonics content introduced by the VSC in the MG can also be studied.

## BIBLIOGRAPHY

- 
- [1] L. MENG, "Hierarchical control for optimal and distributed operation of microgrid systems," PhD Thesis, Aalborg University, 2015.
  - [2] C. Gouveia, "Experimental Validation of Microgrids : Exploiting the role of Plug-in Electrical Vehicles , active load control and micro-generation units", PhD Thesis, University of Porto, 2014.
  - [3] K. De Brabandere, B. Bolsens, J. Van den Keybus, A. Woyte, J. Driesen, and R. Belmans, "A Voltage and Frequency Droop Control Method for Parallel Inverters," *IEEE Trans. Power Electron.*, vol. 22, no. 4, pp. 1107–1115, 2007, DOI: 10.1109/TPEL.2007.900456.
  - [4] Z. Xuesong, G. Tie, and M. Youjie, "An overview on microgrid technology," in *Mechatronics and Automation (ICMA), 2015 IEEE International Conference on*, 2015, pp. 76–81, DOI: 10.1109/ICMA.2015.7237460.
  - [5] C. Moreira "Identification and development of microgrids emergency control procedures", PhD Thesis, University of Porto, 2008.
  - [6] M. S. Mahmoud, S. Azher Hussain, and M. A. Abido, "Modeling and control of microgrid: An overview," *J. Franklin Inst.*, vol. 351, no. 5, pp. 2822–2859, 2014, DOI: 10.1016/j.jfranklin.2014.01.016.
  - [7] D. E. Olivares *et al.*, "Trends in microgrid control," *IEEE Trans. Smart Grid*, vol. 5, no. 4, pp. 1905–1919, 2014, DOI:10.1109/TSG.2013.2295514.
  - [8] J. Simpson-Porco, Q. Shafiee, F. Dorfler, J. C. Vasquez, J. Guerrero, and F. Bullo, "Secondary Frequency and Voltage Control of Islanded Microgrids via Distributed Averaging," *IEEE Trans. Ind. Electron.*, vol. 0046, no. c, pp. 1–1, 2015, DOI:10.1109/TIE.2015.2436879.
  - [9] J. Driesen and K. Visscher, "Virtual synchronous generators," in *Power and Energy Society General Meeting - Conversion and Delivery of Electrical Energy in the 21st Century, 2008 IEEE*, 2008, pp. 1–3, DOI: 10.1109/PES.2008.4596800.
  - [10] H. M. Rustebakke and General Electric Company. Electric Utility Systems Engineering Department., *Electric utility systems and practices*. Wiley, 1983, URL: <https://www.wiley.com/en-us/Electric+Utility+Systems+and+Practices%2C+4th+Edition-p-9780471048909>.
  - [11] D. Glover, M. Sarma, and T. Overbye, *Power System Analysis & Design*, vol. 53, no. 9. 2012.
  - [12] A. Bergen and V. Vittal, "Power Systems Analysis." p. 619, 2010.
  - [13] H. Han, X. Hou, J. Yang, J. Wu, M. Su, and J. M. Guerrero, "Review of Power Sharing Control Strategies for Islanding Operation of AC Microgrids," *Smart Grid, IEEE Trans.*, vol. 7, no. 1, pp. 200–215, 2016, DOI: 10.1109/TSG.2015.2434849.
  - [14] K. Moslehi and R. Kumar, "A reliability perspective of the smart grid," *IEEE Trans. Smart Grid*, vol. 1, no. 1, pp. 57–64, 2010, DOI: 10.1109/TSG.2010.2046346.
  - [15] D. G. F. T. Z. G. Gtz, "Renewables 2010 Global Status Report," *Nucl. Saf.*, vol. 2010, no. 01.02.2011, p. 80, 2010.
  - [16] C. a. Hernandez-Aramburo and T. C. Green, "Fuel consumption minimisation of a microgrid,"

## B I B L I O G R A P H Y

- Conf. Rec. 2004 IEEE Ind. Appl. Conf. 2004. 39th IAS Annu. Meet.*, vol. 3, no. 3, pp. 673–681, 2004, DOI: 10.1109/IAS.2004.1348751.
- [17] P. P. Varaiya, F. F. Wu, and J. W. Bialek, “Smart Operation of Smart Grid: Risk-Limiting Dispatch,” *Proc. IEEE*, vol. 99, no. 1, pp. 40–57, 2011, DOI: 10.1109/JPROC.2010.2080250.
  - [18] O. Hafez and K. Bhattacharya, “Optimal planning and design of a renewable energy based supply system for microgrids,” *Renew. Energy*, vol. 45, pp. 7–15, 2012, DOI: 10.1016/j.renene.2012.01.087.
  - [19] S. Parhizi, H. Lotfi, A. Khodaei, and S. Bahramirad, “State of the Art in Research on Microgrids: A Review,” *Access, IEEE*, vol. 3, pp. 890–925, 2015, DOI: 10.1109/ACCESS.2015.2443119.
  - [20] York Ben, Key Tom, Singhvi Vikas “Microgrids.”, Version 18, 2013.
  - [21] “About CERTS | CERTS.” [Online]. Available: <https://certs.lbl.gov/about-certs>. [Accessed: 15-Dec-2017].
  - [22] W. Jiang, Z. He, and Z. Bo, “The Overview of Research on Microgrid Protection Development,” in *Intelligent System Design and Engineering Application (ISDEA), 2010 International Conference on*, 2010, vol. 2, pp. 692–697, DOI:10.1109/ISDEA.2010.69.
  - [23] R. Lasseter, A. Akhil, C. Marnay, and J. Stephens, “Integration of distributed energy resources. The CERTS Microgrid Concept,” *Econ. Issues*, p. 27, 2002.
  - [24] M. Barnes *et al.*, “Real-World MicroGrids-An Overview,” *2007 IEEE Int. Conf. Syst. Syst. Eng.*, pp. 1–8, 2007, DOI: 10.1109/SYSOSE.2007.4304255.
  - [25] T. Morstyn, B. Hredzak, and V. G. Agelidis, “Distributed Cooperative Control of Microgrid Storage,” *Power Syst. IEEE Trans.*, vol. 30, no. 5, pp. 2780–2789, 2015, DOI: 10.1109/TPWRS.2014.2363874.
  - [26] T. Ackermann, G. Ran Andersson, and L. Sö Der, “Distributed generation: a definition,” *Electr. Power Syst. Res.*, vol. 57, pp. 195–204, 2001, DOI: 10.1016/S0378-7796(01)00101-8.
  - [27] Mehrdad Yazdani and Ali Mehrizi-Sani, “Distributed Control Techniques in Microgrids”, DOI: 10.1109/TSG.2014.2337838.
  - [28] A. Maitra, B. York, H. Kamath, T. Key, and V. Singhvi, “Microgrid A Primer,” 2013. [Online]. Available: [http://nyssmartgrid.com/wp-content/uploads/Microgrid\\_Primer\\_v18-09-06-2013.pdf](http://nyssmartgrid.com/wp-content/uploads/Microgrid_Primer_v18-09-06-2013.pdf).
  - [29] J. A. Peas Lopes, C. L. Moreira, and A. G. Madureira, “Defining control strategies for MicroGrids islanded operation,” *Power Syst. IEEE Trans.*, vol. 21, no. 2, pp. 916–924, 2006, DOI: 10.1109/TPWRS.2006.873018.
  - [30] Y. You, G. Wang, C. Zhang, and J. Lian, “An Improved Frequency Control Method for Microgrid in Islanded Operation,” *2013 2nd Int. Symp. Instrum. Meas. Sens. Netw. Autom.*, pp. 296–299, 2013, DOI: 10.1109/IMSNA.2013.6743273.
  - [31] M. Yazdani and A. Mehrizi-Sani, “Distributed control techniques in microgrids,” *IEEE Trans. Smart Grid*, vol. 5, no. 6, pp. 2901–2909, 2014, DOI: 10.1109/TSG.2014.2337838.
  - [32] Y. Xu, W. Zhang, G. Hug, S. Kar, and Z. Li, “Cooperative Control of Distributed Energy Storage

## BIBLIOGRAPHY

- Systems in a Microgrid," *IEEE Trans. Smart Grid*, vol. 6, no. 1, pp. 238–248, 2015, DOI: 10.1109/TPWRS.2014.2363874.
- [33] M. R. I. F. Katiraei, "Power management strategies for a microgrid with multiple distributed generation units," *IEEE Trans. Power Syst.*, vol. 21, no. 4, pp. 1821–1831, 2006.
  - [34] J. W. Simpson-Porco, Q. Shafiee, F. Dorfler, J. C. Vasquez, J. M. Guerrero, and F. Bullo, "Secondary Frequency and Voltage Control of Islanded Microgrids via Distributed Averaging," *Ind. Electron. IEEE Trans.*, vol. 62, no. 11, pp. 7025–7038, 2015, DOI: 10.1109/TPWRS.2006.879260.
  - [35] V. Nasirian, S. Moayedi, A. Davoudi, and F. L. Lewis, "Distributed Cooperative Control of DC Microgrids," *Power Electron. IEEE Trans.*, vol. 30, no. 4, pp. 2288–2303, 2015, DOI: 10.1109/TPEL.2014.2324579.
  - [36] M. C. Chandorkar, D. M. Divan, and R. Adapa, "Control of parallel connected inverters in standalone AC supply systems," *IEEE Trans. Ind. Appl.*, vol. 29, no. 1, pp. 136–143, 1993, DOI: 10.1109/28.195899.
  - [37] a. G. Madureira and J. a. P. Lopes, "Voltage and reactive power control in MV networks integrating microgrids," *Proc. ICREPQ*, vol. 7, 2007.
  - [38] J. M. Guerrero, J. Matas, L. de Vicuna, M. Castilla, and J. Miret, "Decentralized control for parallel operation of distributed generation inverters using resistive output impedance," *IEEE Trans. Ind. Electron.*, vol. 54, no. 2, pp. 994–1004, 2007, DOI: 10.1109/TIE.2007.892621.
  - [39] A. Dziulko *et al.*, "Implementation of Equal Reactive Power Sharing Algorithm in Droop-Controlled Islanded AC Microgrid," *Prz. Elektrotechniczny*, vol. 1, no. 1, pp. 83–89, 2015, DOI: 10.15199/48.2015.01.15.
  - [40] Q. Guo, H. Wu, L. Lin, Z. Bai, and H. Ma, "Secondary Voltage Control for Reactive Power Sharing in an Islanded Microgrid," vol. 16, no. 1, pp. 329–339, 2016.
  - [41] B. Kroposki, R. Lasseter, T. Ise, S. Morozumi, S. Papathanassiou, and N. Hatziaargyriou, "Making microgrids work," *IEEE Power Energy Mag.*, vol. 6, no. 3, pp. 40–53, 2008, DOI: 10.1109/MPE.2008.918718.
  - [42] P. Piagi and R. H. Lasseter, "Autonomous control of microgrids," in *2006 IEEE Power Engineering Society General Meeting, PES*, 2006, DOI: 10.1109/PES.2006.1708993.
  - [43] B. Lasseter, "Microgrids [distributed power generation]," in *Power Engineering Society Winter Meeting, 2001. IEEE*, 2001, vol. 1, pp. 146–149 vol.1.
  - [44] J. M. Guerrero *et al.*, "Hierarchical Control of Droop-Controlled AC and DC Microgrids&#x2014;A General Approach Toward Standardization," *Ind. Electron. IEEE Trans.*, vol. 58, no. 1, pp. 158–172, 2011, DOI: 10.1109/TIE.2010.2066534.
  - [45] T. L. Vandoorn, J. De Koning, B. Meersman, and L. Vandevelde, "Voltage-based droop control of renewables to avoid on-off oscillations caused by overvoltages," *IEEE Trans. Power Deliv.*, vol. 28, no. 2, pp. 845–854, 2013, DOI: 10.1109/TPWRD.2013.2241793.
  - [46] H. Niu, M. Jiang, D. Zhang, and J. Fletcher, "Autonomous micro-grid operation by employing weak droop control and PQ control," *2014 Australas. Univ. Power Eng. Conf. AUPEC 2014 - Proc.*, no. October, pp. 1–5, 2014, DOI: 10.1109/AUPEC.2014.6966519.

## B I B L I O G R A P H Y

- [47] D. De and V. Ramanarayanan, "Decentralized parallel operation of inverters sharing unbalanced and nonlinear loads," *IEEE Trans. Power Electron.*, vol. 25, no. 12, pp. 3015–3025, 2010, DOI: 10.1109/TIE.2007.892621.
- [48] J. Hu, J. Zhu, D. G. Dorrell, and J. M. Guerrero, "Virtual flux droop method - A new control strategy of inverters in microgrids," *IEEE Trans. Power Electron.*, vol. 29, no. 9, pp. 4704–4711, 2014, DOI: 10.1109/TPEL.2013.2286159 .
- [49] J. M. Guerrero, L. G. de Vicuna, J. Matas, M. Castilla, and J. Miret, "A wireless controller to enhance dynamic performance of parallel inverters in distributed generation systems," *IEEE Trans. Power Electron.*, vol. 19, no. 5, pp. 1205–1213, 2004, DOI: 10.1109/TPEL.2004.833451.
- [50] B. G. Cho and S. K. Sul, "Power sharing strategy in parallel operation of inverters for distributed power system under line impedance inequality," *2013 IEEE ECCE Asia Downunder - 5th IEEE Annu. Int. Energy Convers. Congr. Exhib. IEEE ECCE Asia 2013*, pp. 358–364, 2013, DOI: 10.1109/ECCE-Asia.2013.6579121.
- [51] Y. Guan, J. C. Vasquez, and J. M. Guerrero, "A simple autonomous current-sharing control strategy for fast dynamic response of parallel inverters in islanded microgrids," *ENERGYCON 2014 - IEEE Int. Energy Conf.*, pp. 182–188, 2014, DOI: 10.1109/ENERGYCON.2014.6850426.
- [52] F. Lou *et al.*, "A Triple-Droop Control Scheme for Inverter-Based Microgrids," *IECON 2012 - 38th Annu. Conf. IEEE Ind. Electron. Soc.*, pp. 3368–3375, 2012.
- [53] J. He and Y. W. Li, "An accurate reactive power sharing control strategy for DG units in a microgrid," *8th Int. Conf. Power Electron. - ECCE Asia "Green World with Power Electron. ICPE 2011-ECCE Asia*, pp. 551–556, 2011.
- [54] Y. Zhu, F. Zhuo, and H. Shi, "Accurate power sharing strategy for complex microgrid based on droop control method," *2013 IEEE ECCE Asia Downunder - 5th IEEE Annu. Int. Energy Convers. Congr. Exhib. IEEE ECCE Asia 2013*, pp. 344–350, 2013, DOI: 10.1109/ECCE-Asia.2013.6579119.
- [55] R. Majumder, G. Ledwich, A. Ghosh, S. Chakrabarti, and F. Zare, "Droop control of converter-interfaced microsources in rural distributed generation," *IEEE Trans. Power Deliv.*, vol. 25, no. 4, pp. 2768–2778, 2010, DOI: 10.1109/TPWRD.2010.2042974.
- [56] T. L. Vandoorn, B. Zwaenepoel, J. D. M. De Kooning, B. Meersman, and L. Vandevelde, "Smart microgrids and virtual power plants in a hierarchical control structure," *2nd IEEE PES Int. Conf. Exhib. Innov. Smart Grid Technol.*, pp. 1–7, 2011, DOI: 10.1109/ISGTEurope.2011.6162830.
- [57] L. Che and M. Shahidehpour, "DC microgrids: Economic operation and enhancement of resilience by hierarchical control," *IEEE Trans. Smart Grid*, vol. 5, no. 5, pp. 2517–2526, 2014, DOI: 10.1109/TSG.2014.2344024.
- [58] R. Majumder, B. Chaudhuri, A. Ghosh, R. Majumder, G. Ledwich, and F. Zare, "Improvement of stability and load sharing in an autonomous microgrid using supplementary droop control loop," *IEEE Trans. Power Syst.*, vol. 25, no. 2, pp. 796–808, 2010, DOI: 10.1109/TPWRS.2009.2032049.
- [59] J. He, Y. W. Li, J. M. Guerrero, F. Blaabjerg, and J. C. Vasquez, "Microgrid reactive and harmonic power sharing using enhanced virtual impedance," *Conf. Proc. - IEEE Appl. Power Electron. Conf. Expo. - APEC*, pp. 447–452, 2013, DOI: 10.1109/APEC.2013.6520248.
- [60] N. L. Diaz *et al.*, "2014, Intelligent Distributed Generation and Storage Units for DC Microgrids—

## B I B L I O G R A P H Y

- A New Concept on Cooperative Control Without Communications Beyond Droop Control.pdf," *IEEE Trans. Smart Grid*, vol. 5, no. 5, pp. 2476–2485, 2014.
- [61] Y. Wei, C. Min, J. Matas, J. M. Guerrero, and Q. Zhao-ming, "Design and Analysis of the Droop Control Method for Parallel Inverters Considering the Impact of the Complex Impedance on the Power Sharing," *Ind. Electron. IEEE Trans.*, vol. 58, no. 2, pp. 576–588, 2011, DOI: 10.1109/TIE.2010.2046001.
  - [62] Y. W. Li and C. N. Kao, "An accurate power control strategy for power-electronics-interfaced distributed generation units operating in a low-voltage multibus microgrid," *IEEE Trans. Power Electron.*, vol. 24, no. 12, pp. 2977–2988, 2009, DOI: 10.1109/TPEL.2009.2022828.
  - [63] P. C. Loh, D. Li, Y. K. Chai, and F. Blaabjerg, "Autonomous control of interlinking converter with energy storage in hybrid AC-DC microgrid," *IEEE Trans. Ind. Appl.*, vol. 49, no. 3, pp. 1374–1382, 2013, DOI: 10.1109/TIA.2013.2252319.
  - [64] L. D. Watson, S. Member, J. W. Kimball, and S. Member, "Frequency Regulation of a Microgrid Using Solar Power," *Simulation*, pp. 321–326, 2011, DOI: 10.1109/TIA.2013.2252319.
  - [65] G. Dehnavi and H. L. Ginn, "Load sharing among converters in an autonomous microgrid in presence of wind and PV sources," *2013 IEEE PES Innov. Smart Grid Technol. Conf. ISGT 2013*, pp. 1–6, 2013, DOI: 10.1109/ISGT.2013.6497839.
  - [66] F. Katiraei, M. R. Iravani, and P. W. Lehn, "Micro-grid autonomous operation during and subsequent to islanding process," *IEEE Trans. Power Deliv.*, vol. 20, no. 1, pp. 248–257, 2005, DOI: 10.1109/TPWRD.2004.835051.
  - [67] Y. Li, D. M. Vilathgamuwa, and P. C. Loh, "Design, analysis, and real-time testing of a controller for multibus microgrid system," *IEEE Trans. Power Electron.*, vol. 19, no. 5, pp. 1195–1204, 2004, DOI: 10.1109/TPEL.2004.833456.
  - [68] I. J. B. Álvarez, "CONTROL OF DISTRIBUTED GENERATION FOR GRID-CONNECTED AND INTENTIONAL ISLANDING OPERATIONS By Irvin Joel Balaguer Álvarez," *Unpubl. Michigan State Univ.*, vol. PhD Thesis, no. C, pp. 2005–2008, 2011, DOI: 10.1109/TIE.2010.2049709.
  - [69] M. Shahabi, M. R. Haghifam, M. Mohamadian, and S. A. Nabavi-Niaki, "Dynamic behavior improvement in a microgrid with multiple DG units using a power sharing approach," *2009 IEEE Bucharest PowerTech Innov. Ideas Toward Electr. Grid Futur.*, pp. 1–8, 2009, DOI: 10.1109/PTC.2009.5282145.
  - [70] D. Menniti, C. Picardi, A. Pinnarelli, and D. Sgrò, "Power management by grid-connected inverters using a voltage and current control strategy for Microgrid applications," *SPEEDAM 2008 - Int. Symp. Power Electron. Electr. Drives, Autom. Motion*, pp. 1414–1419, 2008, DOI: 10.1109/SPEEDHAM.2008.4581283.
  - [71] E. Luis and A. Jonás, "B L," 2013, pp. 2656–2662.
  - [72] D. G. Holmes, T. A. Lipo, B. P. McGrath, and W. Y. Kong, "Optimized design of stationary frame three phase AC Current regulators," *IEEE Trans. Power Electron.*, vol. 24, no. 11, pp. 2417–2426, 2009, DOI: 10.1109/TPEL.2009.2029548.
  - [73] O. Wasynczuk, S. D. Sudhoff, T. D. Tran, D. H. Clayton, and H. J. Hegner, "A voltage control strategy for current-regulated PWM inverters," *IEEE Trans. Power Electron.*, vol. 11, no. 1, pp. 7–15, 1996,

## B I B L I O G R A P H Y

DOI: 10.1109/63.484411.

- [74] J. Liu, Y. Miura, and T. Ise, "Dynamic characteristics and stability comparisons between virtual synchronous generator and droop control in inverter-based distributed generators," *2014 Int. Power Electron. Conf. IPEC-Hiroshima - ECCE Asia 2014*, no. 3, pp. 1536–1543, 2014, DOI: 10.1109/IPEC.2014.6869789.
- [75] Q. C. Zhong and G. Weiss, "Synchronverters: Inverters that mimic synchronous generators," *IEEE Trans. Ind. Electron.*, vol. 58, no. 4, pp. 1259–1267, 2011, DOI: 10.1109/TIE.2010.2048839.
- [76] J. Pegueroles Queralt, "Control of voltage source converters for distributed generation in microgrids," PhD Thesis, Universitat Politècnica de Catalunya, July, 2015.
- [77] V. S. Converters, P. W. M. B. Rectifiers, P. Factor, and U. P. Factor, "Three-phase Voltage Source Converters Modeling", DOI: 10.1109/SusTech.2017.8333536.
- [78] T. C. Green and M. Prodanovi??, "Control of inverter-based micro-grids," *Electr. Power Syst. Res.*, vol. 77, no. 9, pp. 1204–1213, 2007, DOI: 10.1016/j.epsr.2006.08.017.
- [79] J. Rocabert, A. Luna, F. Blaabjerg, and P. Rodríguez, "Control of power converters in AC microgrids," *IEEE Trans. Power Electron.*, vol. 27, no. 11, pp. 4734–4749, 2012, DOI: 10.1109/TPEL.2012.2199334.
- [80] J. R. Rodríguez, J. W. Dixon, J. R. Espinoza, J. Pontt, and P. Lezana, "PWM regenerative rectifiers: State of the art," *IEEE Trans. Ind. Electron.*, vol. 52, no. 1, pp. 5–22, 2005, DOI: 10.1109/TIE.2004.841149.
- [81] G. Joós, "Performance Investigation of a Current-Controlled Voltage-Regulated PWM Rectifier in Rotating and Stationary Frames," *IEEE Trans. Ind. Electron.*, vol. 42, no. 4, pp. 396–401, 1995, DOI: 10.1109/TIE.2004.841149.
- [82] D. N. Zmood and D. G. Holmes, "Stationary frame current regulation of PWM inverters with zero steady-state error," *IEEE Trans. Power Electron.*, vol. 18, no. 3, pp. 814–822, 2003, DOI: 10.1109/TPEL.2003.810852.
- [83] M. Malinowski, "Sensorless Control Strategies for Three - Phase PWM Rectifiers," *Ph.D. Thesis, Warsaw, Pol.*, p. 127, 2001, DOI: 10.1016/B978-0-12-381462-3.00110-5.
- [84] H. Akagi, Y. Kanazawa, and A. Nabae, "Instantaneous Reactive Power Compensators Comprising Switching Devices without Energy Storage Components," *IEEE Trans. Ind. Appl.*, vol. IA-20, no. 3, pp. 625–630, 1984, DOI: 10.1109/TIA.1984.4504460.
- [85] R. S. Pena, R. J. Cardenas, J. C. Clare, and G. M. Asher, "Control strategies for voltage control of a boost type PWM converter," *PESC Rec. - IEEE Annu. Power Electron. Spec. Conf.*, vol. 2, no. 1, pp. 730–735, 2001, DOI: 10.1109/PESC.2001.954205.
- [86] R. Brito, A. Carvalho, and M. Gericota, "A new three-phase voltage sourced converter laplace model," *Proc. - 2015 9th Int. Conf. Compat. Power Electron. CPE 2015*, pp. 160–166, 2015, DOI: 10.1109/CPE.2015.7231066.
- [87] M. P. Kazmierkowski, R. Krishnan, F. Blaabjerg, and J. D. Irwin, *Control in Power Electronics: Selected Problems*. 2002.
- [88] B. K. Bose, "Modern Power Electronics and AC Drives," *Prentice-Hall*. p. 738, 2002.

## B I B L I O G R A P H Y

- [89] N. Jaalam, N. A. Rahim, A. H. A. Bakar, C. K. Tan, and A. M. A. Haidar, "A comprehensive review of synchronization methods for grid-connected converters of renewable energy source," *Renew. Sustain. Energy Rev.*, vol. 59, pp. 1471–1481, 2016, DOI: 10.1016/j.rser.2016.01.066.
- [90] G.-C. Hsieh and J. C. Hung, "Phase-locked loop techniques- A survey," *IEEE Trans. Ind. Electron.*, vol. 43, no. 6, pp. 609–615, 1996, DOI: 10.1109/41.544547.
- [91] S. Barsali, M. Ceraolo, P. Pelacchi, and D. Poli, "Control techniques of Dispersed Generators to improve the continuity of electricity supply," in *Proc. PES Winter Meeting*, 2002, vol. 2, pp. 789–794.
- [92] L. Yun Wei and K. Ching-Nan, "An Accurate Power Control Strategy for Power-Electronics-Interfaced Distributed Generation Units Operating in a Low-Voltage Multibus Microgrid," *Power Electron. IEEE Trans.*, vol. 24, no. 12, pp. 2977–2988, 2009, DOI: 10.1109/TPEL.2009.2022828.
- [93] N. Gyawali, "Improved Active Power Sharing Strategy for ELC Controlled Synchronous Generators Based Islanded Micro Grid Application," 2015, ISBN: 9781467367448.
- [94] L. Rese, A. S. Costa, and A. S. e Silva, "A modified load flow algorithm for microgrids operating in islanded mode," in *2013 IEEE PES Conference on Innovative Smart Grid Technologies (ISGT Latin America)*, 2013, pp. 1–7, DOI: 10.1109/ISGT-LA.2013.6554384.
- [95] M. A. Mahmud, M. J. Hossain, H. R. Pota, and N. K. Roy, "Nonlinear distributed controller design for maintaining power balance in Islanded microgrids," *IEEE Power Energy Soc. Gen. Meet.*, vol. 2014–Octob, no. October, pp. 893–903, 2014, DOI: 10.1109/PESGM.2014.6939024.
- [96] K. P. W. Huanhai Xin, Leiqi Zhang, Zhen Wang, Deqiang Gan, "Control of Island AC Microgrids Using a Fully Distributed Approach," *IEEE Trans. Smart Grid*, vol. 6, no. 2, pp. 1–3, 2014, DOI: 10.1109/TSG.2014.2378694.
- [97] R. Mourant, "PSIM User's Manual," *Micro Simulation*, Boston, MA, 1983.
- [98] "PSIM User ' s Guide," *PSIM User's Guid.*, vol. Version 7., no. Release 3.
- [99] C. K. Sao, S. Member, and P. W. Lehn, "Voltage Source Converters," vol. 20, no. 2, pp. 1009–1016, 2005.
- [100] B. Shoeiby, "Current Regulator Based Control Strategy for Islanded and Grid-Connected Microgrids," PhD Thesis, University of Tehran, March, 2015.